SEVER INSTITUTE OF TECHNOLOGY

Doctor of Science Degree

DISSERTATION ACCEPTANCE
(To be submitted by the graduation approval deadline)

DATE: 09/03/93

STUDENT'S NAME: ALAN HOBACK

E.R.S. CODE: _____

This student's dissertation, entitled "Optimization of Steel Pile Foundations with Rigid and Flexible Concrete Slabs"

has been examined by the undersigned committee of three faculty members and has received full approval for acceptance in partial fulfillment of the requirements for the degree Doctor of Science.

Signatures: _____ Chairman

Distribution: (Please make copies)

5 - Dissertation copies
1 - Candidate
1 - Department
1 - Dean's Office
1 - Registrar

WASHINGTON UNIVERSITY

SEVER INSTITUTE OF TECHNOLOGY

OPTIMIZATION OF STEEL PILE FOUNDATIONS WITH RIGID OR FLEXIBLE CONCRETE SLABS

by

Alan Hoback

Prepared under the direction of Professor Kevin Z. Truman

A thesis presented to the Sever Institute of Washington University in partial fulfillment of the requirements for the degree of

DOCTOR OF SCIENCE

December, 1993

Saint Louis, Missouri

WASHINGTON UNIVERSITY

SEVER INSTITUTE OF TECHNOLOGY

ABSTRACT

OPTIMIZATION OF STEEL PILE FOUNDATIONS WITH RIGID OR FLEXIBLE CONCRETE SLABS

by Alan Hoback

ADVISOR: Professor Kevin Z. Truman

December, 1993

Saint Louis, Missouri

An automated design and optimization process for pile foundations with flexible or rigid concrete slabs is presented. The optimization process is applied to lock and dam foundation examples. The goal is to create a computer program that automatically optimizes the design. The designers specify the requirements of the design such as the loading conditions and soil properties. Then the program computes a low cost design. This can save time for the designer and can save on the construction costs. The pile properties and orientations are the only varied properties.

Within the scope of this work the foundation dimensions are not variable.

Two methods of pile slab analysis are used. The methods assume that either the concrete slab is thick and rigid (inflexible) or that it is thin and flexible. A finite element program is used to perform the flexible analysis which is a major component of the optimization. The program uses a novel method of pile assembly. The piles are assembled at any point within the slab elements.

Several advances have been made with the optimality criteria formulation and the general optimization procedures. The Percent method is a new method which has been developed to optimize discrete problems. Previously search methods were used. This required all combinations of the discrete options to be searched through to find the global optimum. The Percent method does not search. It is gradient-based which is much more efficient than searching.

Several examples are shown. The first set of examples demonstrate the performance and usefulness of certain new advances. A second set of examples applies the optimization capabilities to practical problems. The examples demonstrate that optimal sizes, alignments and numbers of piles can be determined by an optimization method. The examples have significant construction cost savings.

TABLE OF CONTENTS

Page

LIST OF TABLES v

LIST OF FIGURES vii

CHAPTER

1. INTRODUCTION 1

THE OPTIMIZATION METHOD 3

ACHIEVEMENTS 4

2. PILE FOUNDATIONS 6

PILE LAYOUTS AND CROSS-SECTIONS 6

PILE STRUCTURE DESIGN VARIABLES AND LIMITS 12

PILE FOUNDATION ANALYSIS 15

PILE ASSEMBLY 16

3. OPTIMIZATION FORMULATION 28

OPTIMALITY CRITERIA FORMULATION 30

APPLICATION AND ADVANCES OF THE OPTIMIZATION METHOD 38

TOPOLOGICAL VARIABLES 39
VARIABLES WITH ZERO WEIGHT GRADIENTS 41
MEMBER SELECTIONS 45
PILE ELIMINATION 46
GROUP OPTIMIZATION 47
THE PERCENTAGE SELECTION METHOD 49
SENSITIVITY ANALYSIS 54

4. PERFORMANCE EVALUATION EXAMPLE 58

5. FULL EXAMPLES 61
EXAMPLE 2, RETAINING WALL 62
WALL GROUP OPTIMIZATION 69
WALL COUPLED OPTIMIZATION 72
EXAMPLE 3, DAM STRUCTURE 75
EXAMPLE 4, LOCK 26R AL-3 83
RIGID ANALYSIS OF AL-3 104

6. SUMMARY AND CONCLUSIONS 108
SUMMARY OF EXAMPLES 108
CONCLUSIONS 110
FURTHER RESEARCH 113

7. ACKNOWLEDGEMENT 115

APPENDICES 116

8. APPENDIX 1: PILE GROUP BEHAVIOR 117
RIGID BODY CONCRETE SLAB ANALYSIS METHOD 117
PILE STIFFNESS 119
DESIGN FEASIBILITY 123

9. APPENDIX 2: FLEXIBLE SLAB ANALYSIS METHOD 128

10. NOMENCLATURE 141

BIBLIOGRAPHY 143

VITA 145

LIST OF TABLES

Table	Page
2-1. Maximum element sizes	24
4-1 Pile fixity example	60
5-1. Retaining wall load cases.	62
5-2. Initial wall pile properties.	64
5-3. Optimized wall pile properties.	65
5-4. Wall branched pile properties.	68
5-5. Optimized wall pile properties.	71
5-6. Branched wall pile properties.	72
5-7. Optimized wall pile properties.	73
5-8. Final wall branched pile properties.	73
5-9. Dam load cases.	75
5-10. Initial Dam pile properties.	78
5-11. Optimized Dam pile properties.	78
5-12. Optimized Dam pile group positions.	78
5-13. Description of the Lock Load Cases.	92
5-14. Initial lock pile properties.	95
5-15. Initial lock pile positions.	95
5-16. Optimized lock pile properties.	98
5-17. Optimized lock pile positions.	100
5-18. Final lock pile properties.	102
5-19. Final lock pile positions.	102
5-20. Optimized rigid slab analysis pile properties.	107
5-21. Optimized rigid slab analysis pile positions.	107
8-1. Pile Stiffness Coefficients.	121

LIST OF TABLES
(Continued)

Table		Page
8-2.	Pile Fixity Constants. (C_1)	122
8-3.	Axial Pile Stiffness Coefficients.	123
8-4.	Pinned Pile Design Moment Factors.	125
8-5.	Recommended Allowable Design Stresses for Steel Piles.	126
9-1.	Gauss points.	137

LIST OF FIGURES

Figure		Page
2-1	Pile Coordinate system.	8
2-2	Minor Axis Moment of Inertia vs. Major Axis Inertia.	10
2-3	Area vs. Major Axis Inertia.	10
2-4	Extreme fiber distance in y-direction vs. Major Axis Inertia.	11
2-5	Extreme fiber distance in x-direction vs. Major Axis Inertia.	11
2-6	Pile assembly theory.	20
2-7	Study of pile assembly.	22
3-1	Gradient vectors.	32
5-1	Initial pile layouts for wall example.	63
5-2	Weight convergence of wall.	66
5-3	Final pile layouts for individual method.	67
5-4	Final pile layouts for group method.	70
5-5	Final pile layouts for coupled method.	74
5-6	Dam structure.	76
5-7	Initial pile positions for dam.	77
5-8	Final pile positions for dam.	79
5-9	Weight of dam.	81
5-10	Percentage convergence.	81
5-11	Lock and Dam No. 26 (Replacement).	84
5-12	Auxiliary Lock 26R.	85
5-13	AL-3 Isometric view.	87

LIST OF FIGURES
(Continued)

Figure	Page
5-14 AL-3 Plan view.	87
5-15 AL-3 End view.	88
5-16 Constructed pile layouts.	90
5-17 Initial pile layouts for AL-3.	91
5-18 Initial pile layouts for optimization.	96
5-19 Weight convergence of AL-3.	97
5-20 Optimized pile layouts for AL-3.	99
5-21 Final pile layouts for AL-3.	101
5-22 Rigid slab optimization.	106
9-1 Numbering of elemental nodes.	129

OPTIMIZATION OF STEEL PILES UNDER CONCRETE SLAB FOUNDATIONS

1. INTRODUCTION

The objective of the research is to develop an automated design process for pile layouts under concrete slab foundations. The design process involves an iterative optimization method to produce designs which have potentially lower costs. The design procedures were developed for the US Army Corp of Engineers for application on large scale projects.

The first application of the method is for reducing the cost of lock monoliths. The cost lock and dam project can easily exceed one billion dollars. Therefore, reducing the construction costs is a primary motivation for the work. Structural optimization has been successfully applied to reduce costs of buildings and other structures (1,2,3).

A secondary motivation for the work is in producing an automated design process. It is desirable to limit the number of repetitive design calculations that engineers must perform. Automated design processes free the engineer to focus their efforts on the major decision making processes.

Automated designing reduces the costs of projects by reducing engineering hours required to create designs.

A computer program OPTPILE was written for pile optimization (4,5). The eventual goal of this research is to produce a design program that requires input of only the soil properties, the slab foundation shape requirement, and the loading conditions. The pile sizes and layouts and the pile alignments are the varied properties. Eventually the structural slab shape could be found by the optimization program. Within the scope of this work the foundation dimensions are not variable.

Optimization requires repetitive analyses of the design. Analysis and optimization programs are combined to produce a design program. Two methods of pile slab analysis can be used. The methods assume that either the concrete slab is thick and rigid or that it is thin and flexible. The US Army Corp of Engineers uses a computer program CPGA (6) for rigid slab analysis and STRUDL for finite element flexible slab analysis. The program STRUDL is not easily compiled with other programs, so a new finite element program FEMPILE was written to analyze flexible slabs.

The finite element program assembles the piles at any point as point springs. The piles do not have to be assembled to the structure at the nodes. The assembly method allows a more coarsely graded finite element mesh to

be used. This greatly reduces the computation time required to perform stiffness analyses and sensitivity analyses.

1.1 THE OPTIMIZATION METHOD

Optimization techniques have come under greater use as the demand has grown for least cost structures. Two categories of optimization methods exist: analytic and numerical methods. Analytic methods can lead to the exact optimal solution, but these methods require all of the optimization parameters to be expressed explicitly in terms of the optimization variables. Numerical methods are used for structural optimization problems. They are used because the problem does not need to be explicitly expressed. Numerical methods usually involve iterative processes which alter an initial design towards an optimal design.

Several numerical optimization methods exist. Each optimization method has advantages and disadvantages. The optimization method must be selected after considering the characteristics of the problem to be solved.

An Optimality Criteria method in the manner of Cheng and Truman (3) was chosen as the optimization method to be used. The Optimality Criteria Method converges quickly, and it controls the design limits or constraints very accurately. Several other methods could have been used but they have deficiencies in application to structural optimization problems. Further discussion of the selection of the optimization method is contained in Section 3.0.

The optimality criteria approach is developed from the nature of an optimal design point. Gellatly and Berke (7) and Venkayya (1) originally presented the optimality criteria method based on a strain energy criterion. The method was developed to solve optimization problems with a large number of variables. The method quickly arrives at an optimal design while using a relatively small amount of computational effort.

1.2 ACHIEVEMENTS

The optimality criteria method is applied to the optimization of pile structures. Truman and Hoback (8) have previously optimized rigid slab structures with steel piles. The current work has applied the optimization to flexible slab in addition to rigid slabs. Several advances have been made in order to allow adaption of the optimality criteria method to pile analysis.

An Optimality Criteria program was written because a program was not commercially available. Having an in-house developed program allowed the Optimality Criteria procedure to be adapted specifically for the problems to be solved.

The Optimality Criteria Method has not been previously applied to topological variables. A new optimality criteria was created to optimize topological variables. Hoback and Truman (9) showed where the topological variable coordinate systems must be placed for maximum computational efficiency.

Several advances have been made with the optimality

criteria formulation and the general optimization procedures. The Percent method is a new optimization method which has been developed to optimize discrete problems. Previously all combinations of the discrete options must be searched through to find the global optimum. The Percent method is much more efficient than search processes.

Another advance includes a novel method of pile deletion by pile group optimization. Eliminating piles from a design is a very effective method to reduce the weight of a design. Piles are eliminated in a new method in which the number of piles is a variable.

2. PILE FOUNDATIONS

A pile foundation consists of a concrete slab supported by piles. Retaining walls, locks, dams, and buildings use this type of foundation.

Various types of pile materials and installation methods are available. Only driven steel piles are used in the designs presented in this research. Steel piles are driven into the earth by striking the head of the pile with a battering hammer. The other common materials are driven wood piles and concrete piles which are either driven or cast-in-place.

2.1 PILE LAYOUTS AND CROSS-SECTIONS

Piles under slab structures are organized into groups. Grouping is also called linking. Each pile does not have an independent cross-section and orientation, but has the same cross-section and alignment as the other piles in the same group. This eases the installation of the piles.

The cross-sectional properties and the orientations of the piles are variables in the optimization. The depth of the pile tips is a constant. Bearing piles are driven to the point where they bear on strong strata. The depth of this strata is considered to be level across a construction site.

The alignment of a pile is measured using the pile coordinate system. The batter of a pile is the ratio of the depth of the pile to the horizontal distance between the

pile head and tip as shown in Figure 2-1(a). Phi (ϕ) is the angle of rotation of the pile about the vertical axis from the global x-axis as shown in Figure 2-1(b). Theta (θ) measures the pile flange alignment as shown in Figure 2-1(c). Major axis bending is in the direction of the local x-axis when theta is equal to zero degrees. Typical construction procedures generally do not allow θ to be any other value than 0 or 90 degrees.

Problems are treated as two-dimensional if they are symmetrical and have the loading contained within a plane. Problems without any expected symmetry are treated as three-dimensional. All of the pile orientation parameters are variables in the three-dimensional examples. The pile cross-section properties are also variable. The angle ϕ is not variable in two-dimensional problems such as a retaining wall.

Variables in the optimization process can be changed either discretely or continuously. In a continuous process the variables may acquire any value within the design space. In a discrete process the variables are allowed to acquire only values contained within a specified set of values. An example of a discrete variable is θ which may only hold two values of 0 and 90 degrees.

The cross-sections are discrete variables, but member cross-sections have been commonly modeled as continuous. (3) The cross-sections are not be restricted to discrete sizes

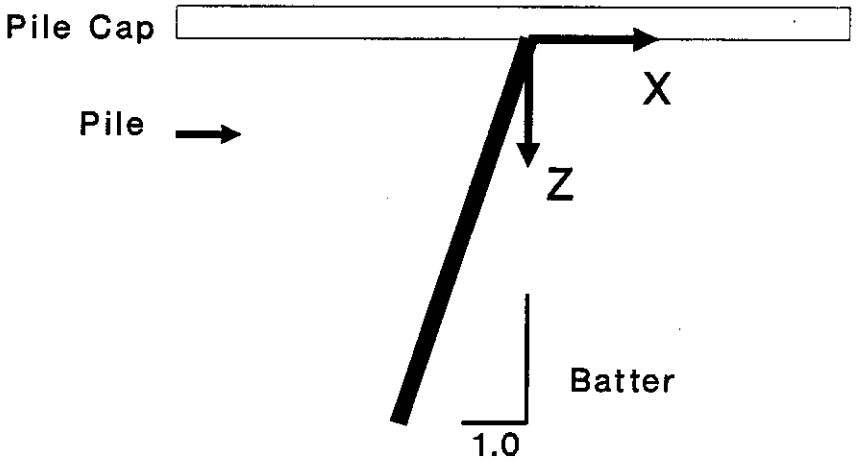

(a)

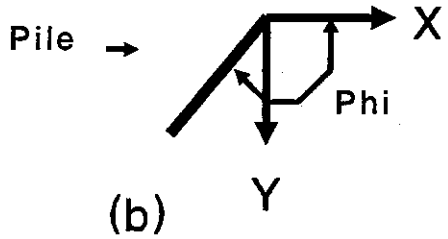

(b)

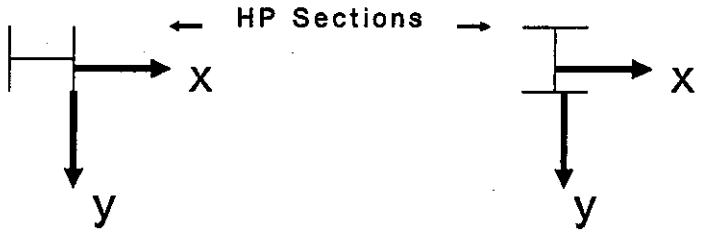

Theta = 0. degrees Theta = 90. degrees

Lower case x and y are the local axes

(c)

Figure 2-1. Pile coordinate system.
(a): Batter, (b): Phi, (c): Theta.

in the first stage of the optimization procedure. A pile is allowed to have an inertia of 800.23 in^4 even though such a size may not be available from a fabricator. A Branch and Bound procedure is used in the second optimization stage to find an available cross-section. This causes the inertias to become discrete.

It is required that one variable should entirely represent the cross-section in the optimization process. All the cross-sectional properties are expressed in terms of one primary variable which is the major axis moment of inertia (I_{xx}). The secondary variables are the minor axis moment of inertia (I_{yy}), the area (A), and the extreme fiber distances (c_x, c_y). The values of the variables are found using the following equations. The continuous set of equations describe HP-14 steel sections by using linear and power law regression. The equations are approximations developed from the AISC Manual for HP-14 sections (10). See Figures 2-2 to 2-5.

$$I_{yy} = 0.37067 I_{xx} - 9.2200 \ (inches^4) \qquad (2.1)$$

$$A = 0.049153 I_{xx}^{0.92180} \ (inches^2) \qquad (2.2)$$

$$c_x = 1.2110 * 10^{-3} I_{xx} + 12.7192 \ (inches) \qquad (2.3)$$

$$c_y = 6.110 * 10^{-4} I_{xx} + 14.139 \ (inches) \qquad (2.4)$$

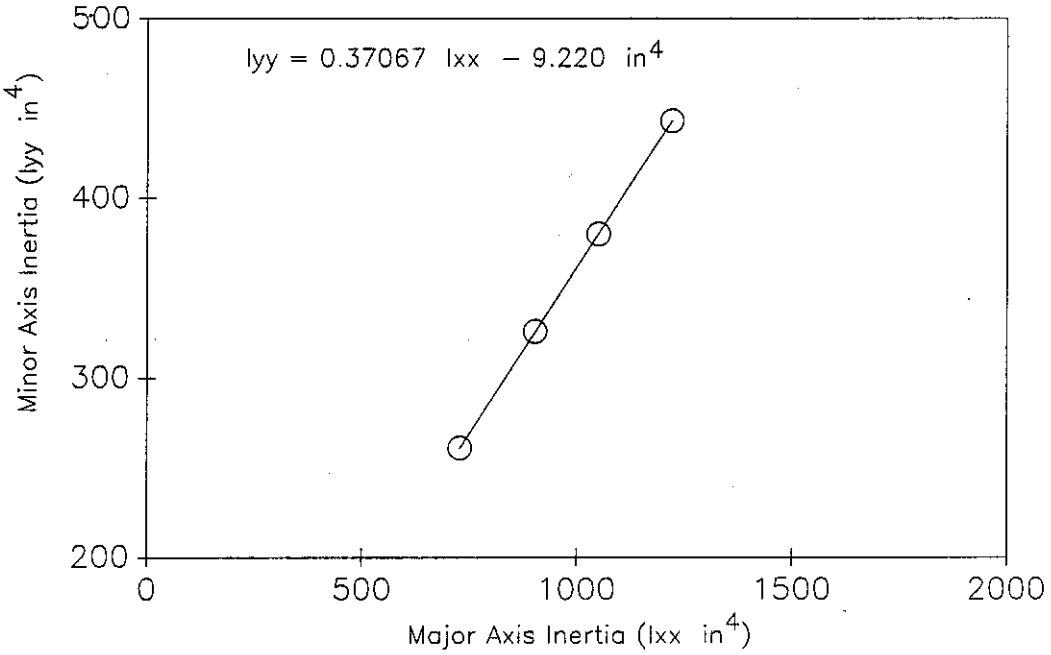

Figure 2-2. Area vs. Major Axis Inertia.

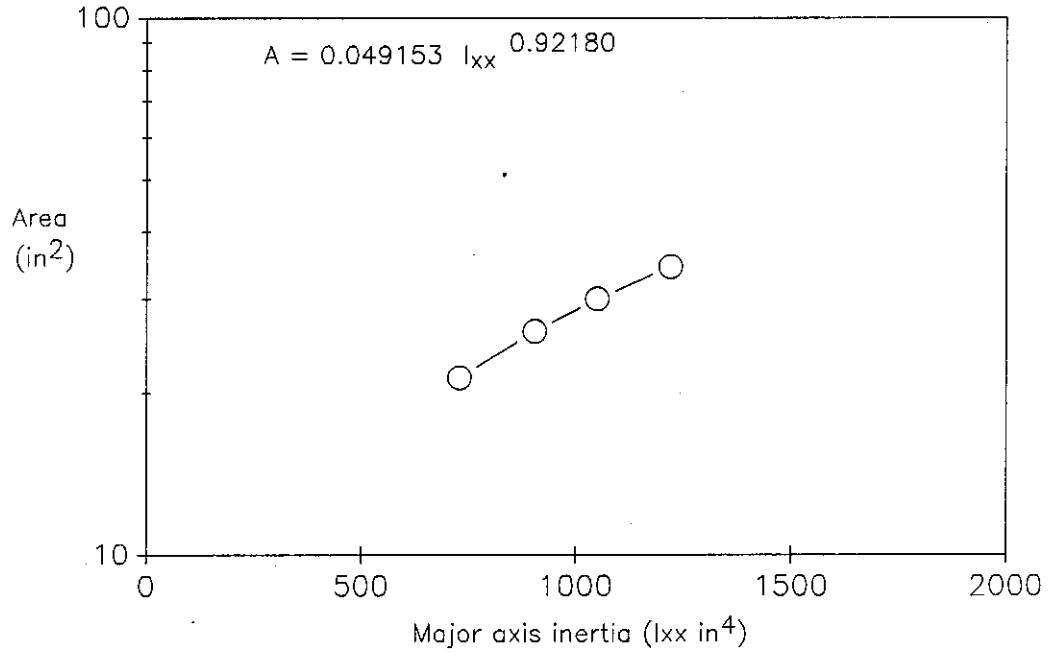

Figure 2-3. Minor Axis Moment of Inertia vs. Major Axis Ineria.

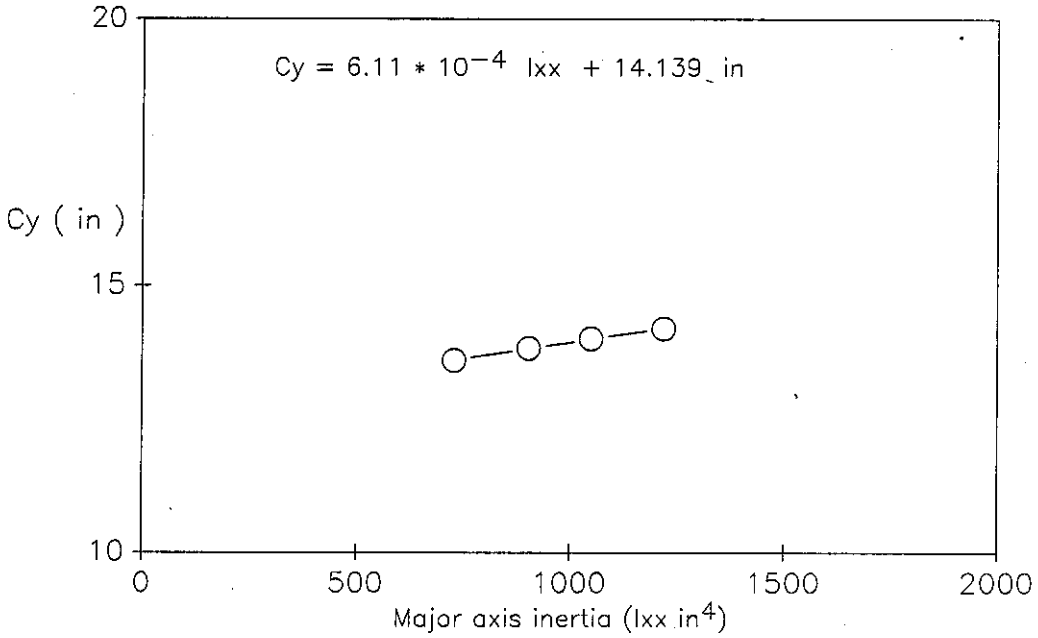

Figure 2-4. Extreme fiber distance in y-direction vs. major axis inertia.

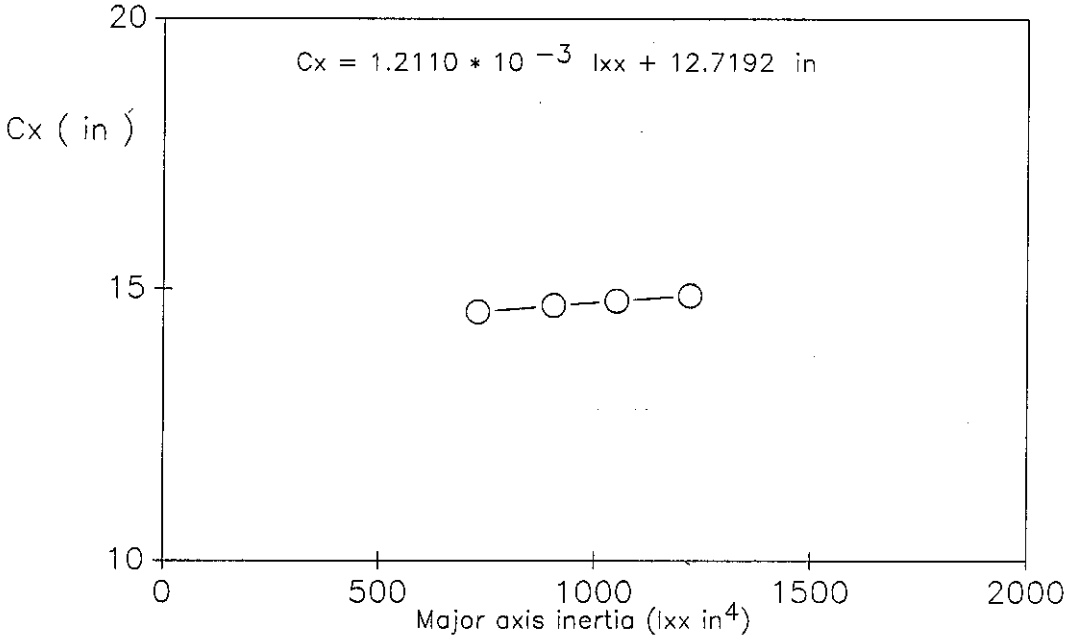

Figure 2-5. Extreme fiber distance in x-direction vs. Major axis inertia.

The reasons that these equations are required is so that temporary cross-sections can be created. During the optimization a pile may have a pile inertia was 800.23 in^4. This cross-section is not a commonly fabricated size. The optimization computes the area and other secondary variables by using the equations since the values are not available from the design code charts.

2.2 PILE STRUCTURE DESIGN VARIABLES AND LIMITS

The pile properties are varied to produce an optimal design. The properties that are variable are: the batter, the sizes, the angles phi and theta, the fixity, and the number of piles, and the positions of the pile groups.

Pile structures are subject to a variety of limits on the designs. The limits are handled in the optimization through use of constraints. Some of the constraints on pile foundations are:

1. Pile stress constraints. The piles are prevented from becoming over-stressed.

2. Soil constraints. The axial force in a bearing pile must not exceed the strength of the bearing strata.

3. Displacement constraints. Lock and dam structures consist of concrete monoliths which come into contact at joints. The displacements of the structures at the joints must be limited to prevent clearance problems.

4. Size constraints. The pile cross-sections are

prevented from advancing beyond the maximum or minimum section sizes available.

5. Minimum batter constraints. The piles may not be battered with a slope beyond a specified angle. It becomes more difficult to install piles as their batters become less vertical.

6. Interference constraints. Piles can not pass through one another.

7. Border constraints. The borders of the pile groups may move. Only one group may occupy a space.

8. Edge constraints. The pile groups must stay within the edges of the slab.

9. Obstructions. The monoliths are usually abutted by other monoliths. The pile tips may not extend under other structures.

10. Sheet pile obstructions. Lock monoliths can have sheet piles around the edges of the lock to lessen seepage. The piles must not intersect the sheet piles but may pass under them.

11. Slab stress constraints. The stress in the concrete slab is prevented from exceeding the maximum allowable value. This is currently not restricted. The slabs can have seemingly unlimited moment capacity by including rebar.

12. Internal constraints. Internal constraints can not be user specified. These constraints control aspects of the

optimization such as the branch and bound procedure and move limits.

The constraints are formulated so that when the constraint h_j is negative, zero, or positive, then constraint j is satisfied, active, or violated, respectively. An active constraint is a constraint which is exactly satisfied.

The constraints generally place an upper or lower bound on the value of a parameter such as stress. An example of a stress constraint is:

$$h_j = \sigma_j - \overline{\sigma}_j \leq 0 \qquad j=1,\ldots,m_1 \tag{2.5}$$

where h_j is the value of the constraint j, σ_j is the stress, $\overline{\sigma}_j$ is the upper bound of the stress in element j, and m_1 is the number of stress constraints. To improve the numerical conditioning of the constraints, Equation 2.5 can be rewritten as:

$$h_j = \frac{\sigma_j}{\overline{\sigma}_j} - 1 \leq 0 \qquad j=1,\ldots,m_1 \tag{2.6}$$

A constraint on the lower bound of a parameter such as member size can be written as:

$$h_j = \frac{-I_{xxj}}{\underline{I}_{xxj}} + 1 \leq 0 \qquad j=1,\ldots,m_2 \tag{2.7}$$

where $\underline{I}_{xxj}$ is the lower bound of the moment of inertia I_{xxj}

for member j, and m_2 is the number of lower limit size constraints.

2.3 PILE FOUNDATION ANALYSIS

The analysis of pile structures is performed with a rigid slab method or flexible slab analysis method. These methods can be used to calculate the forces in the piles. The stiffness of the piles can be expressed at the pile head. This allows the individual pile stiffness to be assembled to the pile slab. The allowable stresses in the piles are found in accordance with the US Army Corps of Engineers document: BASIC PILE GROUP BEHAVIOR (11).

The rigid slab pile system can be analyzed with a preexisting computer program (CPGA) from US Army Corps of Engineers. (6) This method assumes that the foundation is comparatively thick and inflexible. The displacements are found by solving a six degree of freedom system. See Appendix 1 for further details on the analysis of rigid slab foundations.

Some foundation systems have comparatively thin and flexible slabs which can not be accurately modeled as rigid slabs. The flexible slab analysis method consists of representing the concrete slab as a plate element with the appropriate thickness. A finite element program has been created with parabolic isoparametric elements. A Mindlin plate bending element and a plane stress element have been

combined to provide the slab element. The current element shape functions are two-dimensional quadratic after Hinton and Owen. (12) See Appendix 2 for further details about the basic finite element method.

2.3.1 PILE ASSEMBLY

The piles are assembled to the finite element mesh using one of four pile assembly methods. All of the methods assemble the piles to the nodes of the finite element mesh. The first method which is called the nodal method states that the piles must be placed at the nodes. The piles are directly assembled with the nodes. The remaining three methods allow the piles to be offset from the nodes. The second method of assembly is the rigid offset method. The piles are offset from the nodes and rigidly connected to a nearby node by a rigid arm. The third method is a virtual work method. Virtual work is used to form equations for the assembly of the piles. This method uses squared nodal shape function terms. The fourth method is the effective pile assembly method. Effective piles are assembled at the nodes using the shape functions.

The nodal assembly method is inefficient. Given the pile positions the finite element nodes must be placed over every pile. For a large number of piles or irregular patterned piles the mesh can be be excessively refined or misshaped. A typical pile analysis problem can have 800 or more piles and 4000 or more degrees of freedom. Slab

foundations are thick concrete and generally deform in single curvature. Quite often a highly graded finite element mesh is not required to represent slab deflections. A coarse mesh with fewer degrees of freedom is used by the other three assembly methods.

The rigid offset assembly method can be performed by STRUDL (13) and OPTPILE (4). The nodes are no longer restricted to be located at the piles, therefore the piles can be located within an element. The piles are connected to a nearby node by using a rigid connection. The stiffness equations for this are similar to the rigid body analysis equations. The rigid body analysis rigidly connects all of the piles to one common point. The rigid offset uses the same matrices to connect the pile to a node.

The third pile assembly method is the virtual work method. The virtual work method assembles the piles to the nodes using the square of the shape functions. The virtual work method is performed by applying a force **P**. The resulting forces are $\mathbf{K}_{slab}\,\mathbf{D}$ and $\mathbf{K}_p\,\mathbf{d}$, which are the slab and pile forces, respectively. **D** is the global displacement. The displacement at the pile is **d**. The applied virtual displacement is: $\mathbf{D}^*$. The virtual displacement at the pile is: $\mathbf{d}^*$. The equation equating the external and internal work is:

$$D^{*T}P = D^{*T}K_{slab}D + d^{*T}K_p d \qquad (2.8)$$

Substituting the shape functions for the displacements and eliminating the virtual displacements results in:

$$P = [K_{slab} + N^T K_p N] D \qquad (2.9)$$

where **N** is the shape function matrix evaluated at the pile position. The pile stiffness is assembled by pre and post multiplying the pile stiffness by the shape functions.

The fourth method is the effective pile assembly method. The piles are assembled using the shape functions. The shape functions are not squared as in the virtual work method. The piles are assembled by creating effective piles. The effective piles are placed at the nodes of the element containing the pile. These effective piles have the stiffness of the original pile stiffness multiplied by the nodal shape function evaluated at the pile:

$$[K_I^1] = ([K_I^0] + N_I [K_p]) \qquad (2.10)$$

where K_I^1 is the new stiffness of node I, and N_I is the shape function of node I. The sum of the shape functions is 1.0 therefore no stiffness is lost.

The preferred pile assembly method is the effective pile method. This method is accurate for concrete slab--steel pile examples. The nodal method requires too fine of a mesh which dramatically increases the CPU time required for analysis. The rigid offset method is acceptable for a fine mesh spacing of 5 feet or lesser. The error in the

rigid connection is small when the elements are small. This is not preferred because a fine mesh has a larger CPU time. The virtual work method is not preferred because it is inaccurate with fixed piles. The moments in the fixed piles are poorly estimated with the virtual work method.

The effective pile method is accurate for concrete slabs 10 feet thick or greater which have a finite element mesh spacing of 20 feet or closer. It usually has an accuracy of within 2%. A finer mesh could be used for a more accurate analysis. The pile forces converge as the mesh tightens. The optimization may perform 300 analyses. The time required for the optimization is limited by using a coarse mesh. If a 2% inaccuracy is unacceptable then the final design may be checked with a finer mesh.

The pile assembly method uses the assumption that the differential displacements across the finite elements are small compared to the total displacement of the piles. The nodal shape functions are used to describe the displacements throughout the concrete elements. If the shape functions were linear then the displacements must be linear through the element. This is not true when piles are assembled on the element. Figure 2-6(a) shows a simple pile structure. Four piles are located at the midpoints of four elements. Figure 2-6(b) is one of the elements with the appropriate springs applied. Spring K_1 represents the stiffness of the

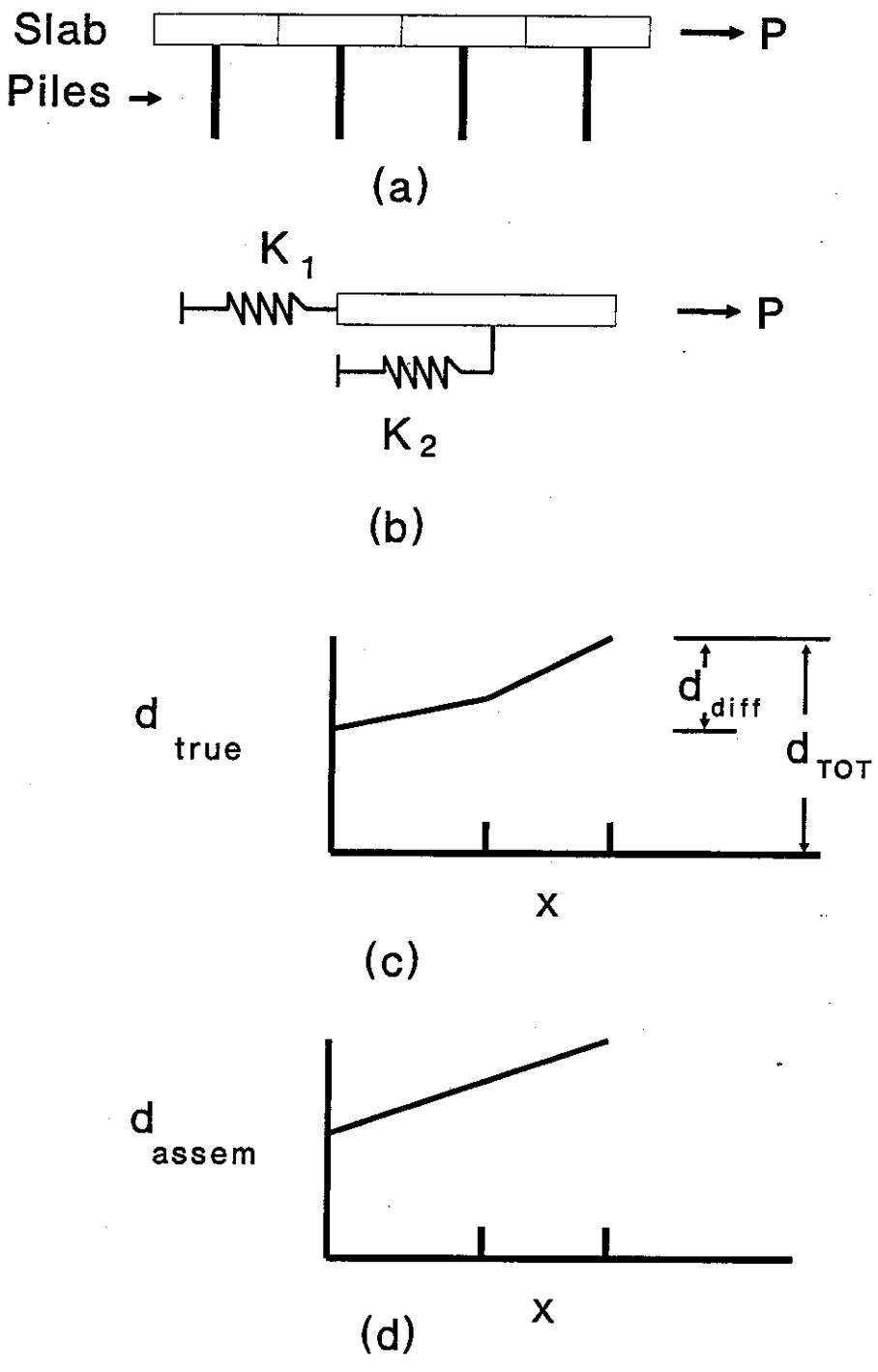

Figure 2-6. Pile assembly theory.

neighboring elements, and K_2 represents the pile stiffness. Figure 2-6(c) shows the true displacements of the slab. The displacements are bilinear about the pile. Figure 2-6(d) shows the assumed linear variation in displacements. The assumption realizes that the bilinear effect is negligible when the differential displacements d_{diff} are smaller than the total displacements d_{tot}. This is true for pile-slab analyses.

The results of using larger elements is that the degrees of freedom are reduced and CPU savings are achieved. It is also much easier to input the required data. The efficiency of the pile assembly method in OPTPILE (4) was compared to the computer program STRUDL (13). A lock example was analyzed using a range of mesh spacings. The OPTPILE lock was analyzed with square elements using mesh spacings from 40 ft (coarse mesh) to 10 ft (fine mesh). STRUDL used only a mesh size of 5 ft because the piles were spaced at 5 ft. An OPTPILE mesh 20 ft or finer was required to accurately model the slab. The CPU time given this spacing was one ninth the STRUDL CPU time. The lock had a slab thickness of only 5 ft. Lock slabs are usually much thicker than 5 ft therefore d_{diff} would be lower. A coarser mesh may be used for thicker slabs.

The three methods of pile assembly are compared. Three pile layouts shown in Figure 2-7 were analyzed. The layouts

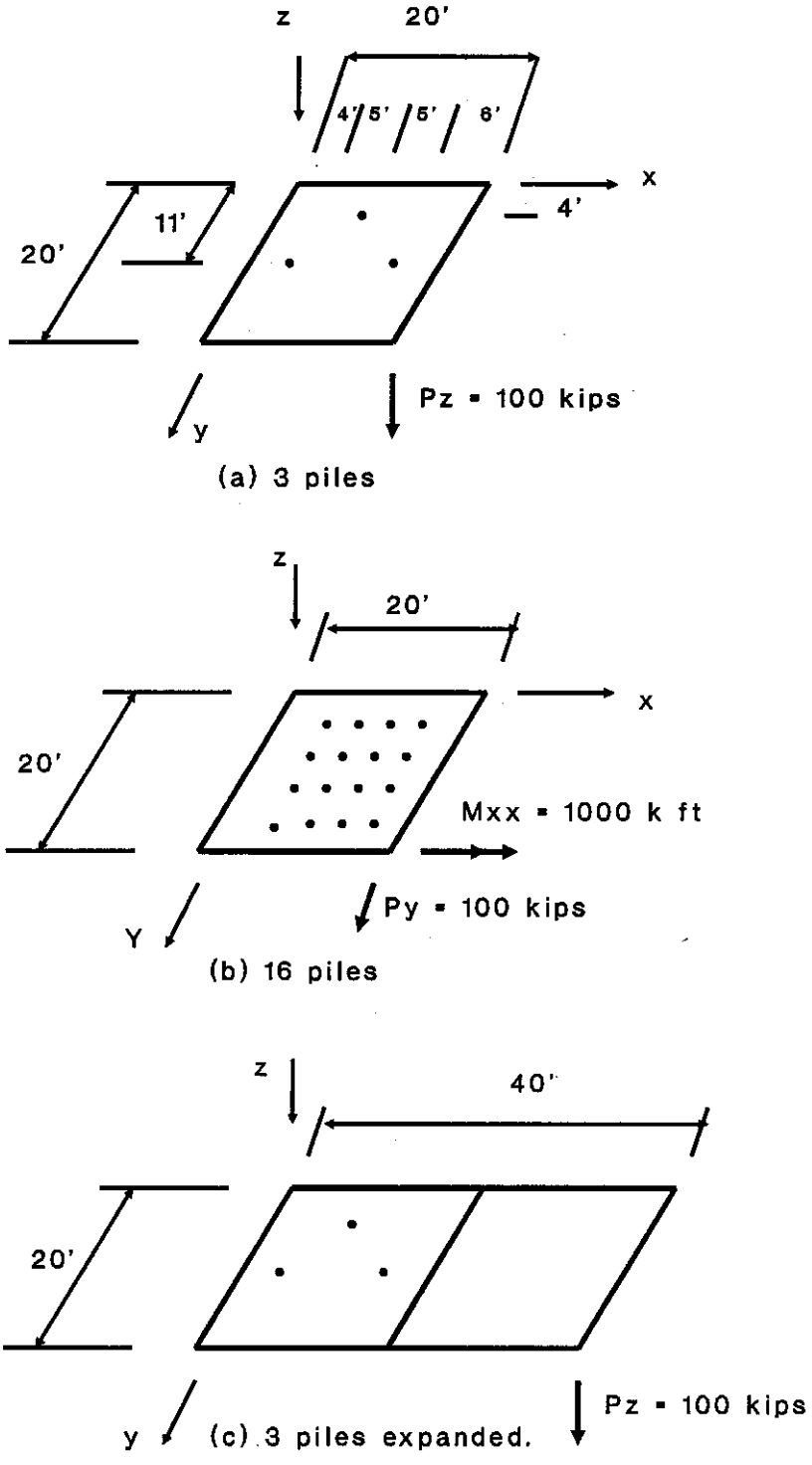

Figure 2-7. Study of pile assembly.

were analyzed first with an exact analysis. A finite element mesh was placed so that each pile could be assembled to a node. None of the elemental pile assembly methods are accurate under every condition. The assembly methods are effected by the thickness of the concrete slab and the spacing of the finite elements. It has been noted that as the mesh spacing decreases the assembly methods approach the exact results.

A study was performed to find the required mesh spacing for accurate analysis of pile structures. The examples were analyzed with the various pile assembly methods. The finite element mesh was refined until the pile forces were within 3% of the exact results. The original sized mesh was a one by one element grid which had 20 ft spacings. Next was a two by two grid with 10 ft spacings. This continues until a five by five grid is formed which has 4 ft spacings. The 16 pile example has piles spaced at 4 ft. This element spacing produced exact spacing of the piles. All the assembly methods with this spacing converged to the exact results. The maximum spacing for the methods is shown in Table 2-1. The examples were varied to produce the worst possible results. The variations consisted of: fixing and pinning piles, battering the piles at a slope or vertically, and orientating the angle phi at 0 and 40 degrees.

Table 2-1. Maximum element sizes (ft).

Thick-ness (ft.)	NK or effective piles		NKN or virtual work		Rigid Arm	
	3 piles	16 piles	3 piles	16 piles	3 piles	16 piles
5	10	10	10	4	10	4
10	10	10	10	5	10	4
15	10	10	10	5	10	4
20	10	10	10	5	10	4

Observations:

1. It was noticed that "NK" or effective pile method was exactly accurate with 10 ft spacings, but inaccurate with 20 ft spacings. The piles were moved away from the load by using the example 3A. The point load is moved away from the piles by using an extra element. The effective load on the original element was smoothed. The results are that the "NK" method was accurate with a 20 ft mesh. This demonstrates the sensitivity of the pile structure analysis to point loads. A lock structure with uniform loads is more accurately modeled with the assembly methods compared to point loads.

2. The rigid arm method is similar to one of the US Army Corps of Engineers STRUDL analysis methods. The rigid method has questionable accuracy compared to the "NK" method.

3. The assembly methods have an odd convergence. Some

pile forces may approach the exact values then diverge, and reconverge again. The examples as a whole had steady convergence to the exact values with mesh refinement. Some forces oscillated but the envelope of the oscillation converged to the exact value.

4. Although the "NK" method was more accurate the "NKN" method had frequently similar results. For example: the "NK" and "NKN" method frequently had similar lateral and vertical forces. The moments in the fixed piles were significantly different except at convergence. The lateral forces and moments are coupled in the fixed piles. This was not assembled accurately by the "NKN" method. If these moments were excluded (pinned piles) then the method converged equally.

5. These same observations were noted in all examples shown and not shown, and in their variations.

AL-3 Lock Example:

A final design for the lock was produced by analyzing it with the "NK" or effective piles method. This final design was analyzed with the "NK" and "NKN" methods. The original mesh spacing was analyzed. This spacing had average element sizes of 20 by 20 ft. This mesh spacing was halved and the lock was reanalyzed so that the convergence of the methods could be judged. The observations are:

6. The "NK" method pile forces change by an average of 2%

during refinement. Therefore the analysis has converged. Both refinements show that zero piles are overstressed.

7. The "NKN" method significantly changes during refinement. The average change is about 8 or 10%. The axial forces are adequately modeled with the "NKN" method but the fixed pile moments change dramatically in refinement. These moments differ greatly from the "NK" method. This agrees with the observation 4. Both "NKN" refinements had an average of 400 failures.

8. The "NKN" forces are generally converging toward the "NK" values. Observation 3 noted that not all forces must converge in every refinement. The forces may oscillate. Therefore "NKN" could be converging to the "NK" analysis.

9. The mesh spacings were initially about 20 ft and then refined to 10 ft. The mesh spacings and slab thicknesses are near the acceptable regions found is the study of spacings.

10. The "NKN" or virtual load assembly method was applied to the lock example optimization. The result is that a significantly higher weight design was produced. This is because the "NKN" method considered a number of piles to be initially overstressed.

The conclusion of this pile assembly study is that the "NK" or effective pile assembly method accurately analyzes piles in lock slab examples. The current mesh spacings are acceptable for optimization. The computer time for a finer

mesh analysis would prohibit optimization. A finer mesh may be used for a final analysis if so desired.

3. OPTIMIZATION FORMULATION

A numerical optimization method is used. Several numerical optimization methods exist. Each optimization method has advantages and disadvantages. The optimization method must be selected after considering the characteristics of the problem to be solved.

An Optimality Criteria method in the manner of Cheng and Truman (3) was chosen as the optimization method to be used. The Optimality Criteria Method converges, quickly, and it very accurately controls the design constraints and limits. Several other methods could have been used but they have deficiencies in application to structural optimization problems.

The Fully Stressed Design Method is a structural design method. This method causes the member stresses to become fully stressed in the final design by proportioning the member sizes by their stress levels. The assumption of the Fully Stressed Design Method is that at the optimum all members are fully stressed. This would be a false assumption for the pile optimization method. Other constraints such as minimum member sizes may control the design. This method can not be used because of its lack of adaptability.

A second method used for structural optimization is Sequential Linear Programming. The primary disadvantage of Linear Programming is that it is slow to reach an optimal

design. This inefficiency causes an increase in the computations required to solve the problems.

Penalty Function methods can be applied to structural optimization. The Internal Penalty Function Method is not useable because it requires that an initial feasible design be used to start the optimization. It is difficult to use this method for large problems since an existing feasible design is not always known. The External Penalty Function Method has a disadvantage that all of the designs are slightly to greatly infeasible. Slight violations of design codes may be acceptable, but it is not an advisable design policy. The External Penalty Function Method is not easily adapted because the process must not be stopped before convergence. The infeasibility is minimized when the process converges.

Previous work has been performed in the area of pile optimization. A program was developed in 1981 by Hill which attempts to optimize the layouts of piles (14). This method was applied to the optimization of only rigid slab foundations. A pile deletion process was used to reduce the weight of steel. The optimization procedure consisted of first finding the optimal pile slopes, then finding the optimal pile spacing within specified zones, and deleting piles until the stresses and displacements were near their limits. The piles were deleted in an iterative process by eliminating the most and/or the least stressed piles.

The Hill method is a trial and error type of optimization. The present research uses an optimization method which is more adaptable and numerically based. All of the design properties are allowed to simultaneously change as a search is made for the lowest cost design. Reducing the number of restrictions on an optimization can greatly improve the performance. The Hill method is highly restricted because only the number of piles is variable in the final stage.

The optimality criteria converges very quickly and all of the constraints are precisely controlled. Therefore, the optimality criteria method is used.

3.1 OPTIMALITY CRITERIA FORMULATION

The optimality criteria approach is developed from the nature of an optimal design point. Gellatly and Berke (7) and Venkayya (1) presented the optimality criteria method based on a strain energy criterion. A minimum weight objective criterion is used here instead of minimization of strain energy.

The objective function of the optimization process is the function to be minimized. The goal of the pile optimization process is to find the minimum weight of steel that can be used to satisfy the given constraints. The

objective function is:

$$W_T = \sum_{i=1}^{N} \rho_i V_i \qquad (3.1)$$

where W_T is the total weight, ρ_i is the density, and V_i is the volume for the structural element i, and N is the number of piles.

The KUHN-TUCKER conditions are necessary conditions for a point in design space to be a local minimum of the given problem. If the design space is convex then the satisfaction of the KUHN-TUCKER conditions is sufficient for a design to be the global optimum. Since the pile orientation optimization problem is non-convex the conditions can only guarantee that a local optimum has been achieved. Forming the KUHN-TUCKER conditions requires the Lagrangian which is:

$$L = W_T + \sum_{j=1}^{m} \lambda_j h_j \qquad (3.2)$$

where λ_j is the Lagrange Multiplier for the constraint h_j, and m is the total number of constraints.

The first necessary condition for a local minimum dictates that a further improvement in the weight is prevented by constraints. See Figure 3-1. Constraints are active when $h_j=0$, and passive if $h_j<0$. The constraints which are active at the optimum design point form a vector

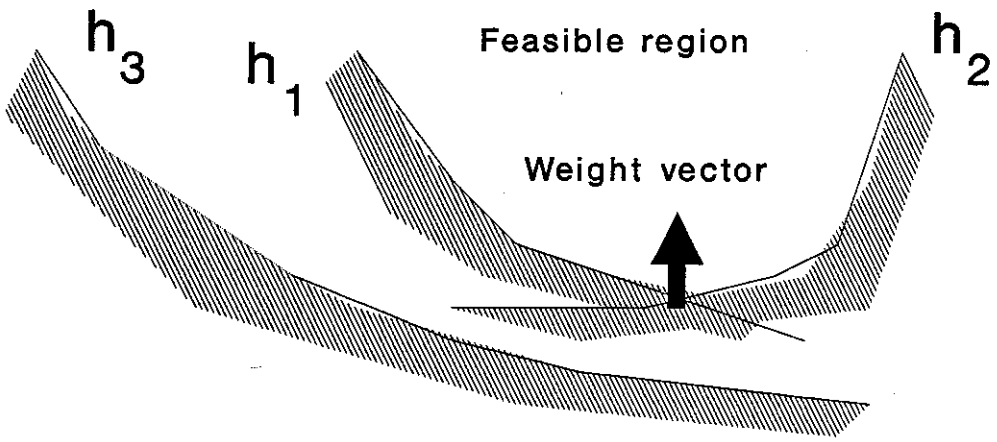

(a)

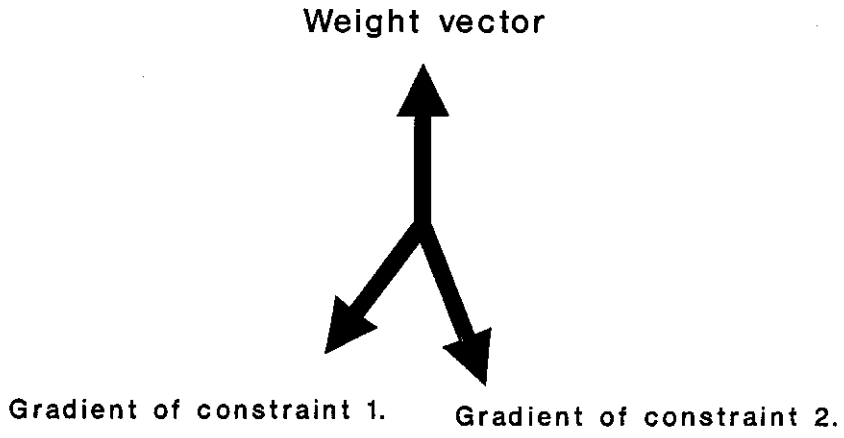

(b)

Figure 3-1. Gradient Vectors.
(a): Constrained space, (b): Gradients.

opposing the weight gradient. In Figure 3-1 constraints 1 and 2 are active. A vector addition of weight and constraint gradients is performed. A scaling variable is required to account for the units of the gradients. The scaling is performed by the Lagrange Multiplier. The formula for the vector addition of the gradients is the same as the derivative of the Lagrangian with respect to the design variables which can be written as:

$$\frac{\partial W_T}{\partial d_i} + \sum_{j=1}^{m} \lambda_j \frac{\partial h_j}{\partial d_i} = 0 \qquad i=1,\ldots,n \tag{3.3}$$

where there are n design variables d_i. This is the first necessary condition. Note that λ_j does not vary at the optimum.

The other necessary conditions are found by looking at active and passive constraints. A constraint gradient is used in the vector sum to oppose improvements in weight only when the constraint is active. This requires that λ_j is zero when h_j is not zero, and h_j is zero when λ_j is not equal zero.

$$\lambda_j h_j = 0 \qquad j=1,\ldots,m \tag{3.4}$$

The final conditions dictate that the Lagrange Multipliers must be positive and the constraint must not be violated.

$$\lambda_j \geq 0 \qquad j=1,\ldots,m \tag{3.5}$$

$$h_j \leq 0 \qquad j=1,\ldots,m \tag{3.6}$$

Selecting the correct set of constraints as active is the most complicated portion of the optimization process. Equation 3.3 is rewritten to provide the optimality criteria:

$$-\left(\sum_{j=1}^{m} \lambda_j \frac{\partial h_j}{\partial d_i}\right) \Big/ \frac{\partial W_T}{\partial d_i} = 1 \qquad i=1,\ldots,n \tag{3.7}$$

This criteria must be satisfied for the n variables.

Linear recurrence equations based on the power law are used to update the design variables as the design progresses toward a more optimal design. The optimality criteria for the i^{th} variable is used as the efficiency of the variable. The i^{th} variable (d_i) is altered by the value of the i^{th} optimality criteria in the following recurrence formula:

$$d_i^{v+1} = d_i^v \left(-\left(\sum_{j=1}^{m} \lambda_j \frac{\partial h_j}{\partial d_i}\right) \Big/ \frac{\partial W_T}{\partial d_i}\right)^{\frac{1}{r}} \qquad i=1,\ldots,n \tag{3.8}$$

where v is the index of the iteration number and r is the convergence control parameter.

The optimality criteria is less than one when the component of the objective or weight gradient for the i^{th} variable is greater than the resistance provided. When the weight gradient is positive, the variable is free to decrease by an amount roughly proportional to the value of the optimality criteria. If the resistance is stronger than

the weight gradient then the optimality criteria is greater than one and the variable should be increased. Taking the r^{th} root of the optimality criteria where r>1 assures that the prediction of d_i for the next iteration does not greatly overshoot the optimum value. A reasonable value for the convergence control parameter (r) is taken as 2.

Rewriting Equation 3.8:

$$d_i^{v+1} = d_i^v \left(1+\left(\left(-\left(\sum_{j=1}^{m} \lambda_j \frac{\partial h_j}{\partial d_i}\right) \Big/ \frac{\partial W_T}{\partial d_i}\right)-1\right)\right)^{\frac{1}{r}} \qquad (3.9)$$

and expanding it using the binomial theorem results in a linear recurrence equation:

$$d_i^{v+1} = d_i^v \left(1+\frac{1}{r}\left(\left(-\left(\sum_{j=1}^{m} \lambda_j \frac{\partial h_j}{\partial d_i}\right) \Big/ \frac{\partial W_T}{\partial d_i}\right)-1\right)\right) \qquad (3.10)$$

The values of the Lagrange Multipliers to be used in the variable recurrence relation must be estimated. Estimation of the multipliers may be performed using either a recurrence relationship or by solving a set of linear equations.

A formula for the change in the active constraints is used to produce the linear equation solution method. The equation for the change in the j^{th} active constraint can be written as:

$$\Delta h_j = h_j^{v+1} - h_j^v = \sum_{i=1}^{n} \frac{\partial h_j}{\partial d_i} \Delta d_i \qquad j=1,\ldots,m \qquad (3.11)$$

where h_j^v is the value of the constraint j at iteration v. The expected value of h_j^{v+1} for the active constraints should be zero. The change in the design variables can be found using the variable recurrence equations. Substituting the variable change:

$$\Delta d_i^v = d_i^{v+1} - d_i^v \tag{3.12}$$

and Equation 3.10 into Equation 3.11 yields:

$$r\, h_j^v = \sum_{s=1}^{m} \lambda_s \sum_{i=1}^{n} \left(\frac{\partial h_j}{\partial d_i} \frac{\partial h_s}{\partial d_i} \Big/ \frac{\partial W_T}{\partial d_i} \right) d_i + \sum_{i=1}^{n} \frac{\partial h_j}{\partial d_i} d_i \qquad j = 1, \ldots, m \tag{3.13}$$

Passive variables are variables which are forced to maintain a certain value. A cross-section size can be held at the maximum or minimum value by making it passive. An additional term is required to account for the change in the constraints by the applied change in the passive variables.

$$r\, h_j^v = \sum_{s=1}^{m} \lambda_s \sum_{i=1}^{n_1} \left(\frac{\partial h_j}{\partial d_i} \frac{\partial h_s}{\partial d_i} \Big/ \frac{\partial W_T}{\partial d_i} \right) d_i + \sum_{i=1}^{n_1} \frac{\partial h_j}{\partial d_i} d_i + r \sum_{i=n_1+1}^{n} \frac{\partial h_j}{\partial d_i} \Delta d_i$$

$$j = 1, \ldots, m \tag{3.14}$$

where n_1 is the number of active variables.

The Lagrange Multipliers are found by solving the linear equations subject to the Kuhn-Tucker conditions (Equations 3.4-6). Equation 3.6 requires that the linear equations apply to only the constraints which are active or assumed to be active. This creates a nonlinear solution process. One method of solution involves a process of

making and updating assumptions about which constraint are active. Each assumption requires a solution of a set of linear equations which contains only the assumed active constraints. This process of making assumptions and updating the assumptions is not guaranteed to converge.

A Gauss-Seidel iteration method (Method of Successive Displacements) was used to solve for the λ_j values. This method is a relatively computationally efficient process. The iteration process requires about the same order of computations as the solution of one set of linear equations.

The Gauss-Seidel iteration method involves successively solving for individual λ_j values. Any λ_j can be solved for if all the other λ_j values are known. Equation 3.13 is equivalent to:

$$\lambda_j = \frac{r\,h_j^v - \sum_{s\neq j}\lambda_s \sum_{i=1}^{n}\left(\dfrac{\dfrac{\partial h_j}{\partial d_i}\dfrac{\partial h_s}{\partial d_i}}{\dfrac{\partial W_T}{\partial d_i}}\right) d_i \; - \sum_{i=1}^{n}\frac{\partial h_j}{\partial d_i} d_i}{\sum_{i=1}^{n}\dfrac{\left(\dfrac{\partial h_j}{\partial d_i}\right)^2}{\dfrac{\partial W_T}{\partial d_i}}\, d_i} \qquad j=1,\ldots,m \tag{3.15}$$

The procedure consists of initially setting the λ_j values to zero. The λ_j values are successively solved for until their values converge. Solving the j^{th} equation for λ_j insures that h_j is satisfied. During the successive solutions if a value of λ_j becomes negative then it is set equal to zero to satisfy Equation 3.5.

The convergence of the Gauss-Seidel procedure is measured by the change in the constraint values. The Lagrange Multipliers quickly change in value in the first iterations. This is because the constraint values have large residuals which indicate that they are highly violated. As the procedure converges the active constraint values are near zero and remain stabile around that point. The problem has converged when the normalized values are only 0.001 for the active constraints.

3.2 APPLICATION AND ADVANCES OF THE OPTIMIZATION METHOD

The optimality criteria method is applied to the optimization of pile structures. Several advances have been made in order to allow adaption of the optimality criteria method. Application of the optimality criteria to topological variables has not been previously developed. Topological variables require reformulation of the optimality criteria objective function, and the coordinate systems. This is shown in Sections 3.2.1 and 3.2.2.

Other advances include innovations in the general optimization methods. A method of pile elimination by pile group optimization has been created as shown in Sections 3.2.4 and 3.2.5.

Another difficulty in applying the optimization is searching for the global optimum. The Percent Selection method in Section 3.2.6 is capable of finding global and discrete optimums.

3.2.1 TOPOLOGICAL VARIABLES

Topological variables layout the positions of structural members. These variables have different characteristics than variables which measure cross-section sizes. A methodology for including topological variables in the optimality criteria process has been developed by Hoback and Truman (9).

The variables which represent the batter of the piles may be measured by using either the angles of rotation or the coordinates of the tip of the piles. Using the tip coordinates as the variables simplifies the pile tip interference constraints.

Each batter is given its own local coordinate system. In this report the distance between the local coordinate system and the current tip position is referred to as slack.

The choice of the origin of the coordinate system has an effect on the convergence of each variable. Consider this example: A variable which has nothing restricting it would decrease itself to zero. This is a passive variable because the lagrange multipliers are zero. If the convergence control parameter (r) is equal to two then the variable would halve itself. (See Equation 3.10.) The tip position of a pile is a topological variable. If the tip is located at a coordinate value of 40 meters and if the tip was not restricted by constraints then the tip would move 20

meters, however the pile behavior may be predictable for a change of only 10 meters.

The slack (coordinate axes position) should be chosen given the nature of the variable and its gradients. If the constraints vary linearly with the variables then the variables have well behaved gradients. This greater predictability would allow an increased slack.

Certain topological variables improve the objective function as their value increases. They have a negative weight gradient. An unrestricted variable with a negative weight gradient should increase. Given the unaltered algorithm all variables which are not actively controlled by a constraint would decrease towards the origin of the local coordinate system. When r is two they would halve themselves.

The variable recurrence formula appears to need reformulation. It was developed using the optimality criteria as a measure of the efficiency. See Equations 3.8 and 3.9. When the weight gradient is larger than the restraining components the variable is unrestricted; which is true for any weight gradient value. The negative coefficients of the negative weight gradient cause the resulting optimality criteria value to be greater than 1 instead of less than 1.

Two methods could be used to adapt the optimization method without altering the recurrence equations. The first

is to simply reverse the sense of the local coordinate system so that the weight gradients are always positive. The second method consists of applying negative slack while maintaining the sense of the coordinates. These methods allow uncontrolled variables to passively move in the correct directions.

3.2.2 VARIABLES WITH ZERO WEIGHT GRADIENTS

A new optimality criteria is presented which allows the optimization of topological variables that have zero weight gradients. Zero weight gradients are not permissible because the optimality criteria recurrence equations become unbounded. (See Equation 3.10)

Some topological variables have zero weight gradients. They are called weightless variables. For example, fixing or pinning a pile to the pile cap has no direct effect on the weight of the design. A second weightless variable is the rotation θ of a pile about the vertical axis. A third weightless variable is the pile batter when the pile is vertical. The first order gradient of the weight with a change in batter is zero for vertical piles.

The topological variables have indirect effects on the weight of the design. Changing a pile connectivity from pinned to fixed could allow the area to decrease which reduces the weight. The indirect effects upon the weight are not readily measurable.

A new optimality criteria has been created that properly models the behavior of topological variables. The weightless optimality criteria is used only for the weightless variables. The standard formulation in Section 3.1 is used for the other variables.

Recall that the standard optimality criteria was developed from the nature of the optimal point. The weight vector holds the design down upon a set of active constraints. The sum of the weight gradient and the constraint gradients is zero at the optimum.

The weightless optimality criteria is a function of only the constraint gradients. The sum of the constraint gradients is zero at the optimum point. This occurs when a variable is fully constrained. The weightless optimality criteria is written initially as:

$$\sum_{j=1}^{m} \frac{\partial h_j}{\partial d_i} \lambda_j = 0 \qquad (3.16)$$

where λ_j is the Lagrange multiplier which acts as the units conversion factor for constraint j. The optimality criteria is taken as the efficiency of the relevant variable. At the optimum the efficiency is one, therefore the weightless

optimality criteria is written as:

$$-\sum_{j=1}^{m} \frac{\partial h_j}{\partial d_i} \frac{\lambda_j}{w_i} + 1 = 1 \qquad (3.17)$$

where w_i is a scaling parameter.

The recurrence equations are developed following the procedures of Section 3.1. The recurrence relations for the variables are based on the power law. The variables are changed in each iteration by the efficiency:

$$d_i^1 = d_i^0 \left(-\sum_{j=1}^{m} \frac{\partial h_j}{\partial d_i} \frac{\lambda_j}{w_i} + 1 \right)^{\frac{1}{r}} \qquad (3.18)$$

which is expanded to:

$$d_i^1 = d_i^0 \left(1 + \frac{1}{r} \left(-\sum_{j=1}^{m} \frac{\partial h_j}{\partial d_i} \frac{\lambda_j}{w_i} \right) \right)$$

The change in the variable is:

$$\Delta d_i = \frac{1}{r} \left(-\sum_{j=1}^{m} \frac{\partial h_j}{\partial d_i} \frac{\lambda_j}{w_i} \right) \qquad (3.20)$$

The linear constraint equations are:

$$h_j^0 = -\sum_{i=1}^{n} \frac{\partial h_j}{\partial d_i} \Delta d_i \qquad (3.21)$$

or:

$$rh_j^0=\sum_{s=1}^{m}\lambda_s\sum_{i=1}^{n_2}\frac{\partial h_s}{\partial d_i}\frac{\partial h_j}{\partial d_i}\Big/\frac{\partial W_T}{\partial d_i}+\sum_{i=1}^{n_2}\frac{\partial h_j}{\partial d_i}d_i + \sum_{s=1}^{m}\lambda_s\sum_{i=n_2+1}^{n}\frac{\partial h_s}{\partial d_i}\frac{\partial h_j}{\partial d_i}\frac{d_i}{w_i} \qquad (3.22)$$

where n_2 is the number of variables with non-zero weight gradients, and $n-n_2$ is the number of weightless variables.

The parameter w_i is a scaling factor to prevent ill-conditioning of the optimization solution. The factor replaces the weight gradient in the optimality criteria. It may be thought of as a pseudo-weight gradient. The value of w_i is taken as a rough estimate of the indirect weight gradient. The indirect weight is discussed in the third paragraph of Section 3.2.2.

Another alteration in the optimality criteria has been made. Notice in Equation 3.19 that the change in the weightless variables is zero when the variables are unconstrained or passive. This greatly affects the passive behavior of the weightless variables. The variables would always decrease when they are passive in the previous standard method. The weight of the design decreases when the pile area passively decreases. However there is no motivation to increase or decrease a weightless variable such as the pile fixity if no constraints are actively applied to it. The passive behavior allows the variable to remain stationary when it has no purpose for changing.

3.2.3 MEMBER SELECTIONS

A branch and bound method has been used to select the optimal discrete cross-sections. Variables such as the cross-sections and the fixity are optimized as continuous variables. The branch and bound process causes the variables to move to available values. For example, a pile with an inertia of 800.23 in^4 is forced to one of the sections available from the fabricators.

The procedure begins by selecting a variable to be made discrete from the variables which are not discrete. The value of the variable lies between two discrete values: a value higher and one lower than the current value. Two branches are created each of which becomes an individual optimization subproblem. The upper branch places a lower limit on the variable at the higher discrete value. The lower branch places an upper limit on the variable at the lower discrete value. A bounding process is done after each branched subproblem is optimized. A branch is selected for further branching by taking the lowest weight feasible branch from all the branches created in the problem. This is continued until a discrete optimum is reached.

The branch and bound procedure significantly increases the computer time required to find the optimum. For example a rigid slab optimization may take only 2 minutes but with branching the optimization time may increase to 30 minutes

real time on a Sun station. A flexible optimization may be increased from 2 to 30 days with branching. One alternative to a branch and bound is to round as many variables as possible to useable values, then branch the remaining variables.

3.2.4 PILE ELIMINATION

It is expected that the greatest cost or weight savings in a pile optimization process will come from the elimination of unnecessary piles. Discrete optimization methods exist that could be adapted for eliminating piles. One method that has been developed is to remove member lower limits of the piles. If a pile is unnecessary then it can zero itself in size. The second phase of the process is to reapply the minimum pile sizes. The Branch and Bound procedure is used to move the piles to useable cross-section sizes.

One difficulty with this type of pile elimination is handling the group behavior of piles. Piles are usually grouped with other piles having the same sizes. This method of pile elimination would require all the piles in a group to zero. A single pile cannot independently zero itself.

This method can be applied for the elimination of single piles. Small structures may have only a few piles. These piles could be ungrouped and allowed to independently delete themselves. The pile elimination procedure is capable of only deleting preexisting piles. It is not

capable of adding piles to overstressed designs. This method is not practical for larger designs.

3.2.5 GROUP OPTIMIZATION

The Group Optimization or Stiffness Multiplier method is a new method to find the optimum number of piles in a design. The goal of Group Optimization is to reduce the total number of piles in a design. The goal is similar to the goal of the pile elimination procedure discussed in Section 3.2.4. The Group Optimization method is more adaptable than pile elimination.

Piles under concrete monoliths are organized into groups of piles which share the same alignments and sizes. This eases installation of the piles. The best optimization method is to find the optimal number of piles in each group through Group Optimization. This is done by allowing the number of piles in each group to be a real variable. The optimal number of piles in a group may be non-integer, but the final design must have only an integer number of complete piles. Partial piles are used temporarily to enable the continuous optimization procedure. The number of piles is made integer by the Branch and Bound procedure.

The most interesting part of the stiffness multiplier method is performing an analysis with a non-integer number of piles. The stiffness analysis of a monolith involves assembling the effective pile stiffnesses over the region of the pile group. One method to assemble the piles is to

smear the total stiffness uniformly over the region of the group. The piles are assembled as a uniform mat stiffness.

The stiffness multiplier method assembles only an integer number of piles, but the stiffnesses are multiplied by a parameter **SM**:

$$K^1_{pile} = SM \; K^0_{pile} \tag{3.23}$$

The stiffness multiplier **SM** is the ratio of the real number of piles to the integer number assembled:

$$SM = \frac{N_{real}}{N_{assem}} \tag{3.24}$$

For example, if 5.5 piles exist in the group then 5 piles are laid-out in a symmetrical grid. The stiffness multiplier of 5.5/5=1.1 is applied to the stiffness of each pile.

The stresses of the piles are evaluated by applying the displacements at the piles to whole single piles. The highest stressed pile in the group is used to form the stress constraint.

The methods of assembling the non-integer piles relies on the assumption that the actual layout of the piles within a group is insignificant. The exact placement of the piles does not effect the structural displacements, but does effect the local concrete stresses. A group of piles is distributed through a specified region of a slab. Displacements do not vary widely within a region of a slab,

therefore the pile stresses do not widely vary. The pile stresses are not significantly dependant upon the exact layout of the piles. The evaluation of stresses in single whole piles is a good estimate of the stresses in a non-integer number of piles. The stiffness multiplier method enables the number of piles to be varied in a numerically efficient manner.

3.2.6 THE PERCENTAGE SELECTION METHOD

The Percentage Selection method is a new method capable of finding global optimums of discrete and continuous problems. It has been shown by Hoback and Truman (15) that the Percentage method can be very valuable in finding the global optimum point through eliminating members. It is also capable of optimizing discrete designs.

The percent selection method's primary application is to select the optimum of two or more discrete options. The method is a new gradient based method to choose between two or more discrete options. An example of a discrete variable is the end fixity of a member which can be either fixed or pinned. Optimizing the member fixities has not been previously made into a gradient based problem. Another type of problem is determining θ.

Formerly the optimum fixity could only be found with discrete search methods. The optimization of discrete options can be solved by search strategies such as a global or genetic search (16). The search strategies involve

searching through many or all of the possible combinations of variables. Discrete optimization searches can require much more computer time than continuous gradient based optimization procedures.

A new method to optimize discrete options with a continuous gradient-based optimization process has been formulated. The Percent Selection method is a quick procedure to find the global optimum of a discrete problem.

The Percent Selection method uses averaged properties to perform the analysis and optimization. This causes the discrete problem to become a continuous problem. A percentage variable is created which measures which discrete option is more efficient. Each discrete option has a percentage associated with it which measures the efficiency of the option. The sum of all the percentages is equal to 100%:

$$\sum_{j=1}^{Nopt_i} p_{ij} = 1.0 \quad i=1,\ldots,n \tag{3.25}$$

where $Nopt_i$ is the number of discrete options for member i, p_{ij} is the percentage of option j for member i, and n is the number of members. This procedure can be applied to discrete problems where each discrete option has its own member stiffness matrix. An equivalent member is used in the analysis. The stiffness of the equivalent member is found by using the percent weighted average of the options:

$$K_i = \sum_{j=1}^{Nopt_i} p_{ij} K_j \qquad i=1,\ldots,n \tag{3.26}$$

where K_i is the total stiffness of member i. The stress constraints of each option are averaged to find an equivalent constraint:

$$h_i = \sum_{j=1}^{Nopt_i} p_{ij} h_{ij} \qquad i=1,\ldots,n \tag{3.27}$$

where h_i is the constraint for member i.

The percentage variable of each discrete option may converge to 0% or 100%. This indicates that one discrete option is optimal. The Branch and Bound procedure is required as the last step when the percent variable does not reach 0 or 100%.

The formal procedure for optimization with respect to discrete options involves adaptions of the analysis and optimization methods. The first step is to create an initial design which includes estimates of the initial percentages and the other variables. The stiffnesses of all the possible member options are computed. For example, the stiffness of a pinned pile and a fixed pile are computed. The equivalent member stiffness is the percent weighted average of the member stiffnesses for each possible case. The members are assembled and a stiffness analysis is performed. The member displacements are applied to every

possible condition of the member. The relevant constraints are formed for each option. The constraints are averaged to provide the member constraint. The Percent Selection procedure can be applied to linear and non-linear stiffness problems.

The percent variables are included in the optimization. Additional constraints are also required. The percents of each possibility must be between zero and one:

$$0.0 \le p_{ij} \le 1.0 \quad i=1,\ldots,n;\ j=1,\ldots,Nopt_i \qquad (3.28)$$

Another application of the percent method is for finding the global optimum design. A local optimum is a design which is the most efficient design in the local region. Optimization problems that are convex have only one possible optimum design, therefore the final design is the global optimum design. Structural optimization problems are generally non-convex. Non-convex problems can have local optimas or dips in the objective function which can trap the optimization. The Kuhn-Tucker conditions only guarantee that the final design is the locally optimum design.

One method to search for the optimal design is to begin the optimization from various starting points. The best resultant design is taken as the optimum.

Another method for finding the optimum is to alter the behavior of the optimization problem. Problems can sometimes be made convex or less non-convex. The Percentage

method can find the global optimum for certain truss and frame structures. Frame structures have local optimums which prevent some members from being eliminated. The percent method overcomes these local optimums. Pile structures do not have this problem because the piles are eliminated through group optimization.

3.3 SENSITIVITY ANALYSIS

The optimization algorithm uses the gradients of the constraints and the objective function with respect to the design variables. The optimization algorithm uses the gradient information to predict how to change the variable to improve the cost of the design without violating the design limits. The gradient information can be obtained through one of three sensitivity analysis methods.

The finite difference method can be used to approximate the gradients. The original structure has design parameters of $\mathbf{d}^o$ and stress constraints of $\mathbf{u}^o$. Each variable d_i is consecutively altered by a small amount (0.5%) to produce new designs $\mathbf{d}^1$. The new secondary structures are analyzed to provide the new constraints $\mathbf{u}^1$. This procedure requires one analysis for each variable. The gradients of each constraint with respect to the variables are computed as:

$$\frac{\partial u_j}{\partial d_i} \approx \frac{\Delta u_j}{\Delta d_i} = \frac{u_j^1 - u_j^o}{d_i^1 - d_i^o} \tag{3.29}$$

The two other common sensitivity analysis methods are the virtual load and pseudo load techniques. These methods form a virtual load vector and solve for the virtual displacements using the structural stiffness matrix. The techniques are identical except with respect to the methods that they use to solve for the virtual displacements. The virtual load technique involves solving for the inverse of

the stiffness matrix and multiplying this by the virtual loads. The pseudo load technique solving for the virtual displacements uses a linear stiffness solution method.

The first step in both methods is to express the stresses and member displacements as a function of the structural displacements:

$$u_j = \{b\}_j^T \{U\} \tag{3.30}$$

where u_j is the stresses or local displacements, **U** is the structural displacements, and **b** is the virtual load vector. The virtual displacements vector is $\mathbf{v}_j$ which can be found by:

$$\{v\}_j = [K]^{-1} \{b\}_j \tag{3.31}$$

or:

$$\{v\}_j^T = \{b\}^T [K]^{-1} \tag{3.32}$$

Taking the derivative of Equation 3.30 with respect to the design variables gives:

$$\frac{\partial u_j}{\partial d_i} = \frac{\partial \{b\}_j^T}{\partial d_i} \{U\} + \{b\}_j^T \frac{\partial \{U\}}{\partial d_i} \tag{3.33}$$

The linear stiffness solution problem is:

$$[K] \{U\} = \{R\} \tag{3.34}$$

where **K** is the structural stiffness and **R** is the load vector. The derivative of Equation 3.34 is taken:

$$[K]\ \frac{\partial\{U\}}{\partial d_i} + \frac{\partial[K]}{\partial d_i}\ \{U\} = \frac{\partial\{R\}}{\partial d_i} \qquad (3.35)$$

or:

$$\frac{\partial\{U\}}{\partial d_i} = [K]^{-1}\left(-\frac{\partial[K]}{\partial d_i}\ \{U\} + \frac{\partial\{R\}}{\partial d_i}\right) \qquad (3.36)$$

The loads are usually independent of the design variables, so the derivative of the loads is usually zero. It is not zero when the dead load of the members is a significant portion of the load on the structure. An example is the concrete slabs over pile foundations which provide the dead load for the structure. For solution with the virtual load method Equation 3.36 is substituted into Equation 3.33:

$$\frac{\partial u_j}{\partial d_i} = \frac{\partial\{b\}_j^T}{\partial d_i}\ \{U\} + \{b\}_j^T\ [K]^{-1}\left(-\frac{\partial[K]}{\partial d_i}\ \{U\} + \frac{\partial\{R\}}{\partial d_i}\right) \qquad (3.37)$$

This can be rewritten as:

$$\frac{\partial u_j}{\partial d_i} = \frac{\partial\{b\}_j^T}{\partial d_i}\ \{U\} + \{v\}_j^T\left(-\frac{\partial[K]}{\partial d_i}\ \{U\} + \frac{\partial\{R\}}{\partial d_i}\right) \qquad (3.38)$$

The solution procedure of the virtual load method is to find the vector {b} with Equation 3.30, solve for **v** with Equation 3.31, then solve Equation 3.38.

The pseudo load method uses a pseudo load vector $\{v_{il}\}$ which is:

$$\{v_{il}\} = -\frac{\partial[K]}{\partial d_i}\{U\} + \frac{\partial\{R\}}{\partial d_i} \qquad (3.39)$$

The procedure involves solving Equation 3.34 using a linear solution method then solving Equation 3.39.

The choice of the sensitivity analysis method is made by comparing the number of computer calculations required for each method. The only difference between the methods is how the stiffness matrix is solved. The virtual load method requires the inverse of the stiffness matrix. Acquiring the stiffness matrix and multiplying it by a vector requires about three times the number of calculations compared to solving a linear system of equations. Therefore the pseudo load method can be more efficient.

The pseudo load method is also very efficient with designs having few constraints. This method requires the solution of the stiffness matrix for only the number of constraints. The virtual load method requires an inversion of all the structural stiffness degrees of freedom for any number of variables. The pseudo load method remains more efficient even when the number of constraints exceeds the number of degrees of freedom. The gradients of the all global displacements are found. The stress constraints can be found using the displacement gradients.

The finite difference method requires the solution of the stiffness matrix for each variable. This has the same number of calculations as the pseudo load method, so the finite difference method is used.

4. PERFORMANCE EVALUATION EXAMPLE

Example 1 Percent Selection of Pile Fixity

The purpose of this example is to provide a simple demonstration of the new percent method for optimization of discrete variables. The fixity of a single pile to a foundation is optimized. This example demonstrates that the Percent Selection method may be used to determine the optimal pile fixity. Previously the fixity would have been determined by a discrete optimization method such as a search.

The foundation is subjected to a horizontal load. The options for connecting the pile to the foundation are (a) fixed, and (b) pinned. The objective is to minimize the pile inertia subject to a displacement constraint. The maximum allowed displacement is 1. As shown in Appendix 1 the lateral stiffness coefficient ($b_{11\,i}$) of a pile is:

$$b_{11\,i} = \frac{C_{oi}\, E_{pile}\, I_2}{R_2^3} \tag{4.1}$$

where:

$$R_2 = \left(\frac{E_{pile}\, I_2}{E_{soil}} \right)^{0.25} \tag{4.2}$$

and E_j is the elastic modulus for material j; and C_{o1}= 1.414 for fixed piles, and C_{o2}= 0.707 for pinned piles. The elastic moduli are set to 1.0 to simplify this example.

Equation 4.1 can be simplified to:

$$b_{11\,i} = C_{oi}\, I^{0.25} \tag{4.3}$$

When P=1 the displacement of the options is equal to:

$$d_i = \frac{1}{b_{11\,i}} \tag{4.4}$$

The displacement constraint for each option is:

$$h_i = \frac{1}{b_{11\,i}} - 1 \le 0 \tag{4.5}$$

The equivalent member constraint is:

$$h = p_{fix} h_{fix} + (1 - p_{fix})\, h_{pin} \le 0 \tag{4.6}$$

The constraint gradients are:

$$\frac{\partial h}{\partial p} = h_{fix} - h_{pin} \tag{4.7}$$

$$\frac{\partial h}{\partial I} = \frac{-I^{-1.25}}{4}\left(\frac{p}{C_{o1}} + \frac{1-p}{C_{o2}}\right) \tag{4.8}$$

This example was optimized with an optimality criteria method. The example converged in six iterations. This example is a well behaved continuous optimization. The iterations are shown in Table 4-1. The optimum is: I=0.25, p=100%. The pile became completely fixed to prevent displacement constraint violations. The Branch and Bound procedure could be used to push the design to a discrete or useable design if the optimum was not 100% or 0%. The

percentage method has been shown to efficiently choose between discrete options.

Table 4-1 Pile fixity example

Iteration	I	p
0 (Initial)	1.000	0.500
1	0.865	0.637
2	0.649	0.722
3	0.496	0.806
4	0.378	0.885
5	0.288	0.958
6	0.250	1.000

5. FULL EXAMPLES

Examples of retaining walls, dams, and locks are shown. Retaining walls are used to support earth at locations where there is a grade level separation. Retaining walls can frequently be modeled as a two-dimensional structure when the walls are symmetric.

Dam structures consist of a thick concrete monolith supported by many piles. The monolith is relatively stiff compared to the piles. The concrete monolith does not significantly deform under loading but the pile heads displace. Dams are frequently modeled as rigid when analyzing the structure.

A lock structure is a system which raises and lowers barges and other river traffic to allow them to pass through dams. A lock has a pool area with an elevation that can be varied. Barges are elevated as the pool elevation changes.

A lock structure has an upstream gate and a downstream gate. The process of passing a barge consists of first opening the appropriate gate to allow the barge to enter. Then the gate is closed and the pool elevation is altered to the new level. The second gate is opened and the barge passes outward.

The concrete monolith for locks consists of two relatively thick side walls connected by a slab under the pool area. Piles are placed under the walls and the slab. The thin slab is relatively flexible. The slab

significantly deform under loading compared with the pile deformation.

The various pool levels and maintenance conditions are the loading cases on the lock. The river level varies over the course of the seasons. This is considered when forming the maximum loading levels.

Another type of structure that may be analyzed as a pile structure is a building foundation. Buildings may be constructed over structural slabs which are supported by piles.

5.1 EXAMPLE 2, RETAINING WALL

A retaining wall is optimized with the program OPTPILE (4). The symmetry of the wall allows the wall to be analyzed using a two dimensional segment. The initial design is shown in Figure 5-1. The wall is subject to two load cases as shown in Table 5-1. The wall is optimized with both the individual pile and group pile optimization methods. The benefits of each method are discussed. This example also demonstrates that the discrete variables can be efficiently optimized.

Table 5-1. Retaining wall load cases.

Load Case	P_x (kip)	P_z (kip)	M_y (kip ft)
1	-220.	440.	500.
2	250.	250.	0.

The optimization optimizes the number, size and

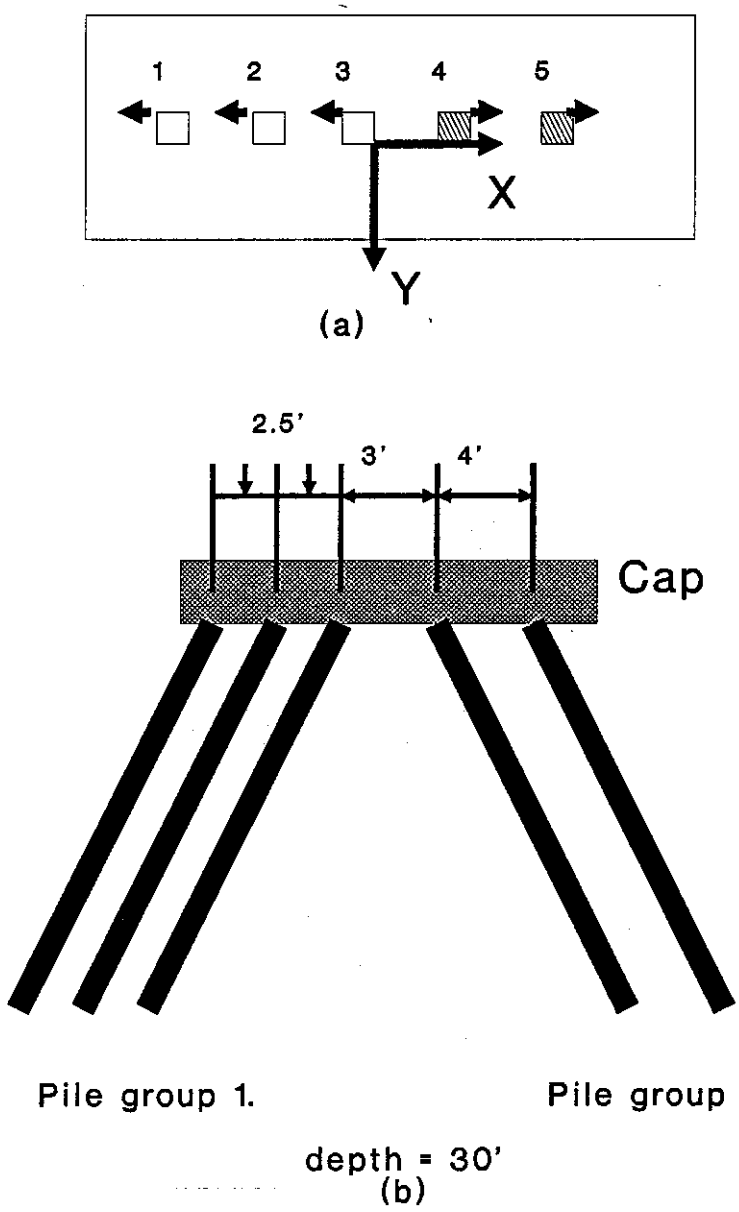

Figure 5-1. Initial pile layouts for wall example.
(a): Plan view, (b): Elevation view.

orientation of the piles, but the pile groups are not be allowed to move. The optimal pile fixities are found with the Percent method.

The initial design has five piles in the wall segment. The initial design is listed in Table 5-2. The piles all have an inertia of 729.0 in^4. The initial fixity and theta percentages are 50%.

Table 5-2. Initial wall pile properties.

Group	Number Piles	I_{xx} (in^4)	Batter	ϕ (deg.)	θ (%0 deg)	fixity (%fix)
1	1	729.	2.	180.	50.	50.
2	1	729.	2.	180.	50.	50.
3	1	729.	2.	180.	50.	50.
4	1	729.	2.	0.	50.	50.
5	1	729.	2.	0.	50.	50.

The individual pile optimization method is first applied to the design. The number of piles is small enough that they do not have to be grouped for ease of installation. Each pile is allowed to have its own size, and orientation.

The fixities and angle theta of the piles are also optimized. It is inefficient to search through all possible combinations of pile fixity for all the piles. The Percent Selection method quickly finds the optimum fixities and thetas.

The optimization reduced the weight of steel from

12,214. lbs to 10,950. lbs in seven iterations. The convergence of the weight is shown in Figure 5-2 as the circles. The optimized inertias for all piles is 729.0 in^4 which is the minimum size available. The final pile layouts are shown in Figure 5-3 and Table 5-3. This design is not a discrete design because the percentages are not 0% or 100%. The piles are most efficient when they are partially fixed, but piles are not allowed to be partially fixed in current design methods.

Table 5-3. Optimized wall pile properties.

Group	Number Piles	I_{xx} (in^4)	Batter	ϕ (deg.)	θ (%0 deg)	fixity (%fix)
1	1	729.	35.4	180.	96.2	51.4
2	1	729.	24.2	180.	100.	57.6
3	1	729.	11.8	180.	87.2	45.4
4	1	729.	8.65	0.	90.5	22.0
5	1	729.	35.1	0.	100.	49.5

A branch and bound procedure is performed to find a discrete or useable least weight design. The inertias remain at 729. in^4 in the final design of all piles. All piles are 0% fixed in the final design. The piles are therefore pinned. The angle theta of each of the piles is 100% of 0. degrees, so the layout of the piles is 0. degrees. The final pile properties are shown in Table 5-4.

The final branch weight is 10,929. lbs which is almost identical to the initial optimized weight. The final

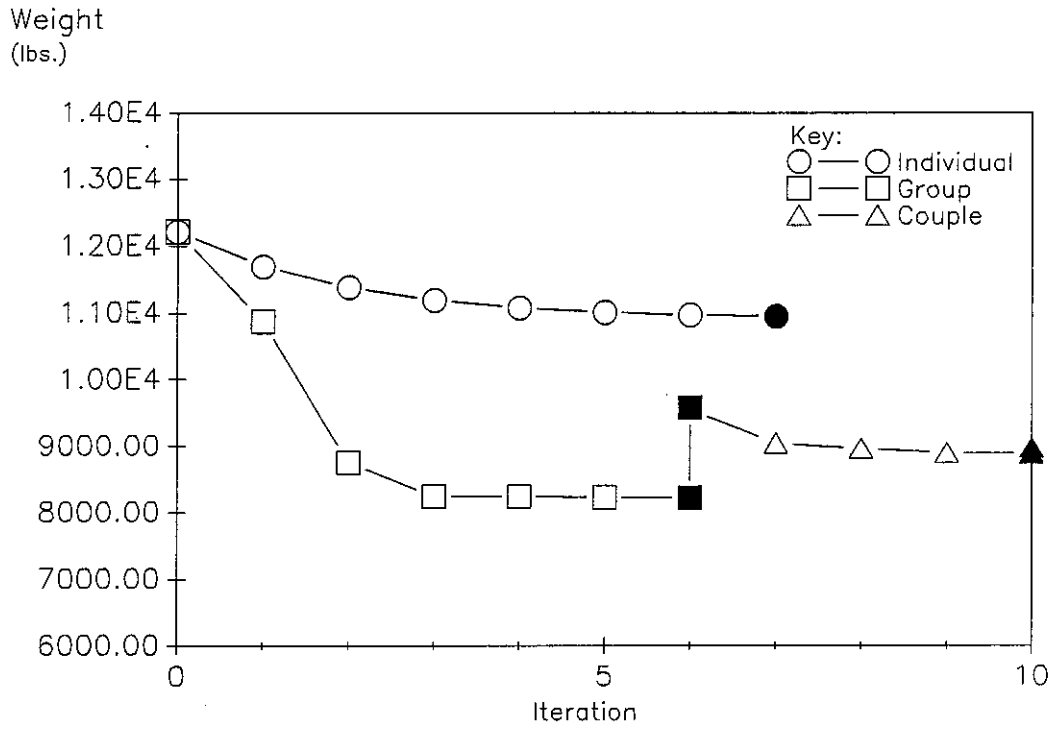

Figure 5-2. Weight Convergence of wall.

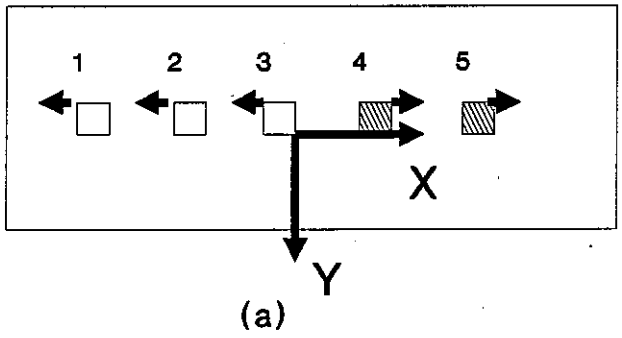

(a)

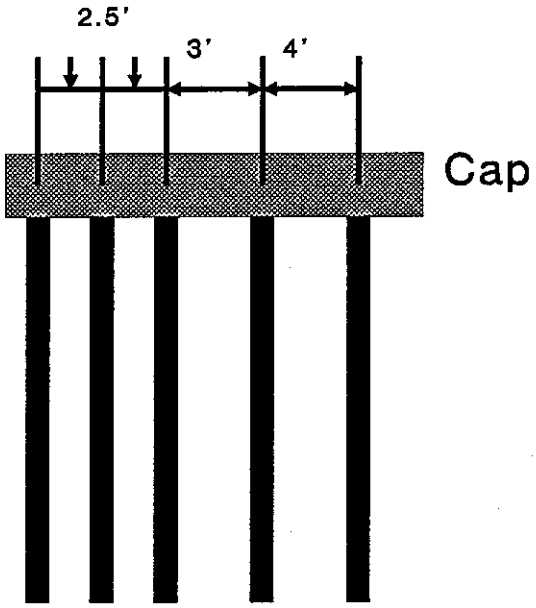

Pile group 1. Pile group 2.

depth = 30'

(b)

Figure 5-3. Final pile layouts for individual method. (a): Plan view, (b): Elevation view.

branched weight is shown in Figure 5-2 as the darkened circle. The design was not penalized for moving from the optimum point to a discrete design. Therefore this example is not highly sensitive to the choice of pile fixity.

Table 5-4. Wall branched pile properties.

Group	Number Piles	I_{xx} (in^4)	Batter	ϕ (deg.)	θ (%0 deg)	fixity (%fix)
1	1	729.	53.	0.	100.	0.
2	1	729.	100.	0.	100.	0.
3	1	729.	100.	180.	100.	0.
4	1	729.	17.	0.	100.	0.
5	1	729.	31.	0.	100.	0.

A small weight savings resulted from making the design discrete. The weight savings was unexpected because it is in disagreement with the branch and bound theories. The branched designs should have higher costs than the original optimized design. The disagreement can be explained by the fact that the original optimization may not have completely converged to the optimum design before the branching was performed.

The only active constraints at the optimum were the minimum pile sizes for all piles. Therefore the current structure is over-designed, and the number of piles should be reduced.

The optimization method quickly converged to the optimum design. The design was not a useable or discrete

design so a branch and bound procedure was performed. The branch and bound required six branches to be optimized. A total of seven optimizations were performed including the initial optimization. These branches were required to move the percentage variables to discrete values. The alternative method would be to do a global search of all fixity and theta options which would have required 1024 optimizations. Therefore, the percentage method was 1024/7=146 times quicker than a global search. The percentage optimization method has significantly quickened the optimization process. It has been proven to be a useful tool.

5.1.1 WALL GROUP OPTIMIZATION

The group optimization method is applied to the initial pile design of the wall. The results from the group and individual methods can be compared to determine which method is more effective. The group optimization method allows the number of piles in each group to be varied as a real number. The number of piles may decrease. A branching method is used to find an integer number of piles.

The initial pile properties are the same as the previous example. Each pile is not be allowed to have its own size and orientation, but must have the same properties as the other piles in the same group. Piles 1,2, and 3 are placed in group 1. Piles 4, and 5 are placed in group 2.

The results are shown in Figure 5-4, and Tables 5-5 and

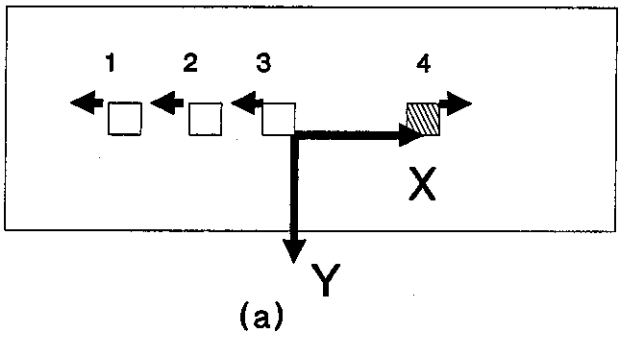

(a)

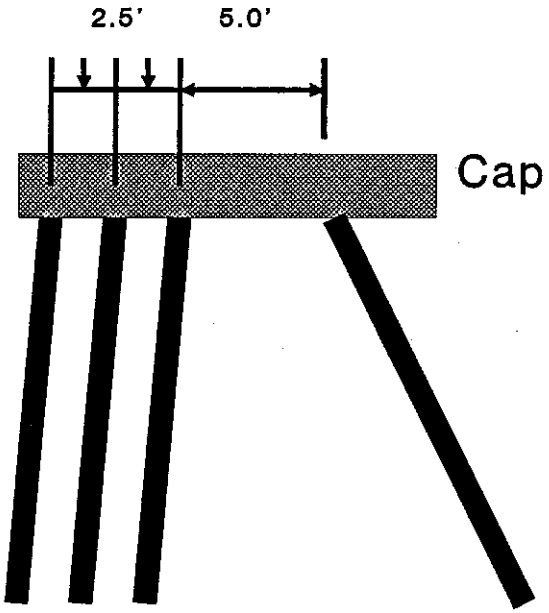

Pile group 1. Pile group 2.

depth = 30'

(b)

Figure 5-4. Final pile layouts for group method. (a): Plan view, (b): Elevation view.

5-6. The group optimization method reduced the weight of steel from 12,214. lbs. to 8218. lbs. in six iterations. The design was not discrete (useable) because the number of piles was non-integer so a branch and bound was performed. The branch and bound increase the weight from 8218. lbs. to 9489. lbs. A total of 35 optimizations were performed to reach this design. The discrete design of 9489. lbs. is lower than the previous design of 10929. lbs. using the individual method. See Figure 5-2. The effect of the branching is shown with the filled squares.

The group optimization method was much more effective than the individual method at reducing the number of piles. It is very effective to optimize the number of piles as real variables. The group optimization method can reduce the number of piles because the initial design is not highly stressed. If the initial design was more highly stressed than the individual method may have been more effective.

There are several active constraints in the optimum design. Several stresses are at their maximum values. The piles are near their minimum available sizes. The pile tips are close to intersecting each other.

Table 5-5. Optimized wall pile properties.

Group	Number Piles	I_{xx} (in^4)	Batter	ϕ (deg.)	θ (%0 deg)	fixity (%fix)
1	2.34	729.	4.51	180.	100.	50.
2	1.22	729.	2.0	0.	100.	32.

Table 5-6. Branched wall pile properties.

Group	Number Piles	I_{xx} (in^4)	Batter	ϕ (deg.)	θ (%0 deg)	fixity (%fix)
1	3	729.	11.3	180.	100.	100.
2	1	904.	2.0	0.	100.	100.

5.1.2 WALL COUPLED OPTIMIZATION

The group optimization and individual pile optimization methods may be coupled for small designs. This example demonstrates that coupling the two methods results in the lowest cost design. The results of the group optimization may be input into an individual pile optimization. If the piles are ungrouped then an additional weight saving may be achieved. The piles need not be grouped in this structure because the number of piles is low. The piles were temporarily grouped so the group optimization method could be used.

The group optimization results are input in to an individual pile optimization. Four iterations are performed to reduce the weight to 8881. lbs. See the weight convergence in Figure 5-2 as the triangles. The optimization began from the branched group optimization weight. The optimized design is not a discrete design because the pile fixities are not completely pinned or fixed. Therefore, a branch and bound was applied which increased the weight to 8971. lbs. The final pile

properties are listed in Tables 5-7 and 5-8. The pile layouts are illustrated in Figure 5-5.

The coupling of the two optimization methods has provided a significant savings in the cost of the structure. The coupling of the methods has produced a design of lower weight than either method could have produced independently. The individual method was incapable of altering the number of piles and so its final cost was too high. The group method reduced the number of piles, but it placed unnecessary restrictions on the design. The coupling produced the most efficient design.

Table 5-7. Optimized wall pile properties.

Group	Number Piles	I_{xx} (in^4)	Batter	ϕ (deg.)	θ (%0 deg)	fixity (%fix)
1	1	729.	37.5	180.	100.	43.
2	1	729.	9.10	180.	100.	64.
3	1	729.	5.17	180.	100.	30.
4	1	729.	3.49	0.	100.	22.

Table 5-8. Final wall branched pile properties.

Group	Number Piles	I_{xx} (in^4)	Batter	ϕ (deg.)	θ (%0 deg)	fixity (%fix)
1	1	729.	14.3	180.	100.	0.
2	1	729.	6.51	180.	100.	0.
3	1	729.	9.83	180.	100.	0.
4	1	729.	2.35	0.	100.	0.

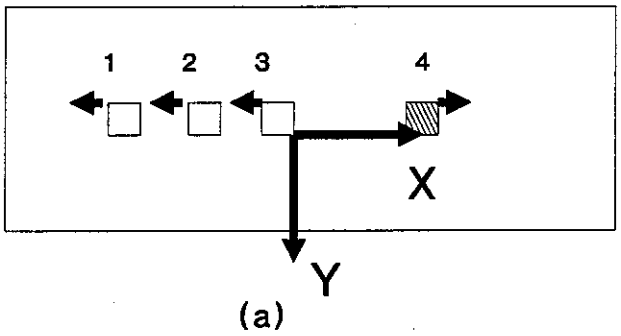

(a)

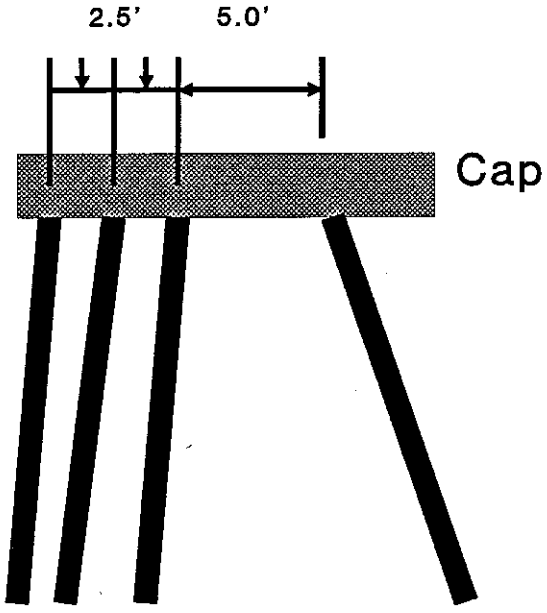

Pile group 1. Pile group 2.

depth = 30'

(b)

Figure 5-5. Final pile layouts for coupled method. (a): Plan view, (b): Elevation view.

5.2 EXAMPLE 3, DAM STRUCTURE

The number of piles under a dam is optimized with the group method. The dam is an existing structure called the Old River Low Sill Control Structure. It has been analyzed with CPGA and the results were shown in the CPGA User's Guide (6). This design is the initial input to OPTPILE (4). The only alteration to the design is that all of the pile tips are set to a depth of 90 feet. Previously all the piles were 90 feet long. The number of piles in each group is optimized with the group method. The purpose of this example is to demonstrate that group and percent optimization methods are effective tools to reduce the cost of structures.

The structure is shown in Figures 5-6 and 5-7. The dam loading is listed in Table 5-9. The initial pile layouts are listed in Table 5-10. Originally the three groups of piles have 60, 52, and 128 piles for a total of 240 piles. Groups 2 and 3 are installed in the same area of the structure. These two groups are allowed to exist in the same area as long as the piles do not intersect.

Table 5-9. Dam load cases.

Load Case	P_x kip	P_y kip	P_z kip	M_y kip-ft	M_y kip-ft	M_y kip-ft
1	0.	-12000	20000	-1.E6	0.	0.

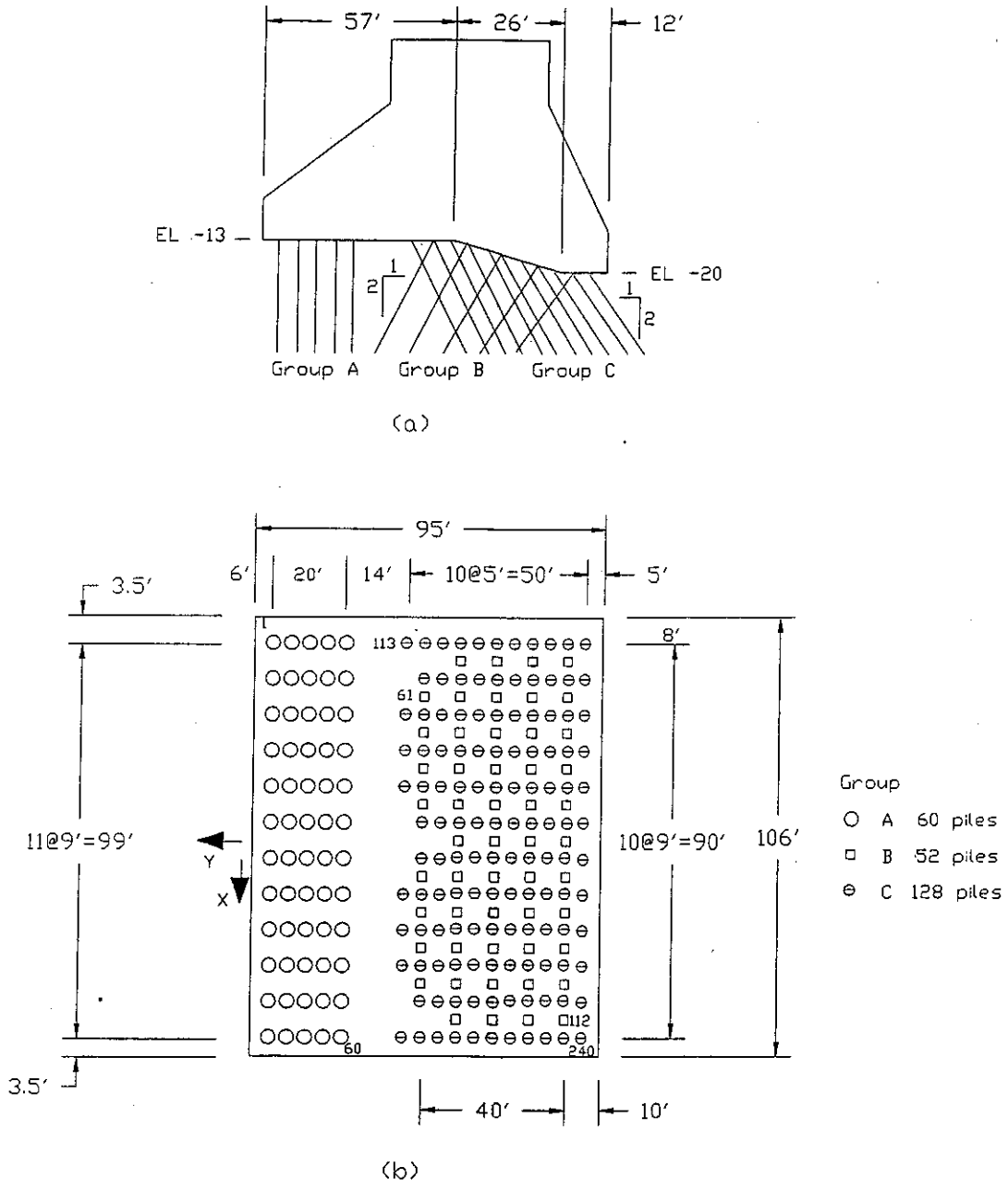

Figure 5-6. Dam Structure.

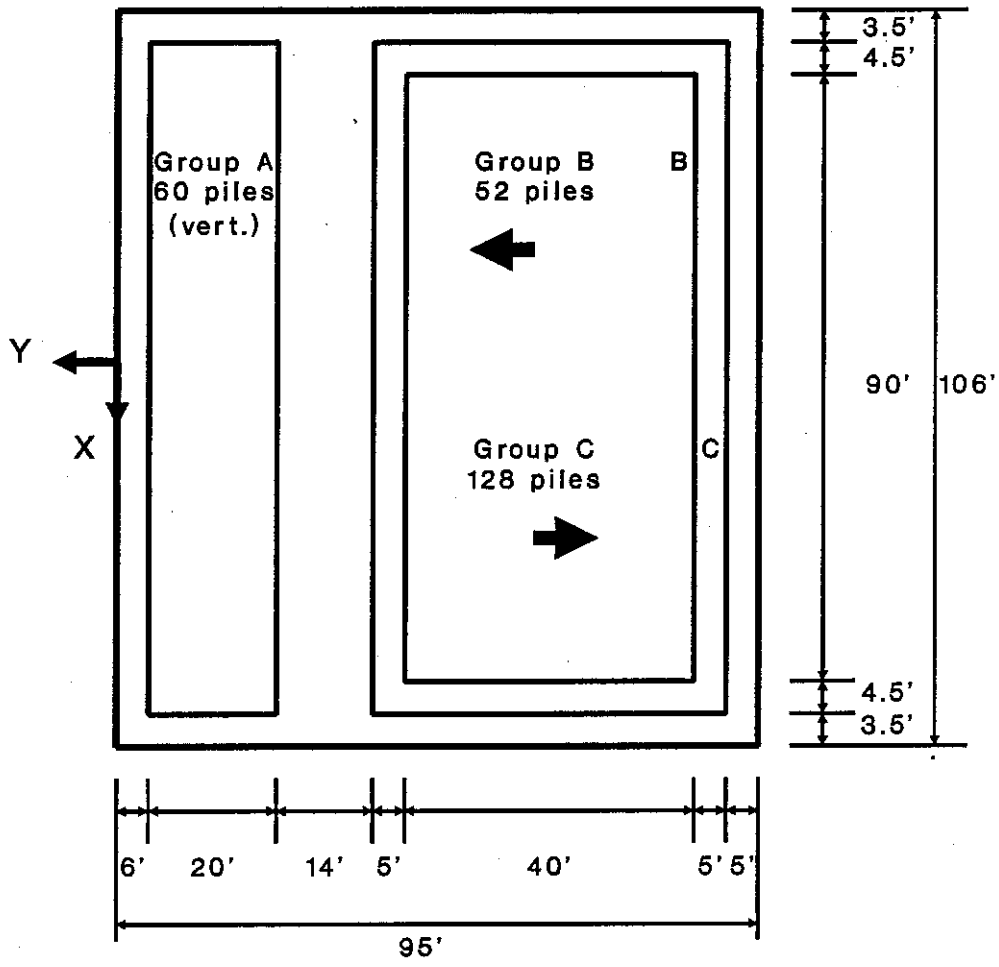

Figure 5-7. Initial Pile Positions for Dam.

Table 5-10. Initial Dam pile properties.

Group	Number Piles	I_{xx} (in^4)	Batter	ϕ (deg.)	θ %0 deg	fixity % fix
A(1)	60	729.	100.	0.	50.	50.
B(2)	52	729.	2.	90.	50.	50.
C(3)	128	729.	2.	270.	50.	50.

The pile layouts are graphically shown by two methods in Figures 5-6, and 5-7. One method shows the position and orientation of each pile and the second method show the positions of the groups of piles. The piles are optimized as groups.

The optimum number of piles in the groups is 23, 19 and 78. The total is 120 piles which is half of the 240 piles in the initial design. The final layouts are shown in Tables 5-11, 5-12, and Figure 5-8.

Table 5-11. Optimized Dam pile properties.

Group	Number Piles	I_{xx} (in^4)	Batter	ϕ (deg.)	θ deg	fixity
1	23	750.	2.23	270.	0.	pin
2	19	730.	2.09	270.	0.	pin
3	78	732.	2.01	270.	0.	pin

Table 5-12. Optimized Dam pile group positions.

Group	x_{low} (ft)	x_{high} (ft)	y_{low} (ft)	y_{high} (ft)
1	-46.8	49.5	-15.7	-10.9
2	-48.9	39.5	-31.6	-24.8
3	-45.3	43.8	-89.5	-45.3

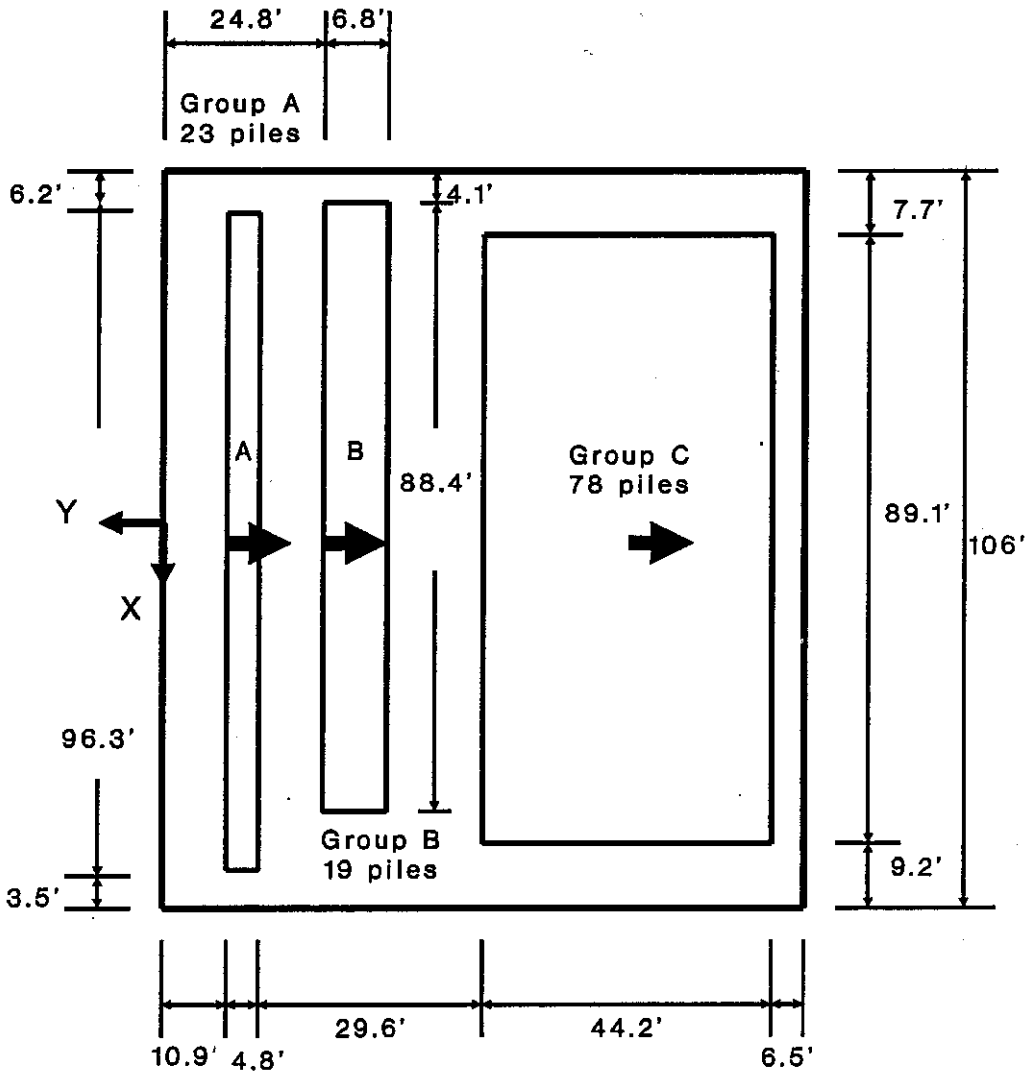

Figure 5-8. Final Pile Positions for Dam.

The weight of steel in the initial design is 1,667,000 lbs. The optimal weight is 870,000 lbs. The weight was significantly decreased from the initial design. The convergence of the weight is shown in Figure 5-9. The weight of steel jumps in the first optimization iteration because the pile allowable stresses were exceeded. The design in the CPGA manual was feasible. The design became infeasible when the pile fixities were set to 50% to start the percentage optimization.

The pile alignments at the optimum are all about the same. This would not occur if more load cases were required. The borders of the pile groups were allowed to move. The borders moved small distances. The final pile inertias are not exactly 729 in^4, but they are very close. The pile sizes are within a tolerance region of a few percents to a fabricated size so they can be rounded down. A branch and bound is not required. The percentage variables for the fixity and angle theta converged quickly to useable values. The convergence of the percents for pile group one are shown in Figure 5-10.

Most of the piles are close to their maximum allowable stresses. Other active constraints are the layout limits on the minimum batters of groups 2 and 3.

This example demonstrates that significant improvements can be made when given an inefficient initial design. This

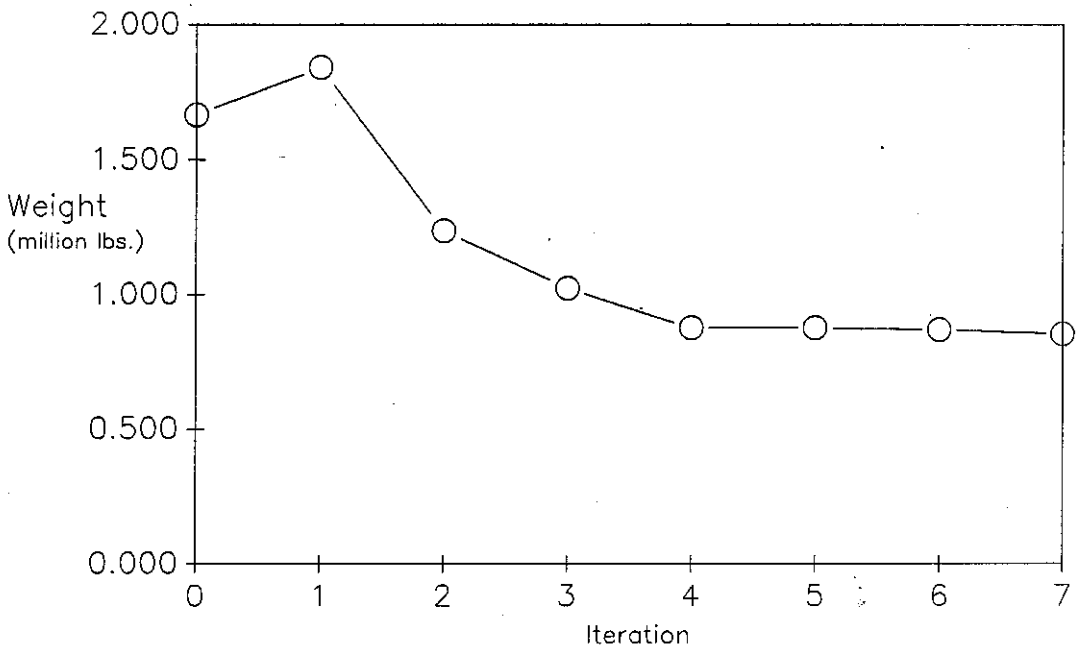

Figure 5-9. Weight of Dam.

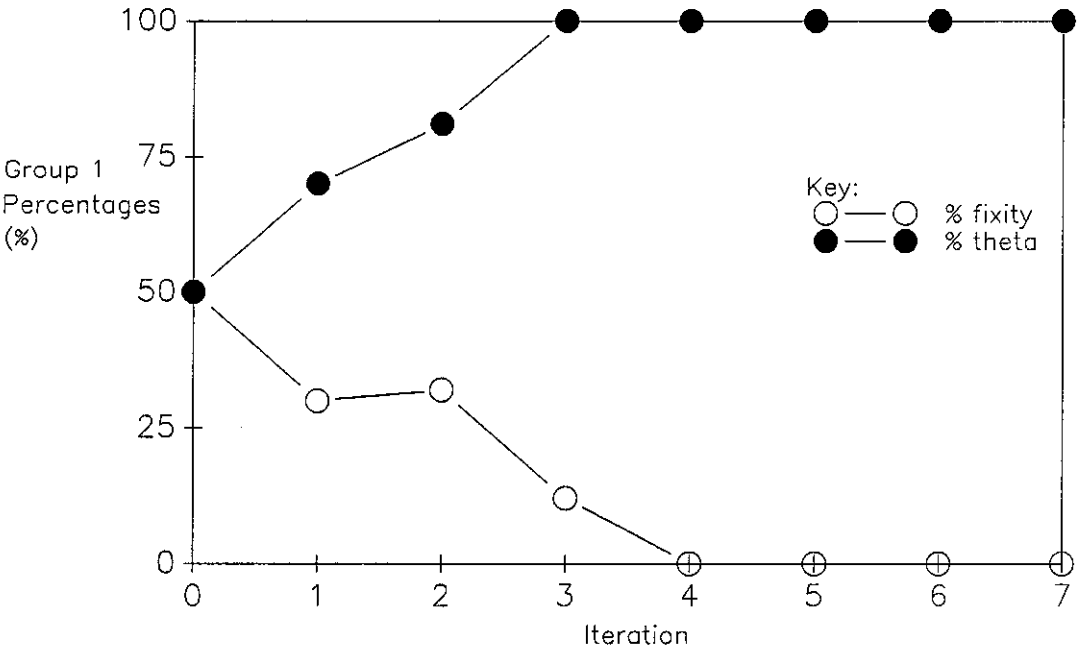

Figure 5-10. Percentage Convergence.

example also demonstrates the effectiveness of the group optimization method which halved the number of piles.

5.3 EXAMPLE 4, LOCK 26R AL-3

The pile layouts under a portion of a lock are optimized. This is an existing structure. The US Army Corps of Engineers is currently completing construction, so this is a real and current example. The pile and concrete monolith designs were obtained from the design documents (17). The engineers at Black and Veatch produced the initial design which is used as a starting point for the optimization. This example demonstrates that the optimization methods can be applied to current projects and that significant cost savings may result.

Description of the Lock:

The lock and dam structure is located on the Mississippi River at Alton Illinois. The river flows in a south easterly direction at Alton. The lock and dam structure has two lock chambers and several dam sections. See Figure 5-11. The locks are located on the Illinois side of the river near the levee. The dam sections extend from the locks to an overflow dike. The overflow dike extends from the dam to the Missouri side of the river.

The smaller auxiliary lock is considered in this example. See Figure 5-12 for a closer view of the auxiliary lock. The lock consists of 11 segments. Each lock monolith has at least one function. Sections AL-1 and 11 are guard walls. Section AL-2 is the intake for the water that is used to fill the chamber. Sections AL-3 and 10 are the

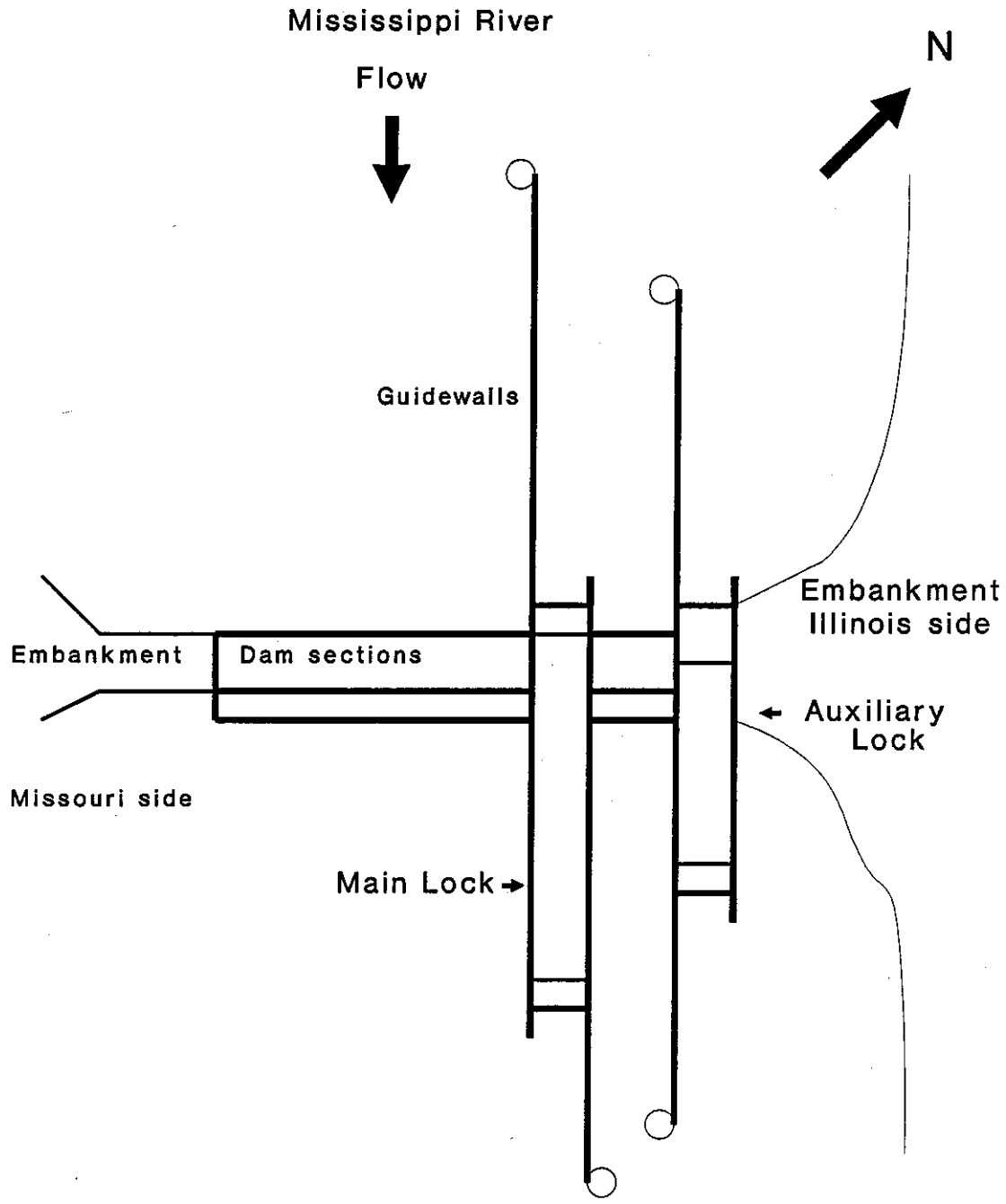

Figure 5-11. Lock and Dam No. 26 (Replacement).

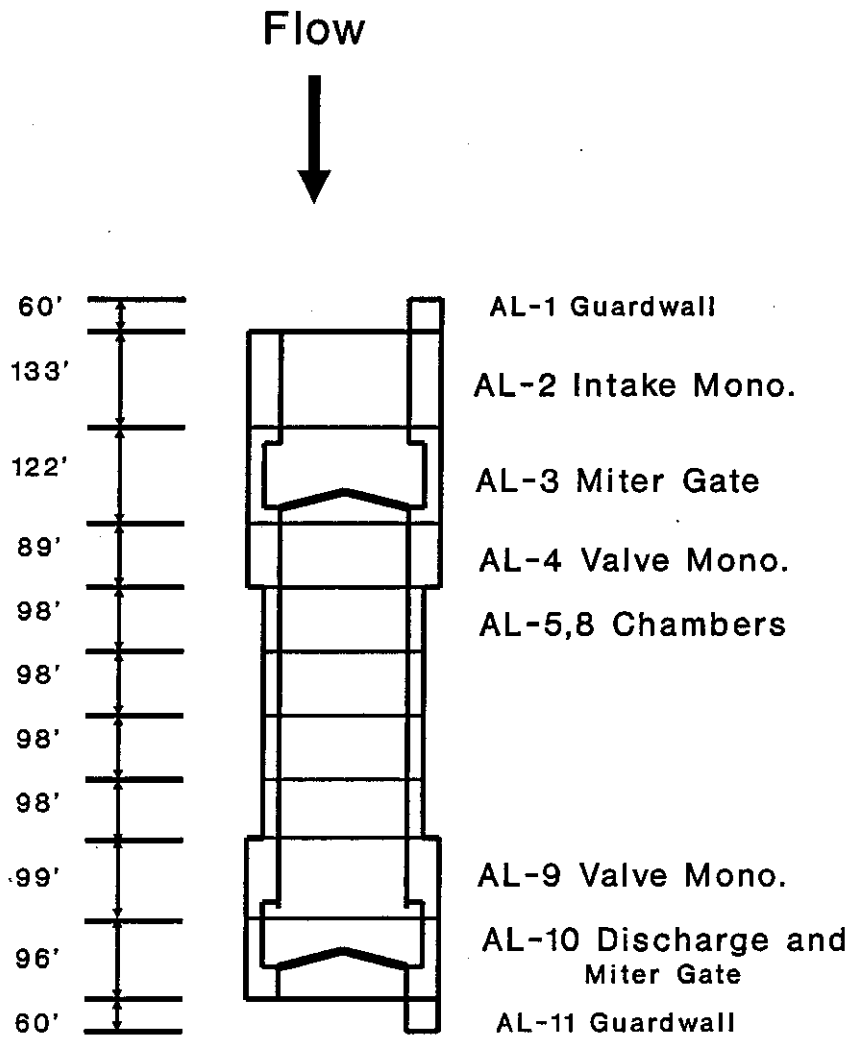

Figure 5-12. Auxiliary Lock 26R.

miter gate monoliths. Section AL-4 and 9 are the valve monoliths. The valves control the intake and discharge flow in the lock chamber. Sections AL-5 to 8 are chambers. The water is vented into the bottom of these chambers to lift or lower the barges. Section AL-10 is the discharge monolith.

The barges and river traffic is raised by the lock by entering through the downstream gate and then the gate is closed. The intake valves are opened to allow water to flow through the culverts into the chambers. The chambers between the two gates are flooded. The upstream gate is opened when the chamber elevation equalizes with the upstream elevation.

An optimization is performed on the AL-3 gate segment of Lock and Dam 26R. A closer view of the AL-3 segment is shown in Figures 5-13, 5-14, and 5-15. The monolith is a U-shaped concrete section which is supported by steel piles driven into the ground. The lock section has thick wall sections with a thickness of 76.5 ft, and a thinner slab section with a thickness of 16 to 18 ft. The miter gate sits on a sill when it is closed. The two pieces of the gate fold into recesses on each side of the lock when they are opened.

The lock walls have voids in them. The square voids at the elevation of the lock floor are the culverts. The culverts are used to fill and empty the lock. Walkways and

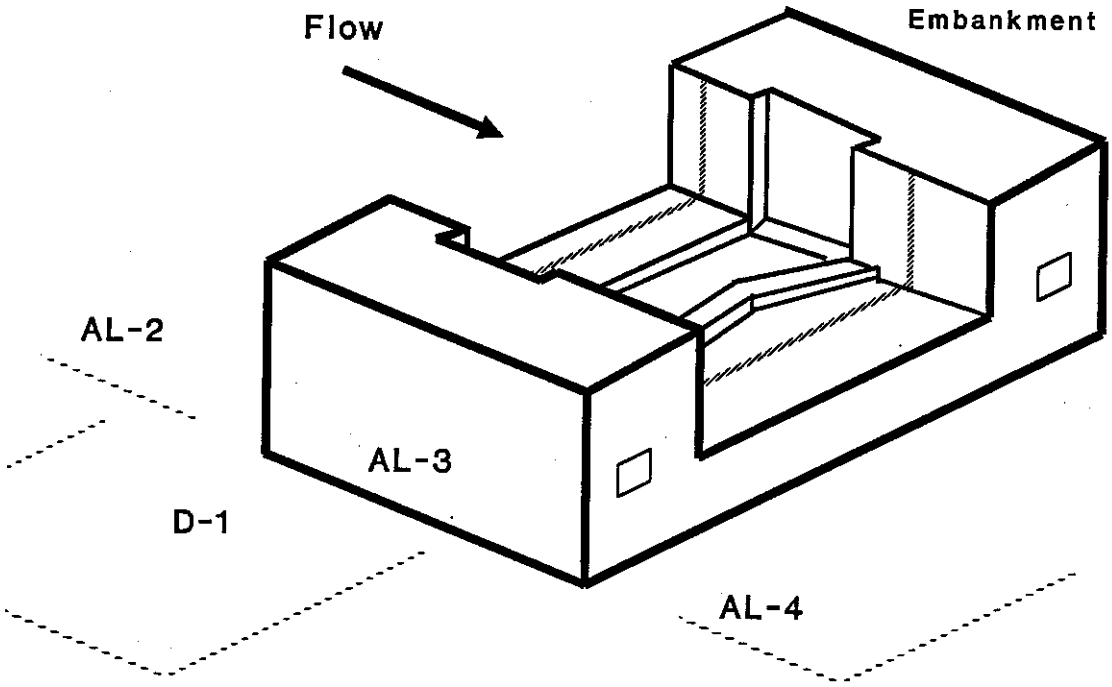

Figure 5-13. AL-3 Isometric view.

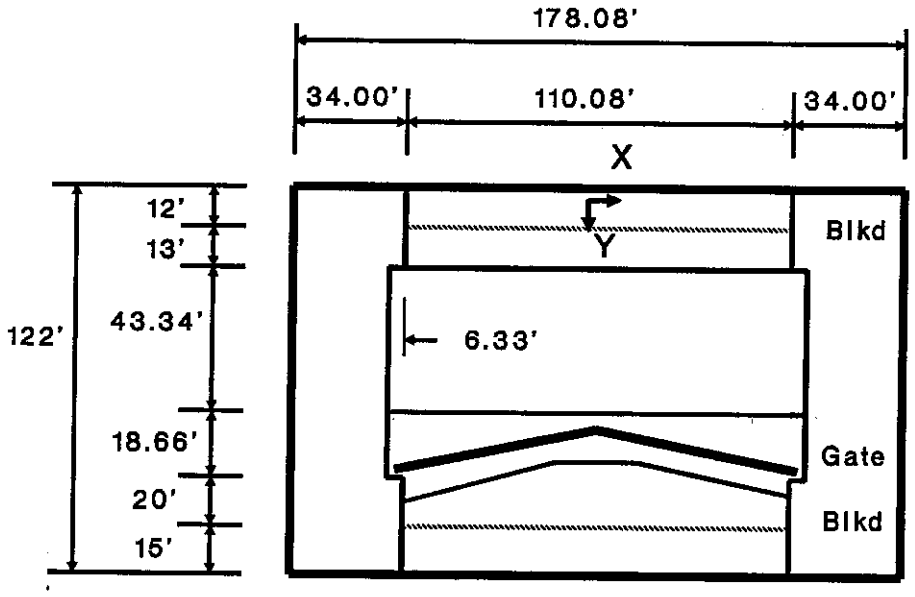

Figure 5-14. AL-3 plan view.

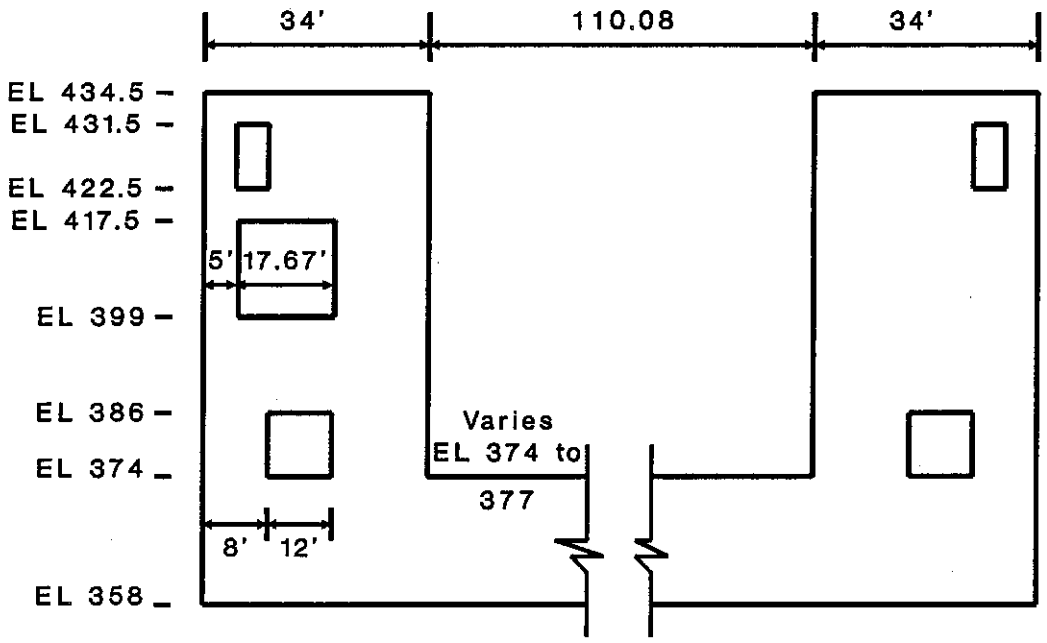

Figure 5-15. AL-3 End view.
Typical voids shown.

machinery voids are unsymmetrically placed throughout the walls. Typical voids have been shown.

There are two sockets for placing maintenance bulkheads. These bulkheads can be lowered into the lock by a crane. The bulkheads seal the chamber so that maintenance can be performed on the gate. This is called lock dewatering. A couple of methods of dewatering can be done. The entire lock could be sealed and dewatered or this individual monolith could be sealed and dewatered.

The initial pile design has 734 piles underneath it. See Figures 5-16 and 5-17. All of the piles are the maximum size of HP-14 piles that can be used. The piles are initially aligned in one of three directions. The 408 piles in group A are vertical. The 67 piles in group B are battered at a slope of 2.5 in the y-direction. The 259 piles in group C are battered at a slope of 2.5 in the negative x-direction. The large number of battered piles were put in the initial design to resist the large lateral forces caused by the backfill.

The loadings on the lock structure are the normal operating conditions, the construction loading, maintenance loadings, and earthquake loadings. The lock is subject to a wide variety of loadings. Over 150 load cases exist. Analysis would be difficult if all the load cases were applied, and the optimization would be infeasible. Most of the load cases are not expected to be active and can be

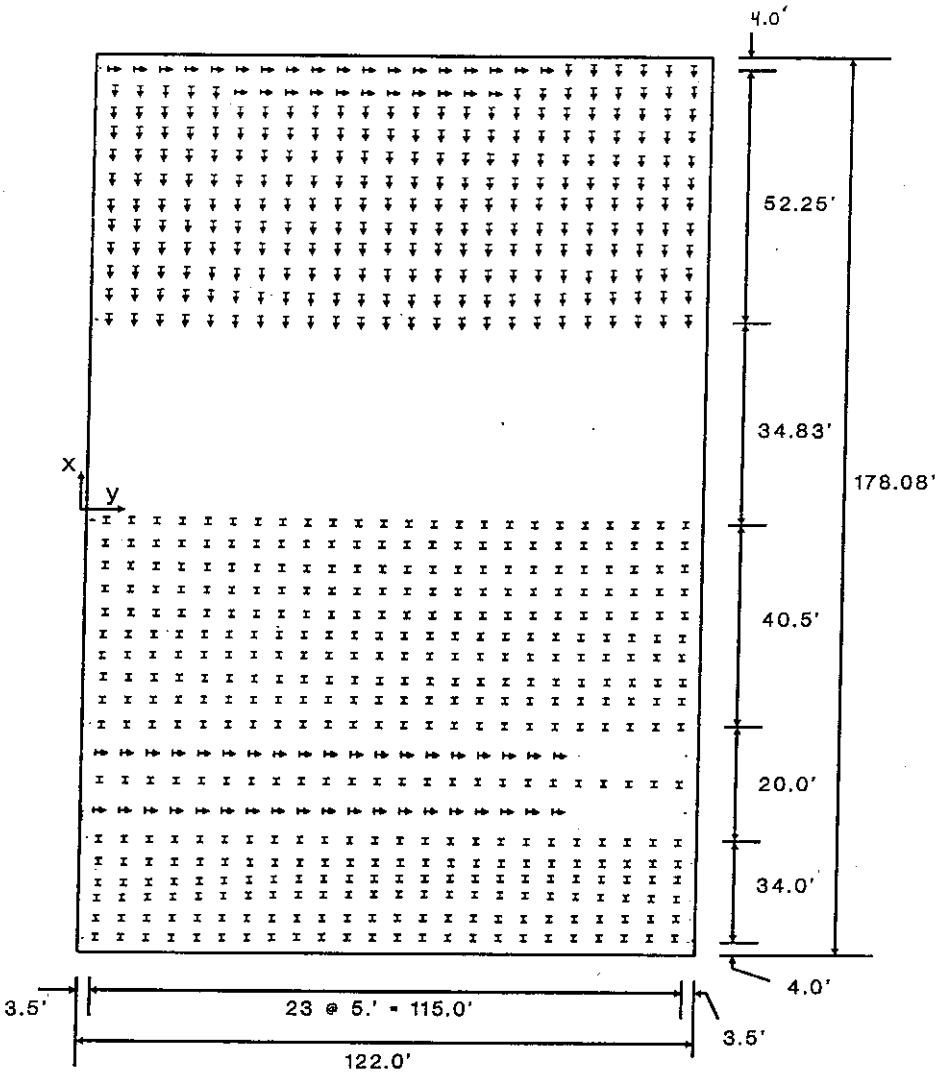

Figure 5-16. Constructed Pile Layouts.

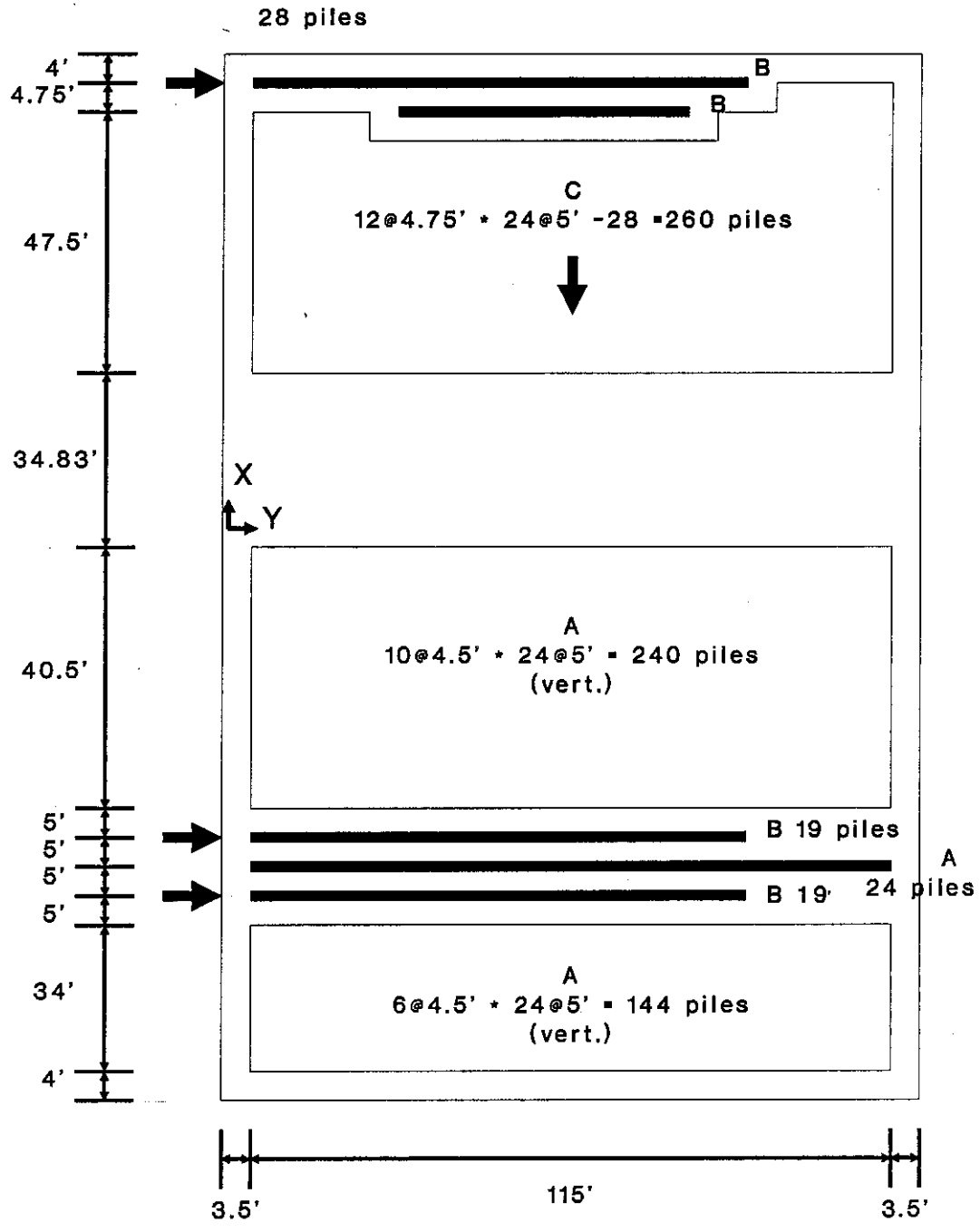

Figure 5-17. Initial Pile Layouts for AL-3.
Arrows indicate batter.

eliminated. Many of the load cases are very similar to other load cases and therefore do not significantly change the results. The previous designers narrowed the load case list to 20 cases. The list has been further narrowed to eight cases. The load cases and a brief description of the case is shown in Table 5-13.

Table 5-13. Description of the Lock Load Cases.

Number	Description
IA (101)	Construction
IIB1 (201)	Normal Operation, Pools at 419 and 395 ft., Upper pool in the lock, maximum uplift.
IIB2 (202)	IIB1 with down drag caused by the backfill.
IIC1 (203)	IIB1 with minimum uplift.
IIC2 (204)	IIC1 with down drag caused by the backfill.
IID1 (205)	Normal Operation, Pools at 419 and 395 ft., Lower pool in the lock, Minimum uplift.
IID2 (206)	IID1 with down drag caused by the backfill.
IIIA (301)	Extreme Maintenance, Lock dewatered with the upstream bulkhead in place.

The load cases have many components. The largest components of the load cases generally are the dead weight, the lateral and vertical force of the backfill, and the effects of the water on the side, top, and underside of the lock. The concrete monoliths have a dead weight which is computed given the monolith thickness, density, and number of voids. The backfill on the Illinois side has significant lateral and vertical components. The vertical component is called down drag. The backfill pressures are chiefly caused

by the soil but are also caused by water seepage. Therefore the backfill force can be different for each load case.

The water causes seven kinds of loading: chamber loads, side pressures, uplift pressures, miter gate forces, bulkhead forces, culvert pressures, and pressures in the joints between the monoliths. The side pressures on the exposed surfaces of the lock are due to the water acting laterally against the lock. The chamber loads are applied when the water is in the chamber. The chamber loads have components acting downward upon the floor and side pressures on the inside of the chamber. The uplift pressures are due to water lifting up the lock from the underside. The uplift pressure usually varies linearly from front to back because of the varying pool elevations. The miter gate and bulkhead forces are due to water acting laterally against them. These devices also have their own self weight. The monoliths have construction joints between them. For example, water may seep into the joint between monoliths AL-2 and AL-3. The side pressure load can vary linearly along the exterior surface. This is because the AL-3 monolith is abutted by dam section D-1. The Dam tainter gate may be open which would cause the water to go through a hydraulic jump on the spill way. This causes a linearly varying side load. Alternatively the tainter gate could be closed and silt could collect on the side of the monolith.

Load cases are grouped into normal operating and extreme cases. The design criteria is made more lenient for the extreme cases. An overstress factor of 1.33 is allowed for the extreme cases and earthquake cases.

Analysis and Optimization:

The initial design was analyzed by Black & Veatch engineers using STRUDL (13). The pile design met there criteria for acceptance. A design is acceptable if its stress and displacements are below allowable limits and the design is constructable. The initial design is overstressed in the normal operating cases. Eighty piles in load case 203 are overstressed. This is acceptable because the piles are only slightly overstressed, by a factor of 1% to 5%. The deflection criteria is very strict in order to maintain compatibility between the adjoining monoliths. Displacements are limited to 0.3 inches, and 0.5 inches in the normal, and extreme load cases, respectively.

The goal of the optimization was to reduce the cost of the structure while maintaining stress and displacement criteria, and constructability. The optimization is capable of changing all properties of the pile design to produce a lower cost design. The unvariable parameters are the site specific soil properties and the lock monolith shape. The optimization varied the pile size, the number of piles, the batter of the piles, the pile fixity, the orientation angles theta and phi, and the positions of the pile groups.

The optimization began from an initial design that is very similar to the Black & Veatch design. The number of piles and orientations were the same but the positions of the piles were slightly altered so that five pile groups could be formed. The initial pile group positions are shown in Figure 5-18. The initial pile data is shown in Tables 5-14 and 5-15.

Table 5-14. Initial lock pile properties.

Group	Number Piles	I_{xx} (in^4)	Batter	ϕ (deg.)	θ (deg.)	fixity
A(1)	168	1220.	100.	180.	0.	fixed
B(2)	38	1220.	2.5	90.	0.	fixed
C(3)	240	1220.	100.	180.	0.	fixed
D(4)	260	1220.	2.5	180.	0.	fixed
E(5)	28	1220.	2.5	90.	0.	fixed

Table 5-15. Initial lock pile positions.

Group	x_{low} (ft)	x_{high} (ft)	y_{low} (ft)	y_{high} (ft)
A(1)	-85.	-58.	3.5	118.5
B(2)	-53.	-48.	3.5	95.
C(3)	-43.	-2.	3.5	118.5
D(4)	32.	75.	3.5	118.5
E(5)	80.	85.	3.5	95.

The number of piles decreased from 734 to 501 and the weight of steel reduced from 6.13 to 2.97 million lbs in ten iterations. See Figure 5-19. The optimization had not reached convergence, because the optimization reached the

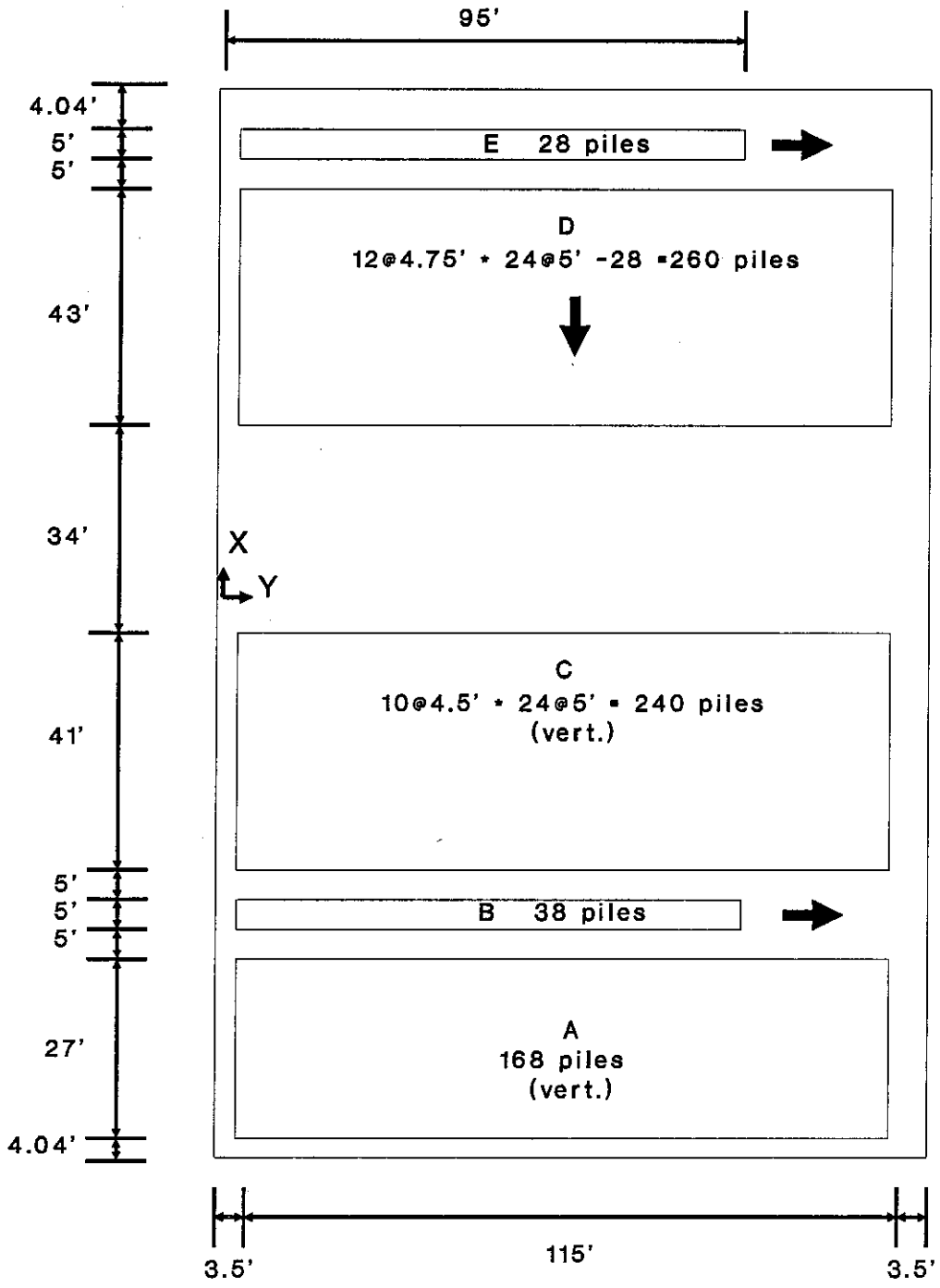

Figure 5-18. Initial pile layouts for optimization. Arrows indicate batter.

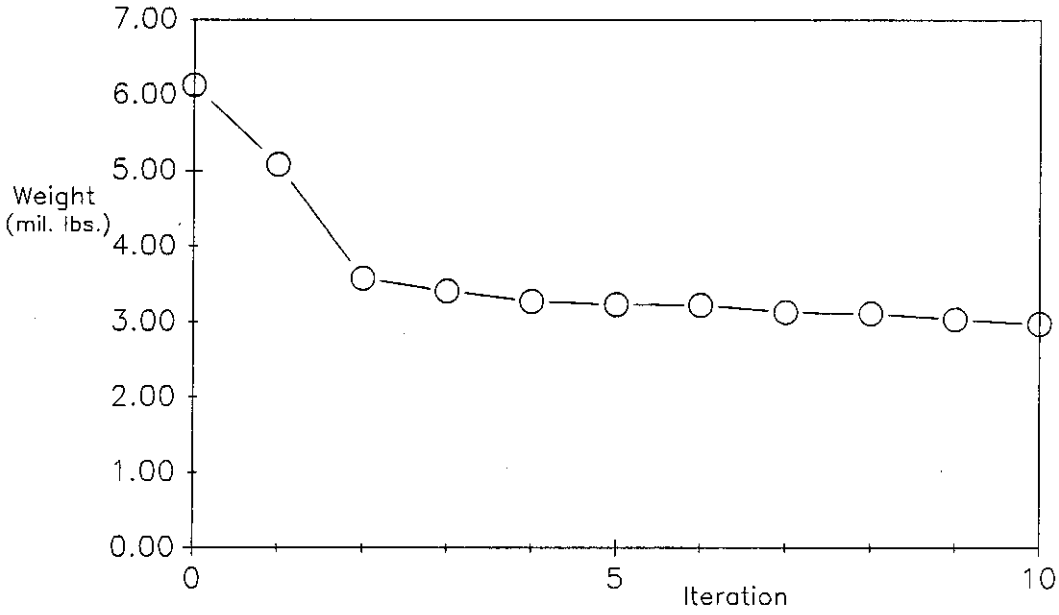

Figure 5-19. Weight convergence of AL-3.

maximum number of iterations allowed. A small additional weight savings may result if the optimization is continued.

The optimized pile layouts are shown in Figure 5-20, and Tables 5-16 and 5-17. Most of the piles are battered in the negative x direction. These piles resist the embankment loads. Previously only one group of piles resisted the embankment. The piles do not intersect each other and do not extend beyond the edges of the slab. The piles are typically constructed with the angle phi parallel to the global coordinate system. The piles in the optimized design are not parallel to the coordinate systems but are orientated in the optimal directions. The optimal design may encourage the common construction methods to be altered.

Table 5-16. Optimized lock pile properties.

Group	Number Piles	I_{xx} (in^4)	Batter	ϕ (deg.)	θ (deg.)	fixity %fixed
A(1)	131	930.	3.50	148.	0.	fixed
B(2)	20	936.	2.00	146.	90.	51%
C(3)	160	729.	5.38	336.	0.	fixed
D(4)	157	729.	2.00	169.	0.	fixed
E(5)	33	1161.	10.9	155.	0.	pinned

The cross-section sizes are not available from a fabricator, and the percentage variables are not 0 or 100%. These variables need to be made discrete by a branching process. A branch and bound procedure could take up to a month on a Sun station for this example so it was not

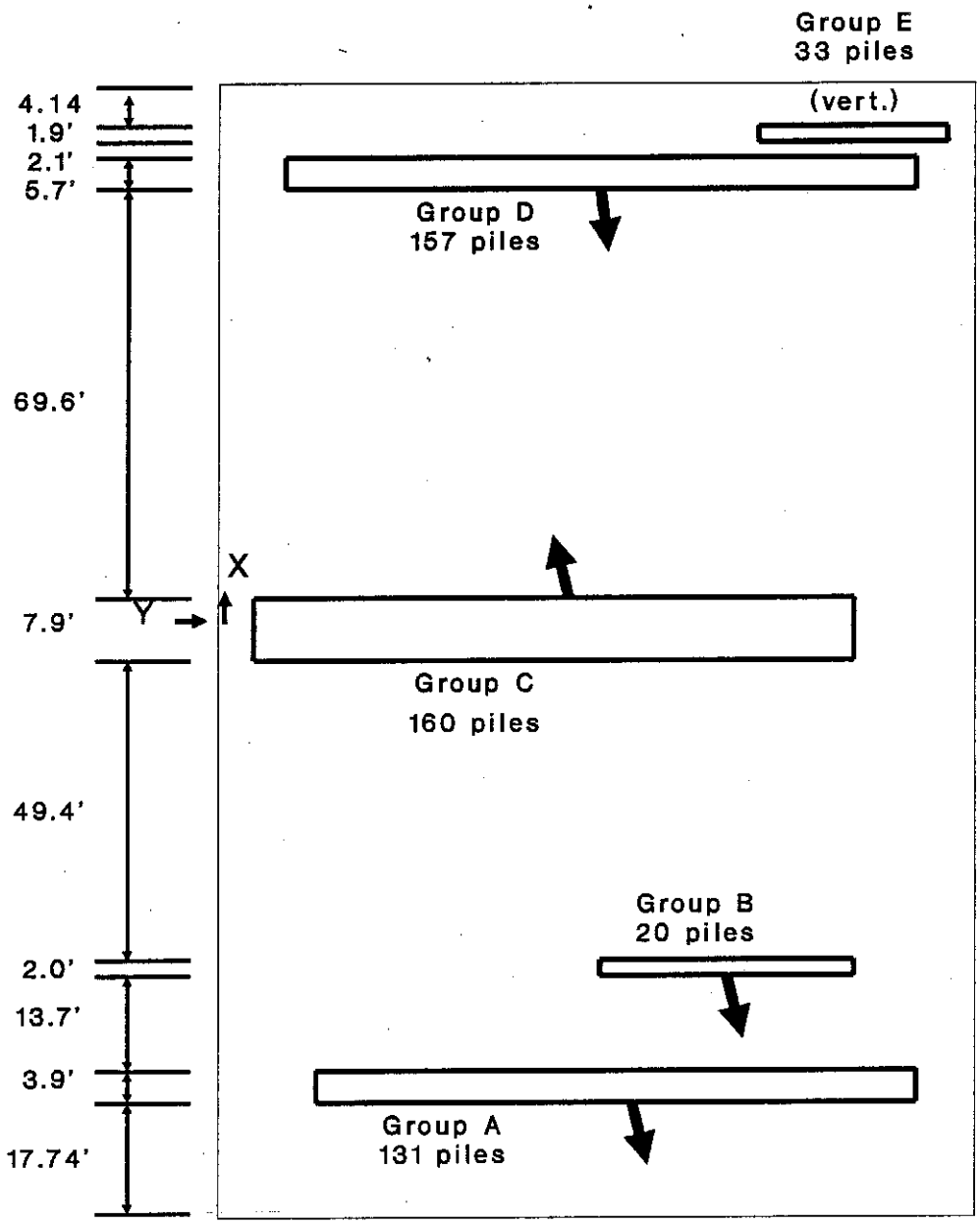

Figure 5-20. Optimized pile layouts for AL-3. Arrows indicate batter.

performed. A rounding process was used. The design parameters are rounded to nearby values and a branching is performed on the not easily roundable parameters.

Table 5-17. Optimized lock pile positions.

Group	x_{low} (ft)	x_{high} (ft)	y_{low} (ft)	y_{high} (ft)
A(1)	-71.3	-67.4	14.6	110.6
B(2)	-53.7	-51.7	70.7	101.6
C(3)	-2.3	5.6	6.2	99.8
D(4)	75.2	80.9	11.6	114.2
E(5)	83.0	84.9	87.0	118.3

The results from the rounding and reoptimizing are shown in Tables 5-18, and 5-19, and Figure 5-21. The final weight of steel is 3.26 mil. lbs. The design was penalized 0.29 mil. lbs for making the design discrete. The number of piles increased from 501 to 557 piles during the reoptimization. Making a design discrete places restrictions on a design such as requiring that the piles must have available sizes. The amount of steel increases because restrictions can only cause an increase in the cost of the design.

The optimization accurately controlled all of the constraints. An example of this is the stress analysis. One pile was overstressed in load case four by less than 1%. All stresses in the other piles were controlled.

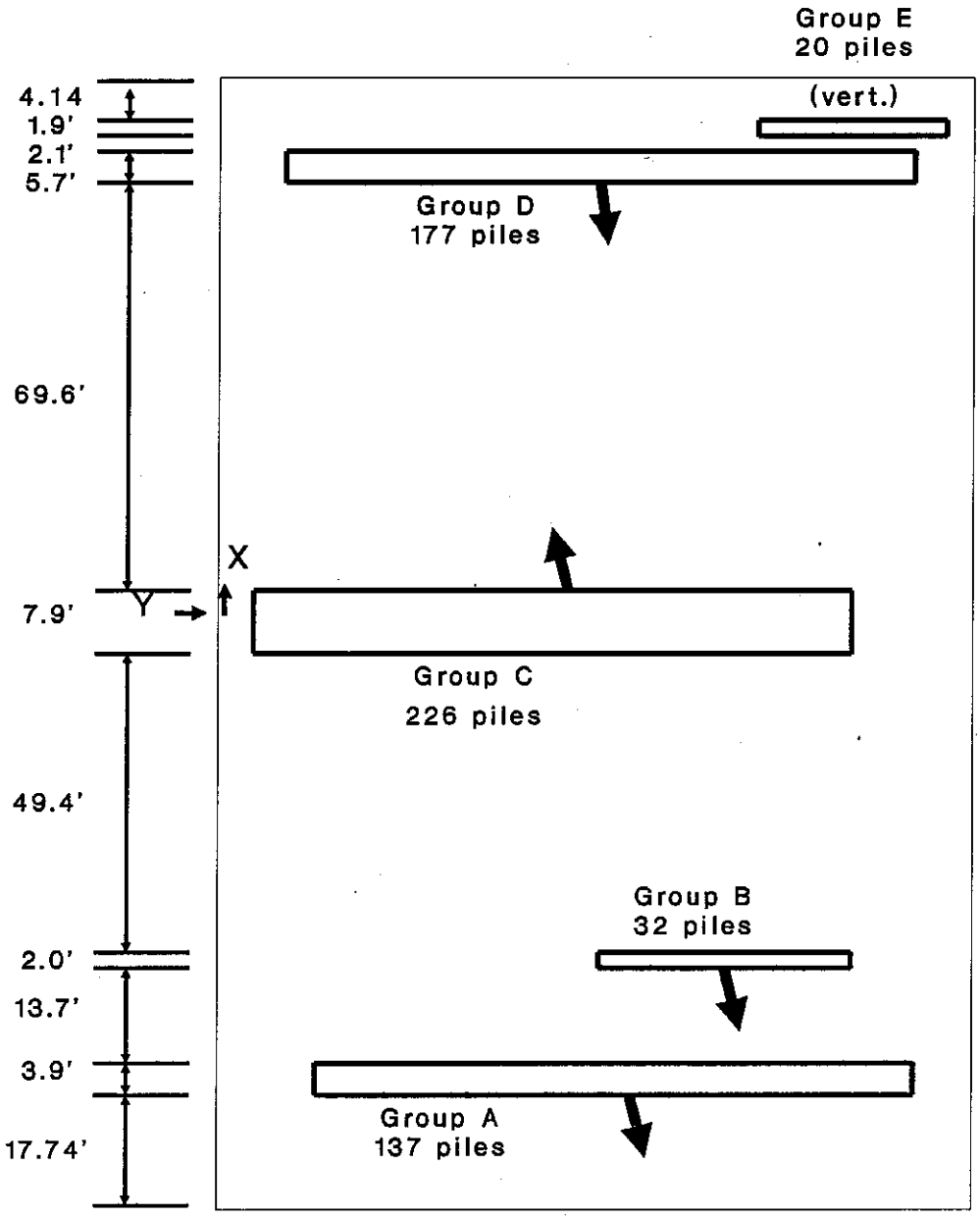

Figure 5-21. Final pile layouts for AL-3.
Arrows indicate batter.

Table 5-18. Final lock pile properties.

Group	Number Piles	I_{xx} (in^4)	Batter	ϕ (deg.)	θ (deg.)	fixity
A(1)	152	904.	3.54	149.	0.	fixed
B(2)	25	904.	2.15	143.	90.	fixed
C(3)	180	729.	5.12	337.	0.	fixed
D(4)	171	729.	2.00	169.	0.	fixed
E(5)	29	1220.	6.51	165.	0.	pinned

Table 5-19. Final lock pile positions.

Group	x_{low} (ft)	x_{high} (ft)	y_{low} (ft)	y_{high} (ft)
A(1)	-71.3	-67.4	14.6	110.6
B(2)	-53.7	-51.7	70.7	101.6
C(3)	-2.3	5.6	6.2	99.8
D(4)	75.2	80.9	11.6	114.2
E(5)	83.0	84.9	87.0	118.3

The discrete design is similar to the originally optimized design. The pile orientations and positions have not significantly changed. The number of piles in each group changed. Group 5 (or E) had an optimized pile inertia of 1161 in^4. This inertia was rounded upward to 1220 in^4. The reoptimization reduced the number of piles in the group from 33 to 29 piles. Therefore, the amount of steel in the fifth group did not change significantly. The rounding of the pile size caused the forces to redistribute in the analysis. The result was that the number of piles in each of the other groups increased. The fixity of group 2 (or B)

was rounded from partially fixed to fully fixed. This caused the piles in group 2 to be less efficient. The result of this was that the number of piles in group 2 increased from 20 to 25 piles.

Five load cases were applied to the design: 203, 204, 205, 301 and 101. It is thought that these load cases will be the active load cases in the optimization. It is possible that some of the other 150 load cases became active. If this design was going to be used in the field testing of more of the load cases upon the final optimal design may be warranted.

The optimization very dramatically reduced the weight of steel in the structure, and it accurately controlled the design limits. The example demonstrated that the optimization can produce efficient designs using an automated procedure.

5.3.1 RIGID ANALYSIS OF AL-3

The analysis and optimization of AL-3 is repeated using a rigid slab analysis. A rigid slab analysis is easier and quicker, but it will be shown that it can be highly inaccurate. This example demonstrates that the type of analysis significantly changes the results. The type of analysis affects the optimization results.

The rigid slab method does not require input of slab properties. The input loads have only six components. The applied loads are the summation of the loads across the structure. For example, the vertical finite element loads are summed to produce the total rigid body load. The analysis is much quicker with a rigid analysis than with a finite element method. The rigid analysis has six degrees of freedom and the finite element mesh can have 1000 degrees of freedom.

The analysis results are much different than with the finite element method. The rigid slab analysis smooths the loads. The finite element loads have high gravity loads under the lock walls, and uplift loads under the chamber. The edges sink downward and the central chamber is lifted up in load case 301. The rigid analysis method smooths the displacements. The average displacement is downward. Many piles have had stress reversals in the rigid analysis compared to the flexible analysis. For example, in load case 204 the flexible analysis shows that 174 piles are in

tension, the rigid analysis shows that 25 piles are in tension. The central piles that were previously in tension are now in compression. Pile 446 had a flexible analysis force of -25.7 kips (tension), but with a rigid analysis had a force of 29.5 kips (compression). This is a dramatic change in analyzed behavior.

Optimization:

The AL-3 lock pile foundations was optimized using a rigid analysis. The results are much different than those for the flexible slab analysis and optimization. The smoothing of the displacements reduces the average stress on the piles. The piles can therefore reduce in size and number below an acceptable level.

The initial pile design is the same as the initial flexible analysis design. The optimized pile design is shown in Figure 5-22, and Tables 5-20 and 5-21. The weight of the steel decreased from 6.13 to 2.41 million lbs in ten iterations. This weight is dramatically below the flexible slab optimized weight. This suggests that the rigid design could be overstressed.

All of the stress criteria are satisfied in the rigid analysis. The final design of the rigid slab optimization was analyzed using the flexible slab analysis. The flexible analysis showed that the design is unacceptable. All of the piles in every load case are overstressed. For example pile

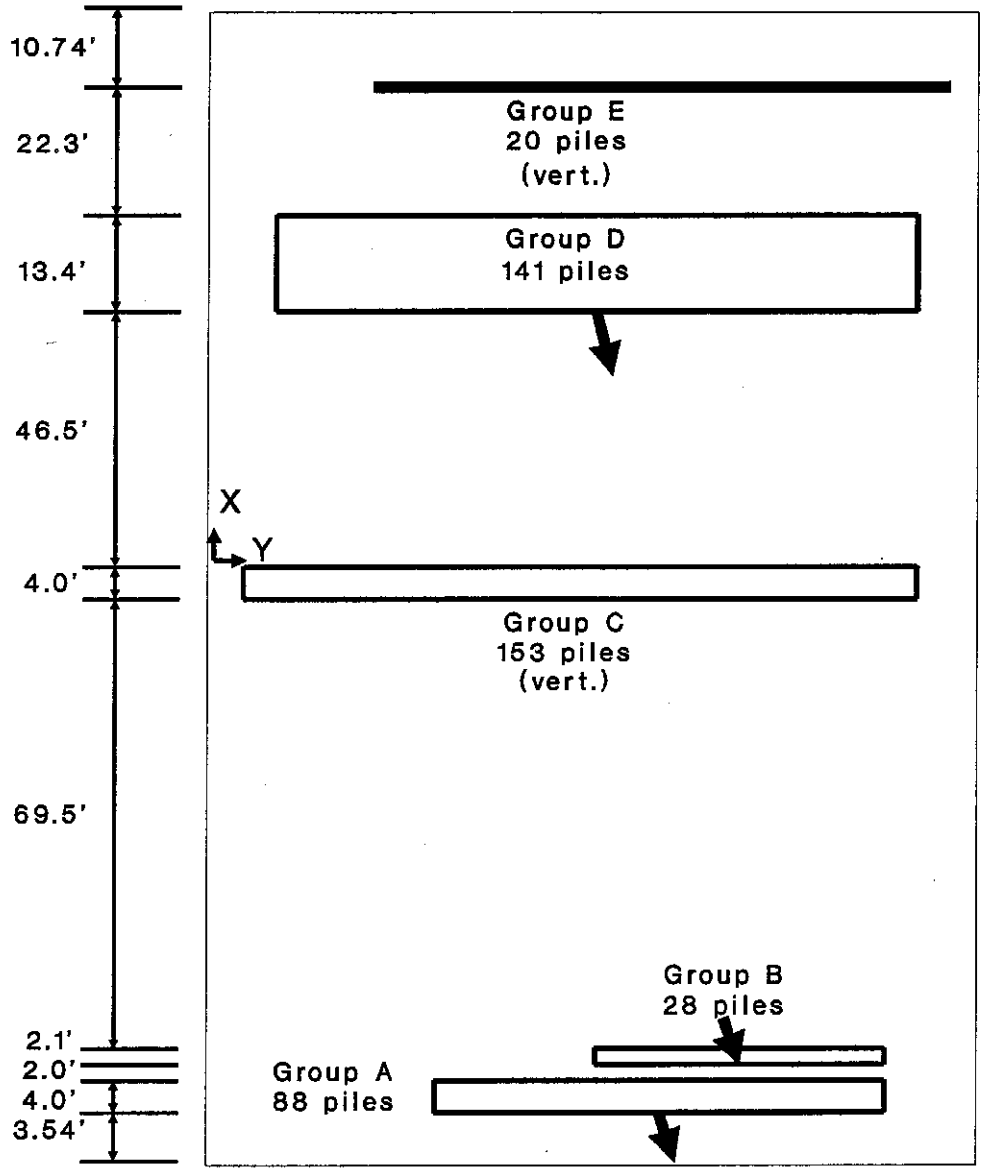

Figure 5-22. Rigid slab optimization.
Arrows indicate batter.

1 in load case 3 has a force to allowable force ratio of 7.73.

The analysis shows that a rigid optimization produces a design that is not acceptable when checked with a flexible analysis. This example demonstrates that although the rigid optimization is quick it is not appropriate for many examples. The flexible slab analysis method should be used for analysis and optimization.

Table 5-20. Optimized rigid slab analysis pile properties.

Group	Number Piles	I_{xx} (in^4)	Batter	ϕ (deg.)	θ (deg.)	fixity
A(1)	88	748.	2.00	154.	90.	fixed
B(2)	28	931.	2.00	154.	90.	fixed
C(3)	153	749.	27.1	327.	90.	fixed
D(4)	141	729.	2.15	163.	90.	62% f.
E(5)	20	871.	100.	79.	0.	56% f.

Table 5-21. Optimized rigid slab analysis pile positions.

Group	x_{low} (ft)	x_{high} (ft)	Y_{low} (ft)	Y_{high} (ft)
A(1)	-85.5	-81.5	42.5	106.2
B(2)	-79.5	-77.4	64.3	105.5
C(3)	-7.9	-3.9	5.2	110.8
D(4)	42.6	56.0	7.8	111.6
E(5)	78.2	78.4	27.5	113.9

6. SUMMARY AND CONCLUSIONS

6.1 SUMMARY OF EXAMPLES

A retaining wall was optimized. A segment of the wall was analyzed as a two-dimensional strip. The wall was optimized with two methods: the individual pile, and pile group optimization. The individual pile optimization allowed each pile to have its own size and orientation. The group optimization found the optimum number of piles in each group by allowing the number of piles to vary as a real number. The group method or stiffness multiplier method was developed specifically for pile optimization. Both the individual and group methods significantly reduced the weight of the steel and the cost of the design. The most beneficial results were obtained by coupling the optimization methods. A group optimization was performed to find the number of piles which was followed by an individual pile optimization to find their final sizes and orientations. This can be done only for examples with a small number of piles.

The number, sizes, orientations, and fixity of the piles under the wall were varied. The pile fixity and angle theta are discrete variables. The piles were allowed to be pinned or fixed, and theta was allowed to be 0 or 90 degrees. These variables each can have only two values. A new percentage method was developed for these variables.

The method varied the discrete values as percentages which resulted in large computation time savings.

An existing dam structure was optimized. The optimization roughly halved the weight of steel in the design. All of the pile properties were variable. The design quickly converged to a discrete (useable) design. A branch and bound optimization was not required. This example demonstrates that the optimization method can be applied to actual structures to produce large cost savings. This example also demonstrates the effectiveness of the percentage optimization, and pile group optimization methods.

The AL-3 segment of Lock and Dam 26R was optimized. The construction of the Lock and Dam is currently being completed. The pile design of the lock was optimized which greatly reduced the number of piles and the total weight of steel under the lock. The weight of steel decreased 43% from the initial design to the final design.

The original designers of the lock allowed small over-stresses in the piles because of the difficulty of finding a useable design. The optimization very accurately controlled the stresses in the piles. A majority of the piles are fully stressed in one or more load cases. This is a good measure of the effectiveness of an optimization procedure.

The program OPTPILE took two days of real-time on a

Sunstation to optimize the lock design. The results were worth the computer resources.

The examples had design limits of various types. The limits or constraints were: maximum stress, maximum displacement, limits on the pile sizes, and limits on the placement and orientation of the piles. The optimization very accurately controlled the these limits. Constraints that were initially violated quickly moved to acceptable levels.

6.2 CONCLUSIONS

Several optimization methods were developed to enable the optimization of steel piles under concrete slabs. The optimization produced large savings in every example. The optimization method is adaptable so that it can optimize walls, dams, and locks, using rigid or flexible analysis methods. The AL-3 lock example demonstrates the usefulness of the optimization procedures. The AL-3 segment is one segment of a Lock structure. If the optimization methods were applied to the other portions of the lock project or to other projects then possible savings would result.

A method of assembling piles into a finite element was developed. Previously the finite element mesh spacing was determined by the pile spacing which caused the element mesh to be overly fine. The program STRUDL allows the piles to be offset from a node. The pile could be connected rigidly to an adjacent node. This allows the piles to be placed

within the elements. The new method of pile assembly allows the piles to be assembled by the shape functions. The piles are assembled to all the nodes of the element instead of one node. The assembly method allows the finite element mesh to be much coarser and quickens the computing time for performing an analysis.

The stiffness multiplier or group optimization method is a new method to vary the number of piles. The stiffness multiplier method is the first attempt to vary the number of structural members as real variables. The stiffness multiplier method involves changes in analysis and optimization. The piles are analyzed by adjusting the stiffness of the assembled piles by a multiplier. This method has proven to be the most effective method to eliminate unnecessary piles. Another possible method that was considered reduces the area of single piles until they are deleted. This is not possible with grouped piles or variables. The single pile elimination method also had difficulties with minimum variable sizes and local optimums. The group method is more effective.

A percentage method was developed to optimize discrete variables. The percentage method can be applied to variables with two or more distinct options. The percentage method uses the weighted average of the options to form the pile properties. The percentage method is usually a very quick method to find the optimum of discrete variables. The

wall example demonstrated that a factor of 146 in computation time could be saved compared to a search. The computational savings increases for larger examples. It was previously impossible to find a guaranteed global optimum of discrete variables. The number of computations was too large for realistic examples. The percentage method was shown to be a useful tool for optimization, and has great potential for use in other structural optimization problems.

The optimality criteria optimization formulation has been applied to topological variables. The optimality criteria method is a very effective method of optimization which can now optimize all types of variables. Previously Hoback and Truman (8) discovered that the coordinate systems of topological variables must be placed such that the weight gradients are positive. Topological variables may have zero-valued weight gradients. An additional optimality criteria has now been developed for these variables. This allows the optimality criteria method to be applied to a greater variety of problems.

The program OPTPILE was written specifically for the optimization of rigid and flexible steel pile structures. It was written in a user friendly manner. The input format is simpler than other analysis programs such as STRUDL. The program OPTPILE may be used as a tool for analysis and optimization.

6.3 FURTHER RESEARCH

Only steel HP-14 piles were optimized in this project. Some pile foundations use driven timber piles and driven or cast-in-place concrete piles. These types of piles could be optimized. This would require programming the allowable load equations for these materials. A subprogram to generate circular or rectangular cross-sections is also required.

The thickness or shape of the concrete monoliths could be simultaneously optimized with the pile foundations. The program OPTPILE can be applied to any foundation that consists of a concrete slab supported by piles. Superstructures can be placed on the foundations. The analysis of superstructures could be coupled with the slab analysis.

The analysis of earthquake and other dynamic loads in OPTPILE is currently limited to applying statically equivalent loads. This may not always be sufficient. The analysis could consider dynamic loads.

The soil has non-linear resistance but properties are idealized as linear. Currently the maximum expected displacements on the piles are used to find the equivalent soil tangent modulus. A non-linear analysis method could be used to more accurately model the soil properties and their effects on the pile foundations.

The group effect on the soil properties should change as the number or spacings of the piles changes. This is not modeled. The input soil properties are considered to be constant throughout optimization.

The program OPTPILE uses free format input in the pattern of the program CPGA. OPTPILE could become more user-friendly by having a graphical windows environment for input and output of data.

Currently OPTPILE requires initial pile data to be input. An accurate guess of a good design is not required. OPTPILE may be programmed to generate an initial pile design. This could be done by having OPTPILE sum the forces in each region of the structure. The initial number of piles would be the load divided by the capacity of an average pile.

7. ACKNOWLEDGEMENT

The author wishes to thank the US Army Corps of Engineers for partially funding this work under contract number DACW39-92-C-0053. The author would like to express his appreciation to Dr. Kevin Z. Truman, Associate Professor of Civil Engineering, at Washington University in St. Louis, for his guidance in conducting this research. The author would like to thank Dr. Gould, Chairman of the Department of Civil Engineering, for supporting him. Finally, the author wishes to thank his parents for encouraging and supporting his education.

APPENDICES

8. APPENDIX 1: PILE GROUP BEHAVIOR

The rigid body slab analysis method, the pile stiffness formulations, and the pile stress evaluation method is shown. These methods have been fully developed before the beginning of this optimization research. The analysis method presented here is a condensation of the materials found in BASIC PILE GROUP BEHAVIOR (11) and User's Guide (6). For a more complete discussion of the pile group analysis method see these references. A computer program, CPGA, was provided by the US Army Corps of Engineers which performs analyses based upon this method.

8.1 RIGID BODY CONCRETE SLAB ANALYSIS METHOD

The analysis method is developed for the static analysis of linearly elastic pile foundations. Certain thick foundations can be analyzed with a rigid body pile cap. The pile cap is not allowed to be flexible. Therefore the pile cap has only six degrees of freedom. The freedoms are the three translations and the three rotations.

The six pile cap displacements are found by inverting the 6 by 6 stiffness matrix:

$$\boldsymbol{D} = \boldsymbol{S}^{-1}\,\boldsymbol{P} \qquad \text{(A1.1)}$$

where **D** is the displacements at the global coordinate system, **S** is the global stiffness matrix and **P** is the global applied forces.

The displacements at a pile D_{GP} is related to **D** by the transformation matrix **C**:

$$D = C\, D_{GP} \tag{A1.2}$$

Given small rotations:

$$C = \begin{bmatrix} 1 & 0 & 0 & 0 & 0 & 0 \\ 0 & 1 & 0 & 0 & 0 & 0 \\ 0 & 0 & 1 & 0 & 0 & 0 \\ 0 & -Z & Y & 1 & 0 & 0 \\ Z & 0 & -X & 0 & 1 & 0 \\ -Y & X & 0 & 0 & 0 & 1 \end{bmatrix} \tag{A1.3}$$

The rotations at the global coordinate system cause x,y, and z displacements at the piles.

The displacements in the local coordinate system of the pile D_L are related to the displacements in global coordinates:

$$D_{GP} = A\, D_L \tag{A1.4}$$

where:

$$A = A_{\phi\beta}\, A_{\theta} \tag{A1.5}$$

$$A_{\theta} = \begin{bmatrix} \cos\theta & \sin\theta & 0 & 0 & 0 & 0 \\ -\sin\theta & \cos\theta & 0 & 0 & 0 & 0 \\ 0 & 0 & 1 & 0 & 0 & 0 \\ 0 & 0 & 0 & \cos\theta & \sin\theta & 0 \\ 0 & 0 & 0 & -\sin\theta & \cos\theta & 0 \\ 0 & 0 & 0 & 0 & 0 & 1 \end{bmatrix}^T \tag{A1.6}$$

$$A_{\phi\beta} = \begin{bmatrix} \cos\phi\cos\beta & -\sin\phi & \cos\phi\sin\beta & 0 & 0 & 0 \\ \sin\phi\cos\beta & \cos\phi & \sin\phi\sin\beta & 0 & 0 & 0 \\ -\sin\beta & 0 & \cos\beta & 0 & 0 & 0 \\ 0 & 0 & 0 & \cos\phi\cos\beta & -\sin\phi & \cos\phi\sin\beta \\ 0 & 0 & 0 & \sin\phi\cos\beta & \cos\phi & \sin\phi\sin\beta \\ 0 & 0 & 0 & -\sin\beta & 0 & \cos\beta \end{bmatrix} \quad \text{(A1.7)}$$

and:

$$\beta = \tan^{-1}\left(\frac{1}{batter}\right) \quad \text{(A1.8)}$$

The pile stiffness matrix **B** relates the local forces $\mathbf{F}_L$ and displacements $\mathbf{D}_L$:

$$F_L = B\, D_L \quad \text{(A1.9)}$$

The contribution to the global stiffness matrix from one pile is found by substitution of the above equations.

$$P = S_{onepile} D \quad \text{(A1.10)}$$

$$C\, A\, B\, D_L = S_{pile}\, C\, A\, D_L \quad \text{(A1.11)}$$

$$S_{pile} = C\, A\, B\, [C\, A]^T \quad \text{(A1.12)}$$

The global stiffness is the sum over all the piles:

$$S = \sum_{IPILE}^{NP} C\, A\, B\, [C\, A]^T \quad \text{(A1.13)}$$

8.2 PILE STIFFNESS

The pile group stiffness coefficients are calculated in the manner of Saul (18). A beam on an elastic foundation

theory is used to find the lateral pile stiffness. The pile and soil interaction is represented at the head of the pile by a linearly elastic pile stiffness. The global stiffness matrix is calculated by assembling the coefficients of all piles.

An analytical method to evaluate the pile stiffnesses is shown. This method requires that the soil modulus can be accurately modeled as having a soil modulus which is either constant or linearly increasing with depth. More complex methods may involve a computer solution for multi-layered soils, nonlinear variation of the soil modulus, and inelastic soil behavior.

The pile is represented in the analysis by the resulting stiffness at the head of the pile. The stiffness of the pile has six degrees of freedom, or five degrees of freedom when torsional pile stiffness is neglected. The non-zero stiffness terms and the stiffness coupling terms are:

$$\boldsymbol{b} = \begin{bmatrix} b_{11} & 0 & 0 & 0 & b_{15} & 0 \\ 0 & b_{22} & 0 & b_{24} & 0 & 0 \\ 0 & 0 & b_{33} & 0 & 0 & 0 \\ 0 & b_{42} & 0 & b_{44} & 0 & 0 \\ b_{51} & 0 & 0 & 0 & b_{55} & 0 \\ 0 & 0 & 0 & 0 & 0 & b_{66} \end{bmatrix} \qquad \textbf{(A1.14)}$$

The lateral stiffnesses as shown in Table 8-1.

Table 8-1. Pile Stiffness Coefficients.

Pile Stiff. Coeff.	Constant E_s	Lin. Var. E_s
b_{11}	$C_1 \frac{EI_2}{R_2^3}$	$C_1 \frac{EI_2}{T_2^3}$
b_{22}	$C_1 \frac{EI_1}{R_1^3}$	$C_1 \frac{EI_1}{T_1^3}$
b_{44}	$C_1 \frac{EI_1}{R_1}$	$C_1 \frac{EI_1}{T_1}$
b_{55}	$C_1 \frac{EI_2}{R_2}$	$C_1 \frac{EI_2}{T_2}$
b_{15}, b_{51}	$C_1 \frac{EI_2}{R_2^2}$	$C_1 \frac{EI_2}{T_2^2}$
b_{24}, b_{42}	$-C_1 \frac{EI_1}{R_1^2}$	$-C_1 \frac{EI_1}{T_1^2}$

The stiffness parameters are defined as:

$$T_1 = \left(\frac{EI_1}{n_h}\right)^{\frac{1}{5}} \quad (inch) \qquad \textbf{(A1.15)}$$

$$T_2 = \left(\frac{EI_2}{n_h}\right)^{\frac{1}{5}} \quad (inch) \qquad \textbf{(A1.16)}$$

$$R_1 = \left(\frac{EI_1}{E_s}\right)^{\frac{1}{4}} \quad (inch) \qquad \textbf{(A1.17)}$$

$$R_2 = \left(\frac{EI_2}{E_s}\right)^{\frac{1}{4}} \quad (inch) \qquad \textbf{(A1.18)}$$

C_1 = pile fixity constant

E_s = horizontal soil modulus. (lb/in^2)

n_h = change in the soil modulus with depth. (lb/in^3)

E = modulus of elasticity of pile. (lb/in^2)

I_j = moment of inertia of pile for local axis j. (in^4)

The Fixity constants, C_1, are listed in Table 8-2 as shown by Dawkins. (19)

Table 8-2. Pile Fixity Constants. (C_1) For Soils With Constant or Linear Variation of Soil Modulus.

Pile Stiffness Coeff.	Constant E_s		Linear Varying E_s	
	Fixed	Pinned	Fixed	Pinned
b_{11}	2.0	1.0	1.075	0.411
b_{22}	2.0	1.0	1.075	0.411
b_{44}	1.0	0	1.5	0
b_{55}	1.0	0	1.5	0
b_{15}	1.0	0	1.0	0
b_{24}	1.0	0	1.0	0
b_{42}	1.0	0	1.0	0
b_{51}	1.0	0	1.0	0

AXIAL STIFFNESS

The two methods of transfer of axial force to the ground are skin friction and pile tip bearing. The axial pile stiffness varies depending upon the assumed method of transfer. The axial stiffness for pure tip bearing is equal

to the stiffness of a supported column (AE/L). This is shown in Table 8-3. The theoretical skin friction stiffness assumes that no force is transferred in bearing, therefore the effective column length is (L/2) and the stiffness is (2AE/L). The true stiffness is (KAE/L) where K ranges over 1.0 to 1.75.

The axial stiffness is a function of the direction of loading. A pile loaded in tension has less stiffness than a pile loaded in compression. The tension stiffness is reduced by about one half.

Table 8-3. Axial Pile Stiffness Coefficients.

Condition	b_{33}
Compressive load, end bearing pile	$\frac{AE}{L}$
Compressive load, friction pile	$\frac{2AE}{L}$

TORSIONAL STIFFNESS

The torsional stiffness of a pile has a negligible effect on the analysis for pile designs containing more than 10 piles. The pile torsional stiffness is neglected for analysis of piles under a flexible slab system. For smaller problems the stiffness can be taken as:

$$b_{66}=C_T\frac{JG}{L} \qquad \textbf{(A1.19)}$$

where:

C_T = constant of distribution of torsional shear to the soil and the transfer of torsional shear resistance from the pile to the structure.

J = pile polar moment of inertia.

G = shearing modulus of elasticity.

L = pile length.

POINT OF MAXIMUM MOMENT

The point of maximum moment in a pile is dependant upon the soil conditions and the fixity of the pile to the cap. Pinned piles do not have a moment at the top of the piles. The pinned piles have a moment beneath the soil which is caused by the lateral forces. The moments are approximated as a constant times the lateral force:

$$M1 = KMP1\ F2 \qquad \textbf{(A1.20)}$$

$$M2 = KMP2\ F1 \qquad \textbf{(A1.21)}$$

where
M1,M2 = design moments
F1,F2 = lateral forces
KMP1,KMP2 = constants found in Table 8-4.

Table 8-4. Pinned Pile Design Moment Factors.

Soil type	KMP1	KMP2
n_h	0.772 T_1	-0.772 T_2
E_s	0.455 R_1	-0.455 R_2

where:

$$T_1 = \left(\frac{EI_1}{n_h}\right)^{\frac{1}{5}} \quad (inch) \qquad T_2 = \left(\frac{EI_2}{n_h}\right)^{\frac{1}{5}} \quad (inch)$$

$$R_1 = \left(\frac{EI_1}{E_s}\right)^{\frac{1}{4}} \quad (inch) \qquad R_2 = \left(\frac{EI_2}{E_s}\right)^{\frac{1}{4}} \quad (inch)$$

8.3 DESIGN FEASIBILITY

The common failure modes of pile structures as listed in BASIC PILE GROUP BEHAVIOR (11) are:

1. Bearing capacity failure of the pile-soil system.

2. Excessive settlement due to compression and consolidation of the underlying soil.

3. Structural failure of the pile under service loads.

4. Bearing capacity failure caused by improper installation methods.

5. Structural failure resulting from detrimental pile installation. This may be due to unforeseen subsoil conditions or to freezing, compaction, liquification, or heave of the soil, or to improper installation.

The failure of piles due to structural loading is avoided by preventing the pile stresses from exceeding the maximum allowable stresses. The allowable stresses of steel

piles are shown in Table 8-5. The allowable stresses are variable in the various regions of the piles. The upper region of the pile are subject to bending and compression. The lower region of the piles are not under significant bending stresses. The pile tips are subject to damage during driving, therefore an increased factor of safety is used in the lower regions.

Table 8-5. Recommended Allowable Design Stresses for Steel Piles.

Compression at Pile Tip (psi) F_a	Compress. Upper Reg. subject to combined stresses (psi) F_a	Tension Upp. Reg. (psi) F_t	Bending (psi) F_b
0.28 F_y (10,000)	0.47 F_y (17,000)	0.50 F_y (18,000)	0.50 F_y (18,000)

The pile stresses are evaluated to determine the feasibility of the design by use of interaction equations. The stresses in the tip of a pile are checked against the allowable stresses as:

$$\frac{f_a}{(F_a)_{tip}} \leq 1.0 \qquad \text{(A1.22)}$$

The allowable stress in the tip is the lesser of the pile tip bearing strength and the bearing strata strength. The axial load at the tip must be less than the damaged cross-section capacity and the soil bearing capacity.

As shown in User's Guide (6) the stresses in the top section of "Steel piles subject to axial load and bending

shall be proportioned to satisfy the following requirements:

$$\frac{f_a}{F_a} + \frac{C_{mx} f_{by}}{(1-f_a/F'_{ex})\,F_{bx}} + \frac{C_{my} f_{by}}{(1-f_a/F'_{ey})\,F_{by}} \leq 1.0 \quad \textbf{(A1.23)}$$

and:

$$\frac{f_a}{F_a} + \frac{f_{bx}}{F_{bx}} + \frac{f_{by}}{F_{by}} \leq 1.0 \quad \left(when \frac{f_a}{F_a} \leq 0.15\right) \quad \textbf{(A1.24)}$$

where:

$$F'_e = \frac{\pi^2 E}{F.S.\ (K_b L_b / r_b)^2} \quad \textbf{(A1.25)}$$

and:

f_a =	computed axial stress (psi)
f_{bx} or f_{by} =	computed compressive bending stress about the x axis and y axis, respectively (psi)
F_a =	allowable axial stress (psi)
F_{bx} or F_{by} =	allowable compressive bending stress about the x and y axis, respectively (psi)
E =	modulus of elasticity (29,000,000 psi)
L_b =	actual unbraced length of pile in the plane of bending (inches)
K_b =	effective length factor as defined by AISC in the plane of bending (inches)
r_b =	radius of gyration in the plane of bending (inches)
C_{mx} or C_{my} =	coefficient about x and y axes, respectively, as defined by AISC
F.S. =	Factor of Safety

9. APPENDIX 2: FLEXIBLE SLAB ANALYSIS METHOD

FINITE ELEMENT METHOD

The concrete monoliths are analyzed with a finite element method. A finite element program was written. The finite element formulation closely follows the formulation of Hinton and Owen (12). Hinton and Owen have presented a plate bending element with 3 DOF and a plane stress element with 2 DOF. The elements are now combined to create a 5 DOF concrete monolith element.

The element is eight noded two-dimensional parabolic isoparametric. The element has to local axes ξ and η which are shown in Figure 9-1.

The shape functions are used to define the geometry and the displacement field. The displacements δ at any point are calculated from the nodal displacements by:

$$\delta = \sum_{i=1}^{n} N_i \delta_i \qquad \text{(A2.1)}$$

where n is the number of nodes per element, δ_i is the displacement at node i, and N_i is the shape function of node i evaluated at the point of interest. The shape functions are based on the Legendre polynomials. The shape functions are:

$$N_1 = -0.25(1-\xi)(1-\eta)(1+\xi+\eta) \qquad \text{(A2.2)}$$

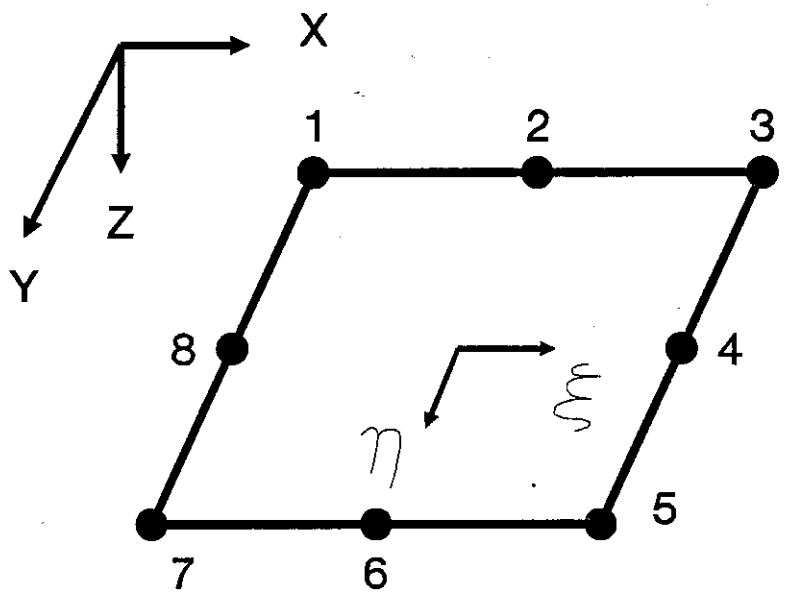

Figure 9-1. Numbering of Elemental Nodes.

$$N_2=0.5(1-\xi^2)(1-\eta) \tag{A2.3}$$

$$N_3=0.25(1+\xi)(1-\eta)(\xi-\eta-1) \tag{A2.4}$$

$$N_4=0.5(1+\xi)(1-\eta^2) \tag{A2.5}$$

$$N_5=0.25(1+\xi)(1+\eta)(\xi+\eta-1) \tag{A2.6}$$

$$N_6=0.5(1-\xi^2)(1+\eta) \tag{A2.7}$$

$$N_7=0.25(1-\xi)(1+\eta)(-\xi+\eta-1) \tag{A2.8}$$

$$N_8=0.5(1-\xi)(1-\eta^2) \tag{A2.9}$$

The total potential energy method is used to formulate the finite element method. The total potential energy is:

$$\pi=\frac{1}{2}\int_V [\sigma]^T\varepsilon\, dV-\int_V [\delta]^T\mathbf{p}\, dV-\int_S [\delta]^T\mathbf{q}\, dS \tag{A2.10}$$

where σ is the stress, ε is the strain, V is the volume, δ is the displacement, $\mathbf{p}$ is the body force per unit volume, S is the surface area, and $\mathbf{q}$ is the applied surface forces. The first term is the internal strain energy, the second term is the work of the body forces, and the third term is the work of the applied surface force.

The stress is expressible as:

$$\sigma=D\varepsilon \tag{A2.11}$$

where $\mathbf{D}$ is the elasticity matrix. The strains are

expressible as:

$$\epsilon = B\,\delta^{e} \tag{A2.12}$$

where δ^{e} is the elemental nodal displacements, and B is the strain matrix.

The total potential energy for element e is:

$$\pi_{e} = \frac{1}{2}\int_{V_e} [\delta^{e}]^{T}[B]^{T}DB\delta^{e}\,dV - \int_{V_e} [N]^{T}\delta^{e}p\,dV - \int_{S_e} [N]^{T}\delta^{e}q\,dS \tag{A2.13}$$

where V_e is the element volume, and S_e is the element surface.

The total potential energy of the structure is equal to the sum of the total potential energies of each element. The derivative of the total potential energy at equilibrium is zero. The derivative of the elemental energy is:

$$\frac{\partial \pi}{\partial \delta^{e}} = \int_{V_e} ([B]^{T}DB)\,\delta^{e}\,dV - \int_{V_e} [N]^{T}p\,dV - \int_{S_e} [N]^{T}q\,dS \tag{A2.14}$$

or

$$\frac{\partial \pi_{e}}{\partial \delta^{e}} = K^{e}\delta^{e} - F^{e} \tag{A2.15}$$

where:

$$K^{e} = \int_{V_e} [B]^{T}DB\,dV \tag{A2.16}$$

The volume can be computed as:

$$\int_{V_e} dV = \iint t\,dx\,dy = \iint t \det \boldsymbol{J}\,d\xi\,d\eta \qquad \text{(A2.17)}$$

where J is the Jacobian of the coordinates. The i,jth term of the stiffness matrix becomes:

$$K_{ij}^{e} = \iint \boldsymbol{B}_i{}^T \boldsymbol{D} \boldsymbol{B}_j\, t \det \boldsymbol{J}\,d\xi\,d\eta \qquad \text{(A2.18)}$$

The Jacobian of the element is found by taking the derivative of Equation A2.1:

$$\boldsymbol{J} = \begin{bmatrix} \frac{\partial x}{\partial \xi} & \frac{\partial y}{\partial \xi} \\ \frac{\partial x}{\partial \eta} & \frac{\partial y}{\partial \eta} \end{bmatrix} = \sum_{i=1}^{8} \begin{bmatrix} \frac{\partial N_i}{\partial \xi} x_i & \frac{\partial N_i}{\partial \xi} y_i \\ \frac{\partial N_i}{\partial \eta} x_i & \frac{\partial N_i}{\partial \eta} y_i \end{bmatrix} \qquad \text{(A2.19)}$$

The plane stress element carries all the forces in the plane of the element. The degrees of freedom are x and y. The plane stress element strain matrix is:

$$\boldsymbol{B} = \boldsymbol{L}\boldsymbol{N} \qquad \text{(A2.20)}$$

where:

$$\boldsymbol{L} = \begin{bmatrix} \frac{\partial}{\partial x} & 0 \\ 0 & \frac{\partial}{\partial y} \\ \frac{\partial}{\partial y} & \frac{\partial}{\partial x} \end{bmatrix} \qquad \text{(A2.21)}$$

Therefore:

$$\epsilon = \sum_{i=1}^{8} B_i \delta_i = \sum_{i=1}^{8} \begin{bmatrix} \frac{\partial N_i}{\partial x} & 0 \\ 0 & \frac{\partial N_i}{\partial y} \\ \frac{\partial N_i}{\partial y} & \frac{\partial N_i}{\partial x} \end{bmatrix} \begin{bmatrix} u_i \\ v_i \end{bmatrix} \qquad \text{(A2.22)}$$

where u_i and v_i are the displacements of node i in the x and y directions, respectively.

The elastic modulus for plane stress is:

$$D_{ps} = \frac{E}{1-\nu^2} \begin{bmatrix} 1 & \nu & 0 \\ \nu & 1 & 0 \\ 0 & 0 & \frac{1-\nu}{2} \end{bmatrix}$$

where ν is poision's ratio.

Plate:

The plate bending element uses the assumptions of Mindlin (20): 1) the deflections of the plate are small, 2) normals to the midsurface before deformation remain straight but not necessarily normal to the midsurface after deformation, and 3) stresses normal to the midsurface are negligible irrespective of loading.

The displacements of the plate are w, θ_{xx}, and θ_{yy} which represent the deflection in the z-direction and the rotations about the x and y axes, respectively. Hinton and Owen use the displacements w, θ_x, and θ_y where $\theta_x = -\theta_{yy}$, and $\theta_y = \theta_{xx}$. The coordinates have been reversed so that the new

coordinate numbering is the same as the pile coordinate numbering. The deformations are:

$$\delta = \begin{bmatrix} w \\ \theta_{xx} \\ \theta_{yy} \end{bmatrix} = \begin{bmatrix} w \\ \frac{\partial w}{\partial y} + \phi_{xx} \\ -\frac{\partial w}{\partial x} - \phi_{yy} \end{bmatrix} \qquad \text{(A2.24)}$$

where ϕ_{xx} and ϕ_{yy} are the average shear deformations about the x and y axes, respectively. The rotations represent the averaged rotations. The actual rotation is variable across the thickness due to the distribution of shear. The uneven warping is adjusted for by changing the shear deformation elasticity by a correction factor α.

The bending deformations are:

$$\chi = \begin{bmatrix} \chi_x \\ \chi_y \\ \chi_{xy} \end{bmatrix} = \begin{bmatrix} \frac{\partial \theta_{yy}}{\partial x} \\ \frac{-\partial \theta_{xx}}{\partial y} \\ \frac{\partial \theta_{yy}}{\partial y} - \frac{\partial \theta_{xx}}{\partial x} \end{bmatrix} \qquad \text{(A2.25)}$$

The moments **M** and the shear forces **Q** are related to the deformations through the elasticity matrix:

$$\begin{bmatrix} M \\ Q \end{bmatrix} = \begin{bmatrix} D_f & 0 \\ 0 & D_s \end{bmatrix} \epsilon \qquad \text{(A2.26)}$$

where:

$$\mathbf{e} = \begin{bmatrix} \chi \\ \phi \end{bmatrix} \tag{A2.27}$$

and $\mathbf{D}_f$ and $\mathbf{D}_s$ are the flexural and shear elasticity matrices, respectively. The elasticity matrices are:

$$\mathbf{D}_f = \frac{E t^3}{12(1-\nu^2)} \begin{bmatrix} 1 & \nu & 0 \\ \nu & 1 & 0 \\ 0 & 0 & \frac{1-\nu}{2} \end{bmatrix} \tag{A2.28}$$

and:

$$\mathbf{D}_s = \frac{E t}{2(1+\nu)\alpha} \begin{bmatrix} 1 & 0 \\ 0 & 1 \end{bmatrix} \tag{A2.29}$$

where α=6/5 is the non-uniform shear correction factor.

The strain matrix is formulated by expressing the deformations in terms of the shape functions and nodal displacements, then taking the derivative. The strain

matrix is:

$$B_i = \begin{bmatrix} B_{fi} \\ B_{si} \end{bmatrix} = \begin{bmatrix} 0 & 0 & \frac{\partial N_i}{\partial x} \\ 0 & \frac{-\partial N_i}{\partial y} & 0 \\ 0 & \frac{-\partial N_i}{\partial x} & \frac{\partial N_i}{\partial y} \\ \frac{\partial N_i}{\partial x} & 0 & N_i \\ \frac{\partial N_i}{\partial y} & -N_i & 0 \end{bmatrix} \qquad \text{(A2.30)}$$

The finite element method uses numerical integration to find the element stiffness. The integration is performed by evaluating the intergrand at a finite number of Gauss points or sample points. An example of numerical integration can be seen by integrating the volume in Equation A2.17. The Integral over coordinates are replaced by summations over all the sample points in each coordinate direction. The integrated parameters t and J are evaluated at each sample point. The total volume is the sum of the components times the weighting factors:

$$V = \sum_{k}^{ngp} \sum_{l}^{ngp} t \det \boldsymbol{J} \, W_k W_l \qquad \text{(A2.31)}$$

The stiffness is the sum of the integrands times weighting factors. Four Gauss points are used for the plane elements and nine points for the plate element. The elemental coordinates and weighting factors are shown in Table 9-1.

Table 9-1. Gauss points.

Num. Gauss pts.	Coordinates	Weights
4	+/- 0.57735	1.
9	+/- 0.77459 0	5/9 8/9

The elemental stiffness is:

$$K^e = \sum_{k=1}^{ngp}\sum_{l=1}^{ngp} B^T D B \det J \, Weight_k Weight_l \qquad \text{(A2.32)}$$

where ngp is the number of gauss points. All of the terms are evaluated at each Gauss point.

The elemental stiffness matrices are assembled to produce the structural stiffness matrix. Each node has five degrees of freedom. Each node has a stiffness which is contributed from one or more adjoining elements. The contribution of the stiffness from each element is summed to produce the total nodal stiffness.

Loading:

The loading of the pile structure consists of in-plane and out-of-plane forces. The in-plane forces are applied to the plane stress element and the out-of-plane forces are applied to the plate element. Distributed and point loads are applied throughout the elements.

Loads are transformed into equivalent nodal loads by use of shape functions. The procedure to transform point loads is developed by using virtual work. An applied load p

and a virtual displacement w^* are applied at the loading point. The resultant forces and displacements at the nodes are $\mathbf{P}$ and $\mathbf{W}^*$. According to virtual work:

$$\boldsymbol{P}^T \boldsymbol{W}^* = p\, w^* \qquad \text{(A2.33)}$$

The isoparametric shape functions transform the virtual displacements as:

$$w^* = \boldsymbol{N}^T \boldsymbol{W}^* \qquad \text{(A2.34)}$$

Substituting Equation A2.34 into A2.33 and eliminating the arbitrary virtual displacements results in:

$$\boldsymbol{P} = p\, \boldsymbol{N} \qquad \text{(A2.35)}$$

Distributed Loads:

Transforming distributed loading involves integration of the surface of load action. Distributed loading is numerically integrated using Gauss points. The forces normal to the plate surface is the integral of the force and the differential area:

$$P_{zi} = \int_A N_i\, q\, dA \qquad \text{(A2.36)}$$

where P_{zi} is the normal force at node i. This is numerically integrated as:

$$P_{zi} = \sum_{k=1}^{ngp} \sum_{l=1}^{ngp} N_{i\,kl}\, q \det \boldsymbol{J}\, Weight_k Weight_l \qquad \text{(A2.37)}$$

Edge Loads

The forces applied along the edge of the elements is the integral of the force and the differential edge area. Forces which are tangential (p_t) and normal (p_n) to the edge may be applied. The equivalent differential forces in the x and y directions are:

$$dP_x = p_t dx - p_n dy \tag{A2.38}$$

$$dP_y = p_n dx + p_t dy \tag{A2.39}$$

The loads are integrated along the edge at the element level. The differential distances are equivalent to:

$$dx = \frac{\partial x}{\partial \xi} d\xi + \frac{\partial x}{\partial \eta} d\eta \tag{A2.40}$$

$$dy = \frac{\partial y}{\partial \xi} d\xi + \frac{\partial y}{\partial \eta} d\eta \tag{A2.41}$$

where $d\eta$ is zero since integration is along the edge. The integration is along the η=+1 face. The procedure is similar for the other faces. The integrals of the forces become:

$$P_{xi} = \sum_{k=1}^{ngp} N_i \left(p_t \frac{\partial x}{\partial \xi} - p_n \frac{\partial y}{\partial \xi}\right) Weight_k \tag{A2.42}$$

$$P_{yi} = \sum_{k=1}^{ngp} N_i \left(p_n \frac{\partial x}{\partial \xi} + p_t \frac{\partial y}{\partial \xi}\right) Weight_k \tag{A2.43}$$

where the differentials are readily available from the Jacobian.

PILE ANALYSIS

An innovative method of assembling the piles into the finite element mesh has been created. Previously the piles could only be assembled to the structure at the nodes of the finite element mesh. The new assembly method allows the piles to be assembled at any point in the mesh. This method is discussed fully in Section 2.2.3.

The flexible analysis and the rigid slab analysis use the same procedure for pile stiffness formulation and pile stress evaluation. This method is presented in Appendix 1.

10. NOMENCLATURE

β = batter slope of a pile.

ϕ = angle of rotation of pile from global x-axis.

θ = angle of rotation of pile flanges about local z-axis.

I_{xx} = major axis moment of inertia.

I_{yy} = minor axis moment of inertia of a given member.

A = area of a given member.

c_x = extreme fiber distance in the direction of a member's local x axis.

c_y = extreme fiber distance in the y direction.

h_j = constraint j.

m = number of constraints.

σ_j = stress in member j.

$\overline{\sigma}_j$ = upper limit on the stress in member j.

$\underline{Ixx}$ = lower bound on the major axis moment of inertia.

$\overline{I}_x$ = upper bound on the major axis moment of inertia.

F = array of forces.

N_I = shape function for node I.

$\mathbf{K}_p$ = pile stiffness matrix.

d = array of displacements.

W_T = total weight of the steel piles.

ρ = density of steel.

V_i = volume of element i.

N = number of piles.

L = Lagrangian.

λ_j = Lagrange Multiplier for the j^{th} constraint.

d_i = design variable number i.

n = number of variables.

r = convergence control parameter.

n_1 = number of active variables.

w_i = scaling parameter equal to the estimate of the secondary effects on the weight.

P_i = global force component i.

D_i = global displacement component i.

SM = stiffness multiplier.

N_{real} = number of real valued piles assembled.

N_{assem} = number of integer piles assembled.

p_{ij} = percentage of a discrete choice for option j, pile i.

$Nopt_i$ = number of discrete options for member i.

M_i = global moment component i.

x_{low} = lower x-coordinate of the borders of a pile group.

x_{high} = higher x-coordinate of the borders of a pile group.

y_{low} = lower group y-coord.

y_{high} = higher group y-coord.

$\mathbf{C}$ = transformation matrix for displacements from the analysis center or center-line to the pile.

$\mathbf{A}$ = transformation matrix for global displacements at a pile to local coordinates.

11. BIBLIOGRAPHY

1. Venkayya, V. B., "Design of Optimum Structures," Computers and Structures, Vol. 1, 1971, pp. 265-309.

2. Xu, L.; Grierson, D.E., "Computer-Automated Design of Semirigid Steel Frameworks," Journal of Struct. Eng., ASCE, Vol. 119, 6, 1993, pp. 1740-1760.

3. Cheng, Franklin Y., Truman, Kevin Z., "OPTIMIZATION ALGORITHM OF 3-D BUILDING SYSTEMS FOR STATIC AND SEISMIC LOADING", In: Ames, W. F. and Vichnevetsky, R. (eds.) Modeling and Simulation in Engineering, Vol. 3, North-Holland, Amsterdam, 1983, pp. 315-326.

4. US Army Corps of Engineers, "User's Guide: Pile Group Optimization Program (OPTPILE)," Technical Report ITL-93, 1993.

5. Hoback, A.S, Truman, K.Z., "Least weight design of steel pile foundations," Engineering Structures, Vol. 15, No. 5, 1993, pp 379-385.

6. US Army Corps of Engineers, "User's Guide: Pile Group Analysis (CPGA) Computer Program," Technical Report ITL-88, 1988.

7. Gellatly, R. A., Berke, L., "Optimal structural design", USAF AFFDL-TR-70-165, 1971.

8. Truman, Kevin Z., Hoback, Alan S., "Optimization of steel piles under rigid slab foundations using optimality criteria," Struct. Optim., Vol. 5, No. 1, 1993, pp. 30-36.

9. Hoback, Alan S., Truman, Kevin Z., Optimization of Steel Pile Foundations Using Optimality Criteria, Report No. 88, Dept. of Civil Engineering, Washington University, St. Louis, MO, 1991.

10. American Institute of Steel Construction, Inc., Manual of Steel Construction, Eighth Edition, 1980.

11. CASE Task Group on Pile Foundations, "BASIC PILE GROUP BEHAVIOR," Technical Report K-83-1, US Army Engineer Waterways Experiment Station, 1983.

12. Hinton, E., Owen, D.R.J., Finite Element Programming, Academic Press, Inc., New York, 1977.

13. GTSTRUDL User's Manual, GTICES Systems Laboratory, Georgia Inst. of Tech., Atlanta, 1989.

14. Hill, James L., "USER'S GUIDE: COMPUTER PROGRAM FOR OPTIMAL DESIGN AND ANALYSIS OF PILE FOUNDATIONS (PILEOPT)," Instruction Report K-81-5, US Army Engineer Waterways Experiment Station, 1981.

15. Hoback, A. S., Truman, K. Z., "A New Method of Finding Global and Discrete Optimums for Structural Systems," Computers and Structures. (In review.)

16. Hajela, P., "Genetic Search-An Approach to the Nonconvex Optimization Problem," AIAA Journal, Vol. 28, No. 7, 1990, pp. 1205-1210.

17. U.S. Army Corps of Engineers, St. Louis District, "Design Memorandum No. 21, Auxiliary Lock & Remainder of Dam," Lock and Dam No. 26 (Replacement), April 1987.

18. Saul, W. E., "Static and Dynamic Analysis of Pile Foundations," J. Struct. Div., ASCE, Vol. 94, No. ST5, Proc. Paper 5936, 1968, pp. 1077-1100.

19. Dawkins, William P., Pile Head Stiffness Matrices, Report for U.S. Army Corps of Engineers Waterway Experiment Station, 1978.

20. Mindlin, R. D., "Influence of rotatory inertia and shear on flexural motions of isotropic elastic plates," J. Appl. Mech., Vol. 18, 1951, pp. 31-38.

Alan S. Hoback

VITA

Date of Birth:	11/20/64
Place of Birth:	Lincoln, Nebraska
Undergraduate Study:	Hastings College, Hastings, Nebraska, B.A. in Physics 1987
	Washington University, St. Louis, Missouri, B.S. in Civil Engineering 1989, cum laude
Graduate Study:	Washington University, St. Louis, Missouri, M.S. in Civil Engineering, May 1991.
	Washington University, St. Louis, Missouri, Dr. Sci. expected Dec. 1993.
Professional Societies:	ASCE, EERI

December 1993

Short Title: Optimization of Pile Foundations Hoback, D.Sc. 1993